NEW FIELD TESTING PROCEDURE FOR MEASURING RESIDUAL STRESS IN PLAIN CONCRETE PAVEMENTS AND STRUCTURES

BY

DANIEL I. CASTANEDA

THESIS

Submitted in partial fulfillment of the requirements
for the degree of Master of Science in Civil Engineering
in the Graduate College of the
University of Illinois at Urbana-Champaign, 2010

Urbana, Illinois

Adviser:

Professor David A. Lange

ABSTRACT

Residual stresses in rigid pavements diminish a pavement's ability to sustain its designed load. When capacity is reduced by residual stress, a pavement is vulnerable to premature failure necessitating costly repairs or replacement. A test method for measuring residual stresses has already been developed for steel wherein a small hole is drilled adjacent to an affixed surface strain gage (ASTM E837 2008). Based on the geometry of the test procedure, the change in strain reading is correlated to a residual stress in the steel material. While rigid pavements are as detrimentally affected by the formation of residual stresses as steel, no similar testing method exists for concrete.

Recent research conducted by the Federal Aviation Administration's (FAA's) National Airport Pavement Test Facility (NAPTF) investigated the strain relaxation of cantilevered concrete beams when a blind-depth hole using core drilling is made in the vicinity of an affixed strain gage. Initial findings indicated that the testing procedure partially quantified the residual stresses. Research at the University of Illinois at Urbana-Champaign (UIUC) improved the testing procedure using cantilevered concrete beams by instead sawing a linear notch near one end of the strain gage and sawing two linear notches near both ends of the strain gage. Results for the doubly notched concrete beam proved to be a much improved method for measuring residual stresses when compared to the core-drilled test procedure.

The current project further improved test procedures and completed additional lab and field testing on in-situ plain concrete pavements. The test procedure was altered in order to observe the strain relaxation in three directions while four saw cuts are made surrounding the strain rosette. When this area of concrete had been appropriately isolated from load-induced stresses, simple calculations determine the residual stress of the material. Three dimensional Finite Element Model (FEM) analyses of these tests further corroborates the findings suggesting that the residual stresses in plain concrete pavements can be reliably measured.

ACKNOWLEDGEMENTS

I want to express my sincere gratitude to my adviser, Professor David Lange, for allowing me to join his research group and to work on this challenging yet rewarding project. I am also grateful for the effort of the previous research assistant, David Marks, in speedily getting me up to date with the project in preparation of my assumption as the new research assistant. Their commitments in maintaining the continuum of knowledge greatly contributed to my own personal growth and success in this research.

I am also greatly indebted to my fellow graduate students for their support in both labor and spirit. In particular, I thank Richard Santos for his ungrudging generosity in providing vehicular transportation to off-campus testing facilities and a much-appreciated second pair of hands during outdoor testing – even in the harshest of winter conditions. I also want to thank Jacob Henschen and Jason Mote for their invaluable insight both offered and sought throughout the project's duration. Additionally, I acknowledge Gustavo Gonzalez and his work under my supervision conducting tests during his time at UIUC as a summer intern.

I am very appreciative of Professor Jeffery Roesler, Associate Director for the Advanced Testing and Research Engineering Laboratory (ATREL), for offering testing facilities and previously constructed concrete pavements for use of experimentation. The testing of these concrete pavements was facilitated by the very helpful ATREL research engineer, Jim Meister. Additional lab support was provided by Gregorz Banas, Coordinator for the Newmark Structural Engineering Laboratory (NSEL).

This project also included a significant amount of FEM analysis that I was unfamiliar with, so I want to thank Professor Eshan Dave, Professor Christian Gaedicke, and graduate students Amanda Bordelon and Kerry Hall for their patient instruction in operating Patran and ABAQUS software.

David Brill, Jeff Gagnon, and Frank Pecht coordinated useful on-site testing at the NAPTF, offered their time in orchestrating wheel load applications and have provided appreciable technical expertise and suggestions toward this project.

Financial support for this project was made possible with funds from the Center of Excellence in Airport Technology (CEAT), funds from the FAA and fellowship funds from the UIUC College of Engineering.

TABLE OF CONTENTS

INTRODUCTION

Residual stresses exist in concrete pavements and structures due to material volume changes, temperature and moisture gradients, changes in support conditions and structural restraints. Unlike stresses associated with live and dead loads, residual stresses are neglected by pavement and structural design procedures and are routinely unknown and overlooked. Yet, in some circumstances, the magnitude of residual stress can rise to a significant fraction of strength, thus diminishing the ability for the concrete to sustain its design load.

During initial construction of a rigid pavement, residual stresses may be built into the material. These residual stresses are characterized as existing in the bulk of the material without the application of an external load or external stress (James and Lu 1996). They can form as a result of a number of issues including differential drying across the profile of the pavement depth and constraining features of the geometry of the structure while the concrete is still in its plastic state. They can also form as a result of changing support and material conditions over the lifetime of the structure. Creep can partially alleviate these stresses over time; however, there is no method to quantify the magnitude of the residual stresses at any age of the pavement structure, particularly in its young life when the material is susceptible to early damage.

The debilitating effect of the built-in stress diminishes the loading capacity of the pavement particularly if the stresses are tensile in nature as this will lead to premature cracking. Cracking in concrete pavements is detrimental to its long-term durability since deteriorating agents like excess water and dissolved gases will accelerate deterioration processes. Additionally, other distresses will manifest themselves as a result of the altered stress state. Blowups can occur more readily since the designed joint spacing is unsuitable for the calculated magnitude of expansion; transverse and diagonal cracking is also more likely to manifest itself because of the differential residual stresses across a pavement's depth (Huang 2004).

While quantifying residual stresses is the principal concern of this thesis, other types of cyclical stresses induced in concrete pavements are notable. Heating and cooling due to cycling of the sun through a 24 hour period induces significant curling stresses in concrete pavements. There exist methods to estimate these stresses by measuring the temperature profile of the concrete pavement and combining them with closed-form solutions of the Westergaard equations (Mohamed and Hansen 1996). However, this does not account for permanent curling stresses as a result of moisture curling, particularly during initial set and hardening of the concrete material.

In any case, the stress-state of the concrete material can be measured with either embedded strain gages or surface strain gages.

Efforts to quantify the stress state in concrete pavements began many years ago using techniques known in the geotechnical field. A. M. Richards published a technique in 1979 detailing the use of electrical strain gages to measure the strain relieved when a "corehole is overcorred" (Richards 1979). More recently, the FAA's NAPTF experimented with a technique that has been standardized in another material – metal (E. H. Guo, et al. 2008). A standardized testing method exists for the determination of residual stresses in steel members by the hole-drilling strain-gage method (ASTM E837 2008). This method entails affixing a strain gage onto the surface of a steel member and recording the strain relieved as a hole is drilled nearby. The stresses are then calculated based on the depth of the drilled hole (full-depth versus partial-depth) and whether the stresses in the material vary uniformly or non-uniformly across its depth. Researchers at the NAPTF applied this testing method to cantilever concrete beams to find that the residual stresses could be partially relieved (E. H. Guo, et al. 2008).

Confirmatory research was undertaken by researchers at UIUC to similarly find that the residual stresses could be partially quantified by the partial-depth hole-drilling method (Marks and Lange 2009). This testing was modified to improve the isolation of induced stresses by instead cutting linear notches at either side of the affixed strain gage. This drastically diminished the effect of the applied load and better characterized the residual stress of the material.

This revised testing procedure was thusly adopted for field testing to better understand the capacity of the testing method to adequately quantify residual stresses in concrete pavements. A rosette of strain gages was affixed in an area of interest along the surface of the concrete. Linear notches of varying depths surrounded the strain rosette in order to characterize the magnitude of relieved strain. This testing method was reiterated in several experiments to find that a minimum notch spacing-to-depth ratio can reliably relieve the majority of residual stresses.

Subsequent FEM analysis was performed to complement the experimental results and to determine the procedure's viability. The FEM analysis, along with testing results, suggest that despite the variability in stress states, a common notch geometry can simply, adequately and reliably quantify the residual stress in plain concrete pavements. However, it is important to account for variability in the final results since it is a depiction of the stress state during the time of testing. Understanding the fluctuation of stress due to temperature and moisture

(environmental conditions) along with changing loading and support conditions over time should indicate trends of stress over time.

These considerations, along with the promising results described in detail in this thesis, suggest that this testing procedure can measure the residual stress in plain concrete pavements. As such, a draft standardized testing procedure is included in the appendix since it is hopeful that this method will advance in future years to widespread acceptance as a useful field test.

CHAPTER 1: RESIDUAL STRESS MEASUREMENT OVERVIEW

1.1 Introduction

The pursuit of quantifying stresses in concrete has spanned several decades as researchers have sought differing ways to approach the problem. At the core of every study is an attempt to improve the previous simplifications in order to more accurately predict the stress state of in-situ concrete. A short review of relevant studies conducted to better characterize stresses in concrete pavements is presented here.

1.2 Historic Testing and Related Rigid Pavement Studies

A closed-form solution for predicting stresses in rigid pavements was first developed by Westergaard, was later corrected by Ioannides and was further developed by Bradbury (Hiller and Roesler 2010). These solutions were originally constructed for slabs of infinite width and length with uniformly distributed loads acting on a circular area with radius *a* (Brink 2003). Situations in which circular or semi-circular loading areas applied as edge and corner loads were also developed. At a later point, these solutions were appended with correction factors for finite slab dimensions by Bradbury (Brink 2003). All of these solutions take into account various estimated parameters including a radius of relative stiffness – a value comprised of the systemic reaction from the rigid pavement layers and its underlying subgrade support (Brink 2003). These analytical solutions are highly idealized and cannot accurately predict the stress states of in-situ concrete pavements.

Stresses that are separate from those idealized stressed induced by applied loads include thermal stresses and stresses due to moisture curling. Typically in analysis, stresses developed by temperature gradients are often simplified as behaving linearly across the depth of the pavement. This simplification is often used since the development of Westergaard's solution for curling in rigid pavements promoted this, but a more thorough and exact characterization would instead use a uniform temperature stress coupled with an equivalent curling stress and a "non-linear self-equilibrating stress" (Hiller and Roesler 2010). Experiments have been constructed that can better link these curling stresses with built-in residual stresses.

Experiments driving towards quantifying built-in stresses caused by permanent thermal and moisture gradients, particularly of irreversible shrinkage caused by gradients during concrete's plastic state and before hardening, by a field testing method have been investigated. One study investigated measuring the degree of moisture and temperature along the profile depth

of a freshly cast concrete pavement (Wells, Phillips and Vandenbossche 2006). That data was then compared to the subsequent cracking of sawn expansion joints. In addition, this data was compared to the slab deflection as it warped over time. A similar study used falling-weight deflectometers to characterize effective built-in temperature differences (Rao and Roesler 2005). Knowing these temperature differences in a pavement can lead to analytical solutions to predict the residual stress in the material (Mohamed and Hansen 1996).

Understanding and quantifying built-in residual stresses is important in certain applications like airfield pavements. While aircraft size and weight has increased regularly in the past few decades, material capacity of concrete runways is maintained until major renovation occurs. Studies have investigated the effect of larger sized aircraft like the Airbus 380 and Boeing 747 on concrete pavements (Caliendo and Parisi 2010). While structural analysis may suggest that a concrete pavement is adequate for these aircraft loads, eventual loss of subgrade support since its casting can induce stresses in a slab which lead to unexpected cracking and failure. Earlier models have incorporated wheel loading and temperature gradients as separate entities to predict slab stresses and subsequently join their results through superposition; however, this is often times an inaccurate depiction of the concrete stress state (Caliendo and Parisi 2010).

Later testing directly correlated strain relaxation due to joint formation in concrete pavements becoming the investigative foundation to pursue residual stress measurements in concrete systems. The distance of the strain measurement to the joint was found to vary in accordance with probable stress states of the material (Guo, Pecht and Ricalde 2010). These stress states would become altered when preparatory spacing joints cracked and propagated through the material as a result of applied dynamic wheel loading. However, observations were made that the stress state up until this point was higher in magnitude and would significantly drop – or be relieved – upon the formation of the joint and subsequent crack. The researchers had concluded that the "pseudo-stress" was unaccountable based on a full scale analysis of their experiment and suggested that the discrepancy in their results were attributable to built-in tensile residual stresses (Guo, Pecht and Ricalde 2010).

1.3 Testing on Concrete Beams by NAPTF and UIUC

Those researchers who made a link between observed, discrepant stresses in concrete pavements performed other work that more rigorously quantified the phenomenon in

cantilevered concrete beams (E. H. Guo, et al. 2008). This work comprised casting rectangular concrete beams and subjecting them to cantilever end loads. Surface strain gages were mounted on the top surface as well as the underside of the concrete beams in order to characterize its response as loads were ramp-loaded. This construct allowed for classical mechanics equations for beams in bending to be utilized in order to determine the induced stresses.

An existing ASTM standard exists which describes an accepted method to measure residual stresses in metal (ASTM E837 2008). This method involves affixing a surface strain gage onto a metal member's web and to drill a small partial or full depth hole in the vicinity of the strain gage. The difference in strain is noted and because the geometry is well understood, an analytical solution using Kirsch's equations can be applied. This solution predicts the stress state at a point beyond a hole in a planar surface subjected to constant stress.

This testing procedure was thusly adapted in the researcher's testing of the cantilevered concrete beams. The top surface of a cantilever is effectively in a planar stress state when loaded with an end load. The core-drill would be used to generate a partial-depth core in the vicinity of the affixed surface strain gage thus presumably altering the stress state in accordance with Kirsch's assumptions. The calculated difference in measured strain could thusly reveal the residual stress in the concrete material. However, their method relied heavily on partial-depth core drills as opposed to full-depth core drils which only partially quantified the residual stress.

Researchers at UIUC worked in conjunction with the researchers who had developed this novice method for measuring residual stress in cantilever concrete beams (Marks and Lange 2009). A revision to the procedure was made which took advantage of the simple geometry of the cantilever concrete beam. Instead of core-drilling near the top surface, linear saw cuts would be made in order to achieve the same affect. This resulted in similar results wherein the residual stress was partially quantified. A second iteration was devised wherein linear saw cuts would be made on both sides of the surface strain gage. Those results proved a viable means to more fully diminish the effect of the applied end load. As a consequence of its classical geometry, the discrepancy between the strains induced by the applied load and the total strain relieved is characterized as strains caused by the relieving of residual stresses.

1.4 Data Collection and Calculation

Third-wired quarter bridge strain gages manufactured by Tokyo Sokki Kenkyujo Co., Ltd. were used throughout this project. These surface foil gages have a gauge length of 30

millimeters (1.18 inches) and a gauge factor of 2.13 ± 1 %. Their resistivity is 119.5 ± 0.5 ohms and they are operable in temperature ranges of -4^{o}F to 140^{o}F.

The length of the gages was determined suitable by previous testing. Future testing and field testing should consider using sizeable strain gages of at least 20 millimeters in gauge length in order to ensure that underlying aggregates beneath the surface of the concrete do not significantly alter the expected strain results. While concrete is a heterogeneous material, its observations can become homogenous if the gauge length is smaller than the largest anticipated aggregate size used in the concrete mix.

These strain gages were connected to Model P3 Strain Indicator and Recorder. This device sends a self-configured excitation voltage to the strain gage and measures voltage changes throughout recording. These voltage readings are converted to units of microstrain whose magnitudes are displayed on an LCD screen in real time. This data recording device was also used to measure the magnitude of load from a custom-built load cell.

A 30 kip-capacity aluminum metal load cell constructed at the NSEL was used to record the magnitudes of load applied with a bottlejack to several tested concrete slabs. This full bridge load cell had a signal output of 3.675 milliVolt for every 1 Volt of excitation. The top portion of the bottlejack piston was corrugated and this was found to damage the load cell during loading, so a small steel plate was situated between the load cell and the bottlejack.

The strain results were noted and, given their orientation, stresses could be calculated. These calculated stresses are valid only on the surface of the concrete on which the measurement was undertaken. Using the biaxial form of Hooke's Law, the stresses can be computed:

$$\sigma_x = E / (1 - \upsilon^2) * (\varepsilon_x + \upsilon\varepsilon_y) \qquad \text{(Eqn. 1.1)}$$

$$\sigma_y = E / (1 - \upsilon^2) * (\varepsilon_y + \upsilon\varepsilon_x) \qquad \text{(Eqn. 1.2)}$$

In the above equations, the elastic modulus, E, was estimated at approximately 3,500 to 5,000 psi depending on the concrete while the Poisson's Ratio, υ, was estimated at 0.15.

CHAPTER 2: PROOF-OF-CONCEPT TESTING ON DISCARDED SLABS

2.1 Introduction

UIUC conducted confirmatory testing on several instrumented, cantilevered concrete beams in a lab setting. The concrete beams material varied in materials, geometry and loading. Through this testing, a revised procedure was developed where linear notches were sawn on either side of an affixed surface strain gage. This revised method of sawing linear notches was adapted for proof-of-concept testing on discarded slabs available at ATREL in Rantoul, IL.

These discarded slabs originated from a road test strip that had been subjected to millions of Equivalent Single Axle Loads (ESALs) in the span of weeks (Cervantes and Roesler 2009). Two plain concrete slabs measuring 6 feet x 6 feet x 6 inches had been lifted from this road test strip and tested to fracture. The four fragments of the slabs were suitable for additional testing, so they were collected and prepared for proof-of-concept testing for this project.

The first slab tested was laid on a concrete floor and supported simply by wood wedged along its underside to prevent it from teetering. This first test identified whether saw cuts sawn around a strain rosette could indeed relieve appreciable material stress. The geometry of the cut was constructed to closely mirror the preliminary success of the concrete beam testing where parallel cuts perpendicular to the strain gage would be made. In a strain rosette, two perpendicular strain gages – along with a third gage set at 45 degrees from those two – necessitate four cuts forming a square. The size of this square was varied across numerous tests.

After a successful first test of the unprepared concrete slab, an industrial saw cutter was used to form the three remaining irregularly shaped slabs into 72 inch x 36 inch x 6 inch rectangular slabs. The underside of the slabs were uneven on account of having been cast on an aggregate base, so the slabs were flipped and a thin layer of Hydrocal plaster was applied in order to produce a smooth underside. These three prepared slabs were tested in a manner as to produce calculable stress magnitudes. Their setup was designed to be slabs in bending whose width was larger than that of the concrete beams previously tested. This would allow for appreciable strain relaxation along the material's width that would not have been discernable in a thin-width beam.

2.2 Procedure

Three strain gages of 30 millimeters length (1.18 inches) were affixed within a 2 inch x 2 inch squared area in the middle of the top surface of the slab; this location was 36 inches along

the length and 18 inches along the width of the slab. A set of four linear notches measuring 10 inches in length were made about this 2 inch x 2 inch squared area to produce an isolated square of material measuring 3 inches x 3 inches. The separation between the 2 inch x 2 inch squared area and the 3 inch x 3 inch square area was no more than 0.5 inches in either Cartesian direction.

When the underside of the concrete slabs had been evened with an appropriate layer of Hydrocal plaster, they were flipped right-side up and positioned atop steel beams. This effort was undertaken in order to induce either compressive or tensile stresses along the top surface of the concrete slab. The steel beams were thusly positioned at either the extreme ends of the slab in order to cause compressive bending on the top side of the slab due to self-weight, or positioned along the interior of the slab in order to cause tensile stresses due to the slab bending in self-weight along the top surface.

The flanges of the steel beams measured 4 inches and were positioned such that the underside surface of the Hydrocal-prepared concrete slab was wholly supported across its width. This resulted in a 64 inch span along the length of the slab in the case of creating a compressive top surface. Given the geometry of the slab and its supports, a calculated compressive stress of 43 psi was estimated at the center of the top surface of the slab due to self-weight. Alternatively, the 4 inch steel beams were positioned near the center in order to induce a top surface in tension. The steel beams were positioned 33 inches from the ends and created two cantilever sections measuring 31 inches in length and a center span measuring 2 inches in length. Given the geometry of the slab and its supports, a calculated tensile stress of 44 psi due to self-weight was expected. The stresses were calculated using:

$$\sigma = Mc / I \qquad \text{(Eqn. 2.1)}$$

$$\text{where } I = bh^3 / 12 \qquad \text{(Eqn. 2.2)}$$

In order to alternatively measure the effect of the increasing depth of the notches surrounding the strain rosette, two masses each weighing 220 pounds were positioned atop the concrete slab in a manner to complement the aforementioned state of stress. In the case of the concrete slab whose top surface is in compression, the masses were positioned approximately 4 inches away from either side of the center. This induced an additional compressive stress of approximately 28.5 psi. For the case where the concrete slab was centrally supported resulting in the top surface being in tension, the masses were positioned along the extreme edges

approximately 2 inches from the edge of the slab. This resulted in the addition of 32 psi tension stress at the center of the slab.

An initial set of four saw cuts was made at a depth of 0.5 inches in depth. These cuts were produced using a handheld circular saw with a 7.5 inch diameter masonry saw blade. After the strain readings stabilized, a second set of four cuts measuring 1.0 inch in depth were made. The strain readings were allowed to stabilize again thereafter a third set of cuts measuring 1.5 inches in depth was made. All quadrilateral saw cutting sequences followed a similar procedure wherein the first two cuts were made in the transverse direction while the second two cuts were made in the longitudinal direction.

Additionally, edge loads of 220 pounds were positioned along the outer edges of the slab while it was centrally-supported in order to amplify the tensile stresses along the top concrete surface during testing. These loads were repeatedly applied and removed throughout testing in order to demonstrate the diminishing response of the centrally located strain rosette as the quadrilateral set of notches increased in depth.

2.3 Results for Discarded Slabs

The strain readings during testing are depicted in the figures at the end of this chapter. The final strain readings have been calculated for their maximum and minimum principal stresses. Whichever value is greater in magnitude is denoted as the residual stress. It is important to realize that the direction of relieved stress is opposite of the stress state of the material. A calculated tensile stress in the isolated concrete material suggests that the material had been in a compressive state. Similarly, a calculated compressive stress in the isolated material suggests that it had been in a tensile state.

Preliminary strain results in the first tested slab reveal a trend in which there is appreciable change strain for increasing notch depths. As seen previously in cantilevered concrete beam tests, an abrupt fluctuation of the strain measurement is observed as the saw cut is made and is followed by a period of time where the strain stabilizes. Initial, shallow cuts seem to stabilize more quickly while later, deeper cuts require more time to stabilize. This behavior has been attributed to thermal cooling of the concrete material as a large amount of heat is generated from the passing saw blade (Marks and Lange 2009). This heat, in part, causes expansion which contracts upon cooling. The successive number of saw cuts resulted in an ultimate average depth of 2.0 inches and a calculated residual stress of 220 psi in compression.

The second test used masses at the ends of a centrally supported slab inducing a total tensile stress of 76 psi at the surface of the concrete material. When notched to a final depth of 1.6 inches, the strain response signified a tensile stress of 88 psi. This tensile stress was calculated using a stiffness value of $5x10^6$ psi and a Poisson's ratio of 0.15. While it is possible to alter the calculated stress value to more suitably match the experimental value by modifying the stiffness of the material, the similarity in order of magnitude suggests an appropriate stress value based on the geometry of the structure can be calculated.

The third test was performed in compression where the total induced stress was 72 psi, but the longitudinal strain gage was damaged when the 220 lb masses were removed. Thus, the calculated residual stress before strain gage damage was through an average notch depth of 0.5 inches of 190 psi in compression. This result is questionable, however, because initial strain values had not stabilized to zero suggesting that creep and other micro-cracking was occurring as the slab was situated over the rail beam supports.

A second test in compression (fourth overall test) was conducted where no masses were used (in order to prevent strain gage damage). This left a calculated 43 psi in compression along the top surface of the material. The cutting of a 1.7 inch notch depth resulted in 370 psi tensile stresses. However, significant drifting of the 45 degree strain gage was noted, so an alternative calculation was made only considering the longitudinal and transverse stresses as denoted by the longitudinal and transverse strain gages. Using the biaxial form of Hooke's Law, the longitudinal stress was calculated to be 75 psi in tension while the transverse stress was calculated to be 30 psi in tension.

This fourth test revealed an unexpected but alluring discrepancy: a surface loaded in compression had indicated tensile forces as its primary stress state. The longitudinal direction had been subjected to a compressive state of 43 psi suggesting that the residual stress, if unloaded would be 138 psi. The tensile stress in the transverse direction, largely unaffected by the self-weight bending of the material, measured 30 psi across the width of the concrete material. A tensile residual stress measuring on the order of 100 can be a significant detriment to premature cracking as upwards of 20 – 40% of the materials modulus of rupture is pre-loaded and built-in.

These initial proof of concept test results suggested that proceeding with this testing procedure on in-situ pavements would yield viable results. The application of a strain rosette

surrounded by four saw cuts had two clear advantages: the maximum and minimum principal stresses could be readily solved for regardless of saw cut geometry surrounding the strain rosette; and the directional stresses (longitudinal and transverse stresses) could be calculated if the cuts remained perpendicular to their direction. It was decided to proceed with this geometry because of its ease of use.

However, it is evident that low-magnitude applied loads would be insufficient to induce quantifiable induced strains. The application of the end masses on centrally supported slabs and the application of interior masses on end-supported slabs generated minimal stress values. Future testing would need to incorporate applied loads similar to that of vehicular traffic. The testing facility at ATREL where these discarded slabs had been identified would offer additional testing opportunities.

2.4 Figures and Graphs

Figure 2.1 Slab flipped exposing its underside. Form fitted at its edges in preparation for Hydrocal plaster

Figure 2.2 Centrally supported concrete slab with 220 lb edge loads applied to produce tension along the top surface

Figure 2.3 Close-up view of centrally supported slab, the 2 inch span and flange supports

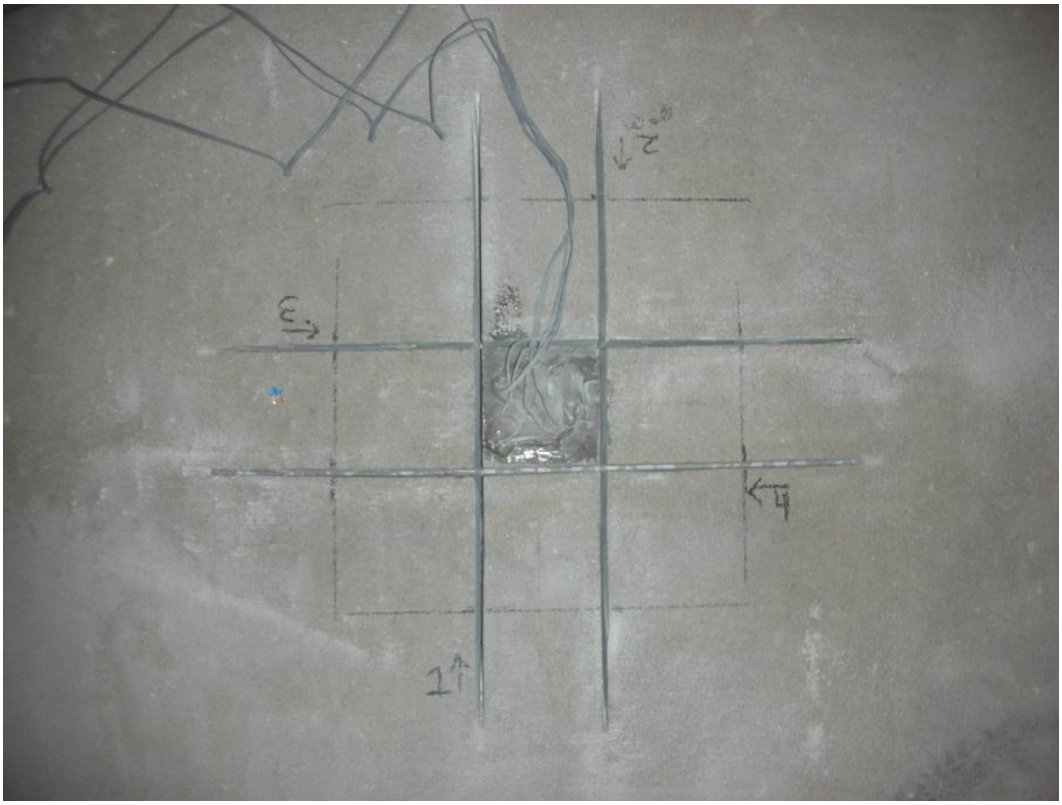

Figure 2.4 Four saw notches surrounding a rosette of 30mm strain gages cut to a depth of 1.0 inch

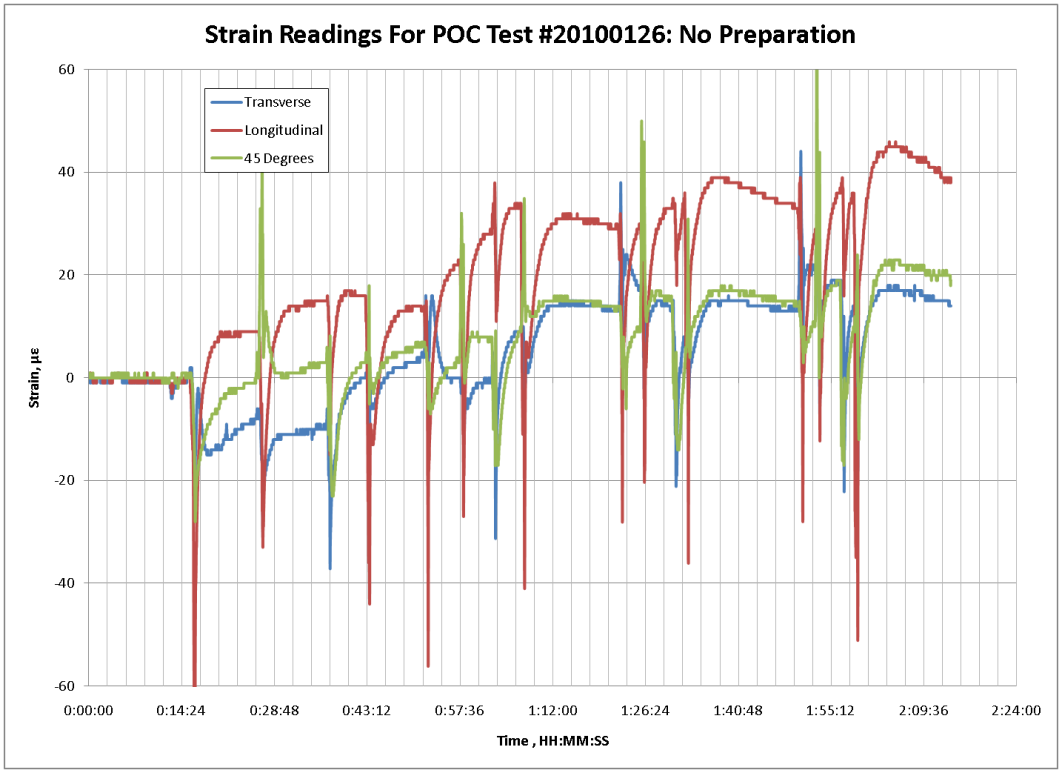

Figure 2.5 Strain readings as multiple sets progressive cuts are made around a rosette of 30mm strain gages for an unprepared concrete slab

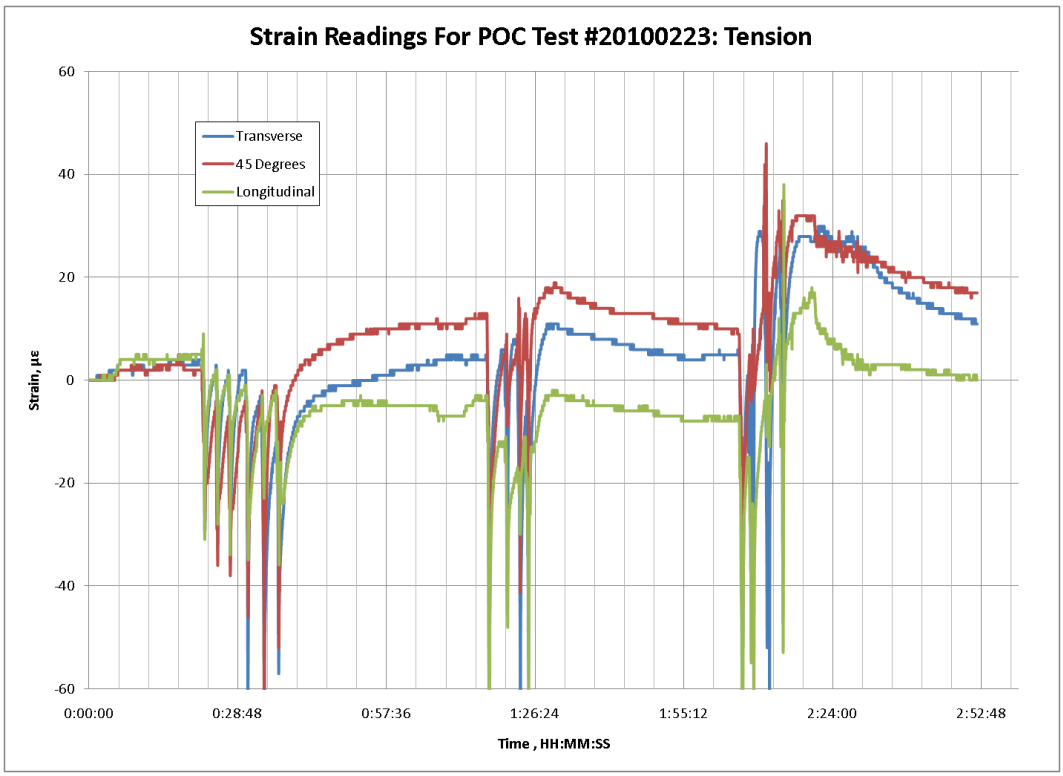

Figure 2.6 Strain readings as cuts of 0.5 in, 1.0 in, and 1.5 in are made around a strain rosette on a concrete slab whose top surface is in tension

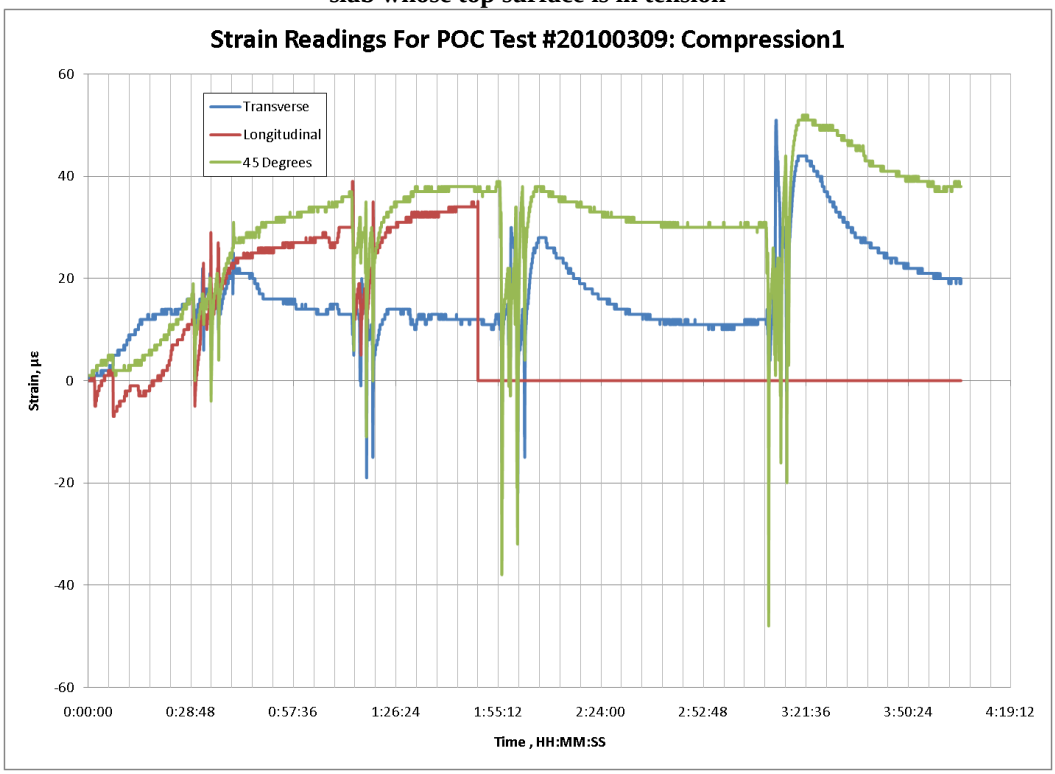

Figure 2.7 Strain readings as cuts of 0.25 in, 0.5 in, 1.0 in and 1.5 in are made around a strain rosette on a concrete slab whose top surface is in compression. The longitudinal strain gage is damaged approximately 2 hours into testing

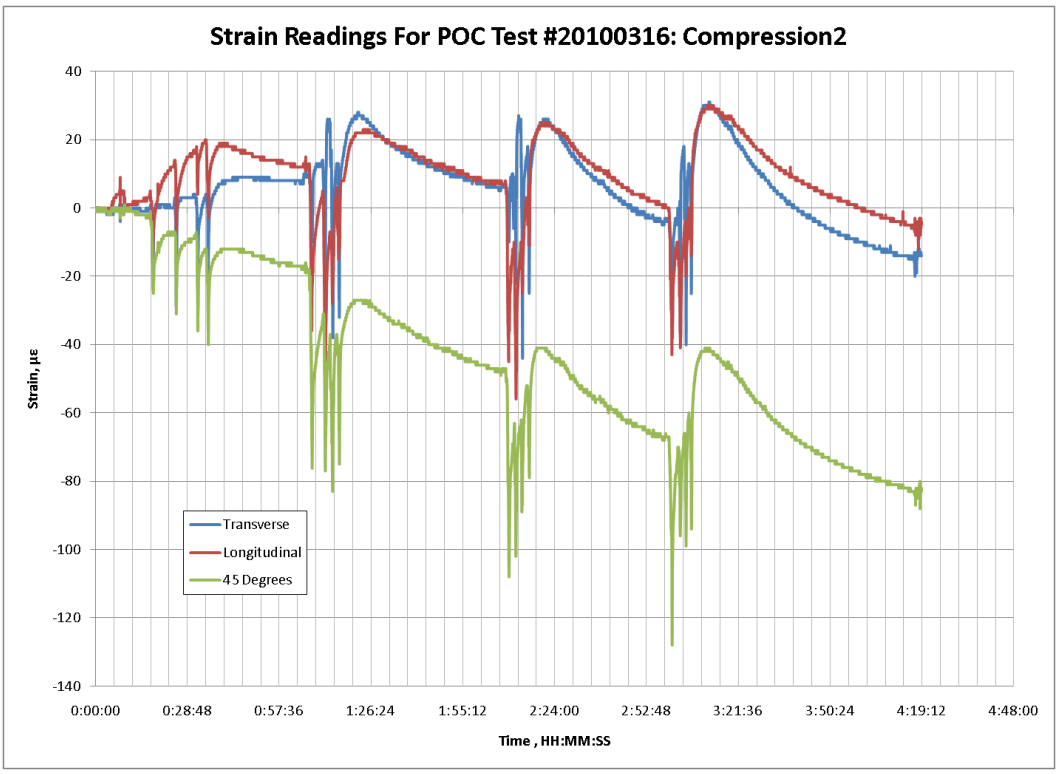

Figure 2.8 Strain readings as cuts of 0.25 in, 0.5 in, 1.0 in and 1.5 in are made around a strain rosette on a concrete slab whose top surface is in compression. Significant and questionable strain drifting occurs in the 45 degree strain gage

CHAPTER 3: RESIDUAL STRESS TESTING ON IN-SITU SLABS AT ATREL

3.1 Introduction

The discarded slabs which had been prepared and tested in bending had come from a road strip which was still atop the original soil on which it was cast at the ATREL facility. This road strip had been subjected to millions of ESALs in the span of weeks in a previous experiment (Cervantes and Roesler 2009). While this testing had been completed, a large traffic simulator named the Accelerated Transportation Loading Assembly (ATLAS) remained in place. Along the underside of ATLAS is a wheel carriage with an attachment for either a truck tire or jet airplane tire. These tires could subject the concrete pavement to thousands of pounds of load while it moved along the road strip's 100 foot length. The machine was designed to apply dynamic loads, but could potentially be used to induce static loads on an in-situ concrete slab.

The 12 foot width road strip was comprised of jointed plain concrete pavement which had areas of surface damage typified by cracking. Six slabs were identified for testing based on having little to no surface cracking. However, cracking within the material was not visible, nor was it investigated. However, choosing these slabs provided an opportunity to demonstrate the viability of the testing procedure on field testing. The concrete slabs measured 6 feet x 6 feet x 6 inches and had been saw notched soon after casting.

3.2 Procedure

The width of the road strip was 12 feet and was partitioned into two halves by a joint spaced 6 feet from either edge. Along the length of the road strip, joints were spaced regularly in 6 foot intervals. This resulted in concrete slabs measuring 6 feet by 6 feet. In order to simplify future FEM analysis, an industrial concrete saw cutter was used to wholly separate the concrete slabs from one another to prevent aggregate bridging. The saw cut was lowered along existing joints and used to cut through the full 6 inch depth of the slabs. Thus each slab was separated from its three adjoining slabs. The fourth edge of the slab was always a free edge and required no saw cutting.

As a result each slab had a symmetric orientation where one edge was along the midline of the road strip while its opposite edge was along the free end. In order to produce a symmetric stress field and reduce the complexity of the slab loading, a 12 inch x 12 inch steel plate was positioned along the interior edge adjacent to the midline. This 1 inch thick steel plate was placed so that it could distribute the applied wheel load across a single square-foot area.

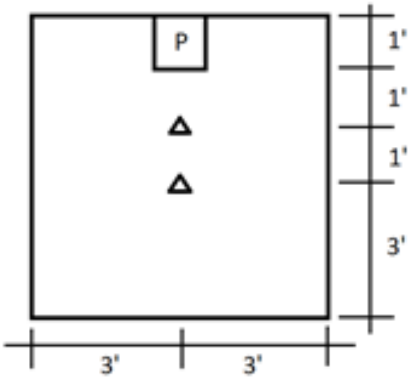

Figure 3.1 Plan view of 6 ft x 6 ft slab with square steel plate, P, and locations of affixed strain rosettes, triangles

Strain rosettes were placed in one of two locations: either 2 feet from the midline edge of the slab or 3 feet from the midline edge of the slab. The orientations of the strain gages were in the longitudinal, latitudinal and 45 degree directions. The symmetry of the loading presumed a saddle response in the slab upon loading – that is tensile bending in the longitudinal direction and compressive bending in the latitudinal direction.

The strain measurements were actively recorded throughout testing while wheel loads were applied and removed. A regiment was developed so that saw cutting could be performed safely in the vicinity of high wheel loads. The slab would be loaded, the load would be sustained and then the load would be removed. The strain magnitudes would be recorded during this initial loading for later calculation. After this loading sequence, four saw cuts would surround the strain rosette in a pre-determined geometry. The notch spacing of the saw cuts would be controlled and would be identical in both longitudinal and latitudinal directions. This action ensured that a squared area of material would always be isolated as opposed to other rectangular shapes. The depth of the four notches would vary in approximately 0.5 inch increments.

A circular saw fitted with a masonry blade was used to create the cuts in the material. The amount of saw blade exposed past the circular saw flush-guide was leveled to the surface of the concrete surface to be cut. Markings on the circular saw itself indicated approximate cutting depths, so the saw blade would be adjusted accordingly. However, a high precision measuring device – a caliper – was used to record the actual depth of the notch after the cut was made. The depths of the cuts were measured at three points along the length of each cut resulting in 12 overall measurements. These 12 measurements were averaged together to ascertain the average notch depth of the four cuts.

After a set of four cuts had been made and measured, sufficient time – approximately 40 to 60 minutes – was allowed to pass in order for the strain readings to stabilize. Upon stabilizing, the wheel load would be re-applied. Approximately 20 to 30 seconds elapsed before this wheel load was removed. This effort was performed in order to determine the diminished effect of the strains induced by an applied wheel load. A second set of cuts of approximately 0.5 inches deeper depth were made along the same grooves made with the initial cuts. This process would be repeated until approximately a depth of 1.5 to 2.0 inches. At this point, two observations were typical: firstly, the change in magnitude of the strain being relieved would approach zero; secondly, the inducement of strain from the applied load would become negligible.

ATLAS was initially used to apply the wheel load, but several problems became apparent immediately. Instead of gradual load application inducing elastic behavior in the concrete material, the wheel load would be applied rapidly inducing unexpected strain results. The unlikely strain readings from the strain rosettes, particularly those spaced 2 feet from the midline edge, were likely as a result of sudden compaction of the underlying aggregate base support and other phenomenon. Additionally, the electric motor of ATLAS introduced pulsing peaks in the strain data measurements. This electrical motor was used to maintain the position of the wheel carriage during static loading. Turning off this electric motor while the hydraulic pumps were used to apply the static load proved problematic as well, as the carriage would shift unexpectedly during testing leading to erroneous results.

As a consequence, the loading application was altered such that a 20 ton capacity bottlejack was situated between the steel plate and the wheel carriage. A 30 kip load cell was positioned between the bottlejack and the wheel carriage so that load magnitudes could be collected as the piston in the bottlejack was raised. The electrical motor and hydraulic pumps of the ATLAS device were turned off and no disruption to the data collection occurred thereafter.

After this sequence was fine-tuned, saw-cutting tests were performed on six concrete slabs. Three tests were conducted where the strain rosette was situated 2 feet from the midline edge while another three tests were conducted where the strain rosette was situated 3 feet from the midline edge. The sequencing of the saw cuts were varied between these tests so that a better understanding of the relieving strain could be developed.

3.3 Results for ATREL Slabs

There are several key points to be made for the data presented at the end of this chapter. Firstly, the magnitude of strains induced in the longitudinal and latitudinal directions are as expected: tensile in the longitudinal direction and compressive in the latitudinal direction. Additionally, the magnitudes of the induced strains are comparable given their distance from the applied load are similar. For the two tests where the strain rosettes were spaced 2 feet from the applied load, the longitudinal strains measured 34 με and 24 με while the transverse strains measured -52 με and -50 με. For the two tests where the strain rosettes were spaced 3 feet from the applied load, the longitudinal strains measured 16 με and 12 με while the transverse strains measured -20 με and -22 με. This suggests that while there is discrepancy in the amount of damage to each slab as a result of the accelerated traffic simulation, their underlying support and materials are comparable yielding comparable results.

Figures 3.6 through 3.10 at the end of this chapter also depict the diminishing response of the applied load on the strain rosettes as the notches are made deeper. Initial loading, when no saw cuts have been made, have a linear slope indicating that the measured data is in the elastic regime. The slope of this line approaches zero as the saw cuts are deepened. The direction of the decrease coincides with the initial stress state: positive, tensile strains induced in the longitudinal direction reduce to zero slope while negative, compressive strains induced in the latitudinal direction increase to zero slope. Near the end of their respective experiments, the slope of zero denotes a limited strain response due to an applied load and is indicative that the square area has been suitably isolated from its surrounding applied and material stresses.

It is also interesting to note the magnitude of the strain measurements. In the previous experiment set-up where beams were subjected to bending, the magnitude of the strain relaxation is approximately the same as in this case, regardless of the induced strains by the applied load. This suggests that the material inherently contains a constrained amount of stress that is relieved. The calculated residual stresses for an estimated Young's modulus of $4x10^6$ psi and Poisson's ratio of 0.15 of the six test cases are tabulated below:

Table 3.1 Results for six field tests performed at ATREL

Date	ID	Notch Spacing (in)	Notch Depth (in)	Notch D/S (in/in)	E-W Strain (με)	45° Strain (με)	N-S Strain (με)	Max Stress (psi)	Min Stress (psi)	Residual Stress (psi)
20100603	2N	3	1.0	0.34	48	56	45	252.3	185.4	252
20100607	2S	3	1.3	0.45	0	10	23	94.5	13.8	94
20100609	3S	3	1.2	0.39	21	8	20	140.0	53.0	140
20100610	4N	3	1.4	0.46	34	4	0	154.4	5.6	154
20100630	1N	4	1.9	0.47	17	22	13	95.9	45.3	96
20100714	5S	4	2.0	0.50	-24	-26	-13	-54.7	-119	-119

The calculated relieved stresses are largely in compression except for the concrete slab labeled 5S that, because of the negative sign in the direction of relieved stress, must have been in tension. However, it is interesting to note the similarity of the results, particularly of those tested within a week's time. While these slabs were tested in the summer with severe thunderstorms moving through the region, several days of drying denoted by the separation in testing dates is seemingly adequate to quantify the material stresses themselves and discard significant moisture gradations.

The results were obtained for each test by deepening the notches with saw cuts until the effect of the applied load was no longer appreciable. This usually coincided with the point at which the strain relieved due to material relaxation was unaffected by deepening cuts. A data collection error occurred with Slab 5S, however, and is evident in Figures 3.20 and 3.21. After the second sequence of cuts and subsequent stabilization, the data collector malfunctioned resulting in the loss of data. That is why there is a large gap where there would normally have been additional data. However, the magnitude of the stabilized strain reading at the end of this second iteration had been recorded in field notes. Thus, testing was able to continue where the new strain readings were corrected for their magnitude. This is evident in the graphs where the strain in the longitudinal direction started at -5 με, the strain the latitudinal direction started at -21 με and the strain in the 45 degree direction started at -14 με.

3.4 Figures and Graphs

Figure 3.2 View of slabs, ATLAS wheel carriage, bottlejack, tarp to shade from sunlight and miscellaneous testing equipment

Figure 3.3 Bottlejack using ATLAS wheel carriage as reaction frame, load cell and steel beam for flush surface

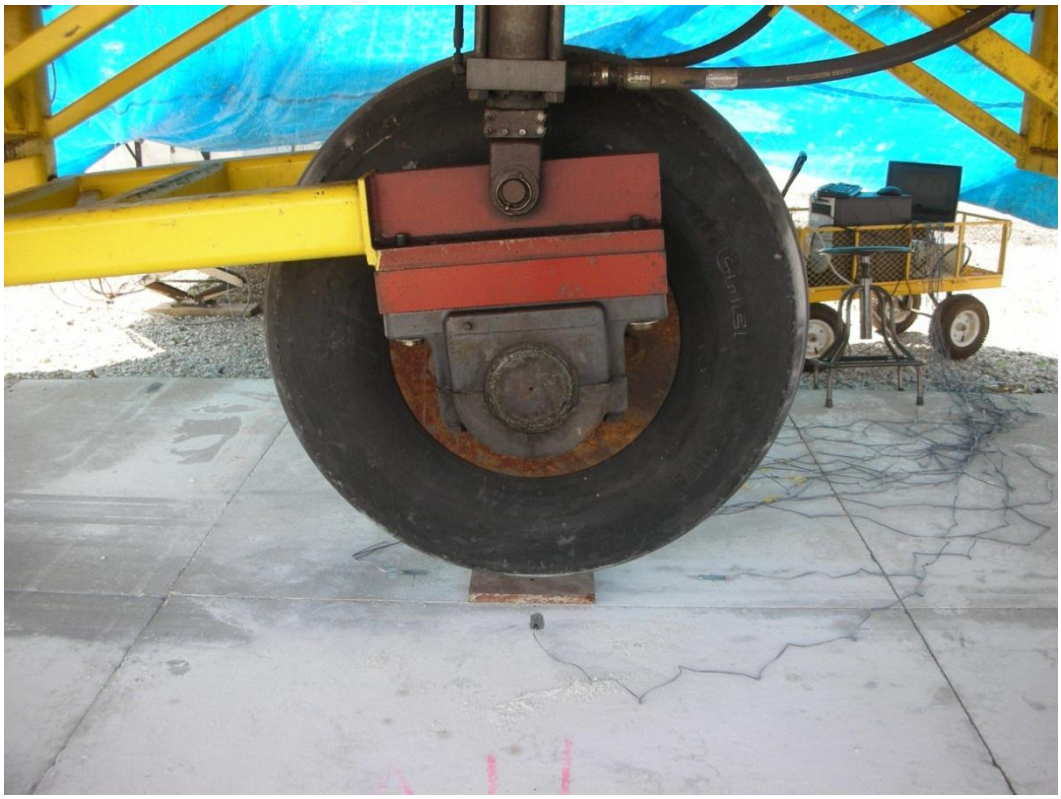

Figure 3.4 ATLAS tire used for static loading of in-situ pavement during initial configuration

Figure 3.5 Strain rosettes spaced either 2 feet or 3 feet from applied load

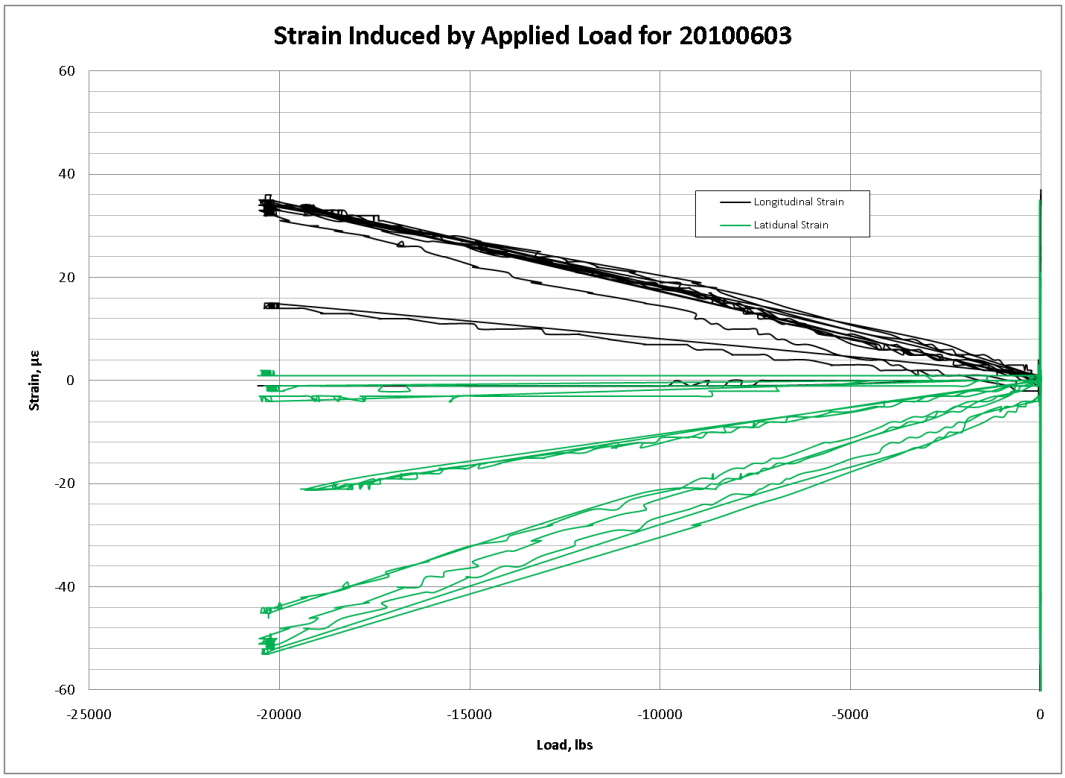

Figure 3.6 Slab 2N loaded and unloaded after various cutting sequences

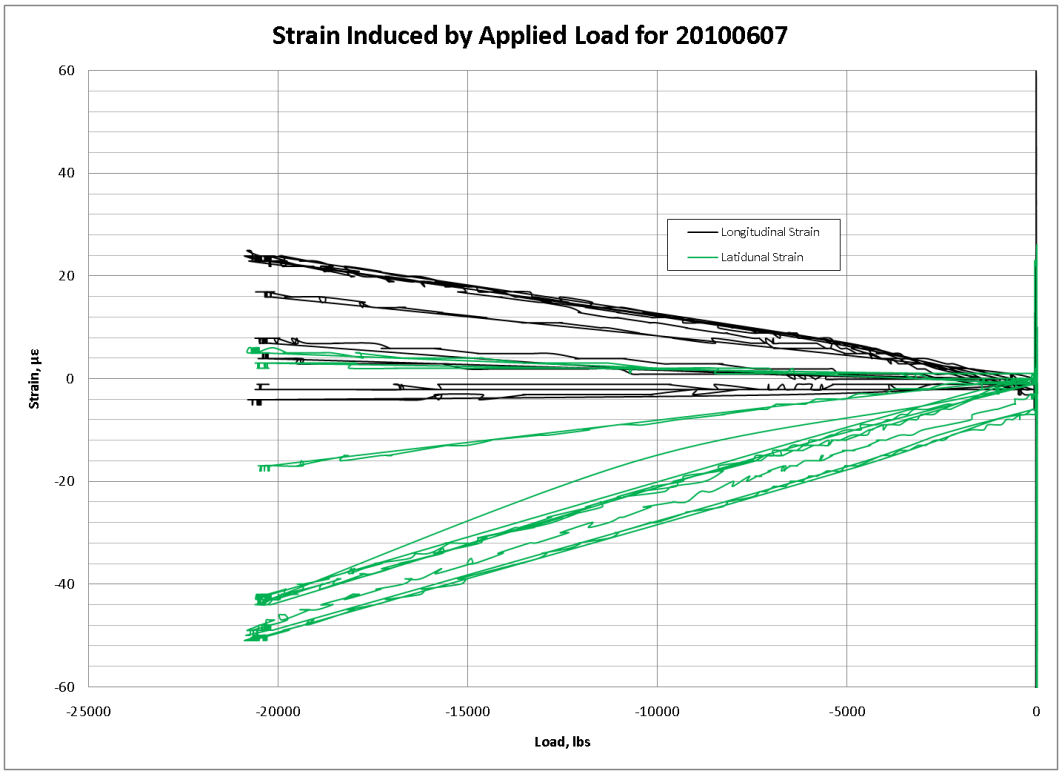

Figure 3.7 Slab 2S loaded and unloaded after various cutting sequences.

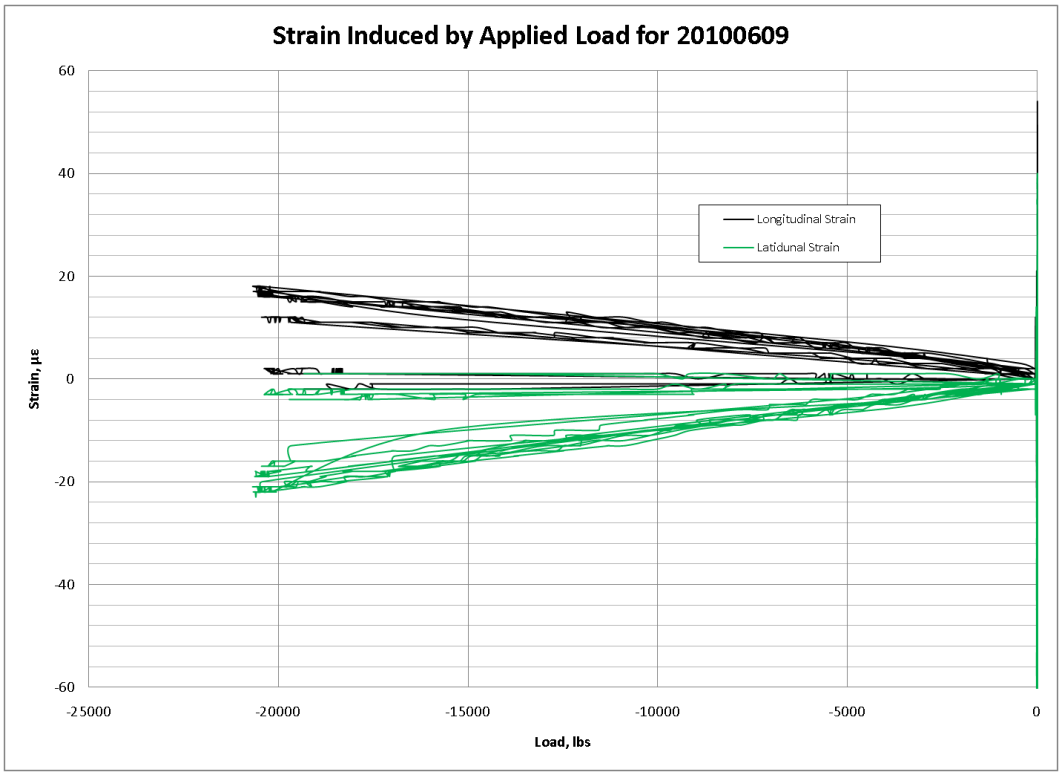

Figure 3.8 Slab 3S loaded and unloaded after various cutting sequences

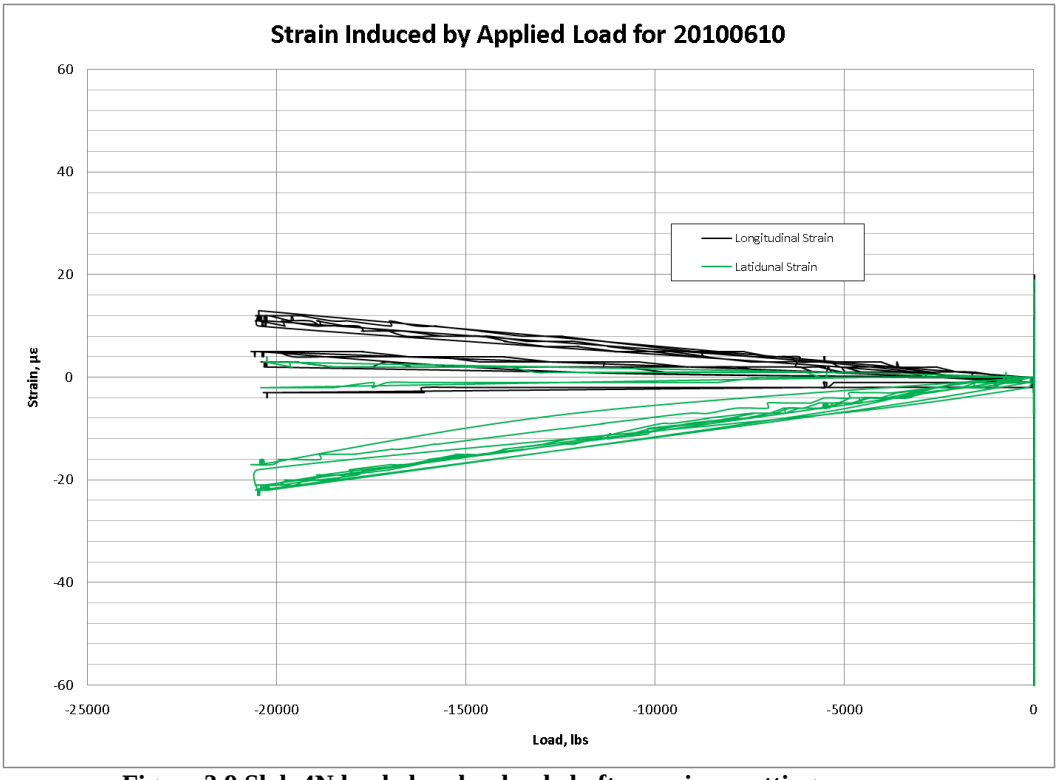

Figure 3.9 Slab 4N loaded and unloaded after various cutting sequences

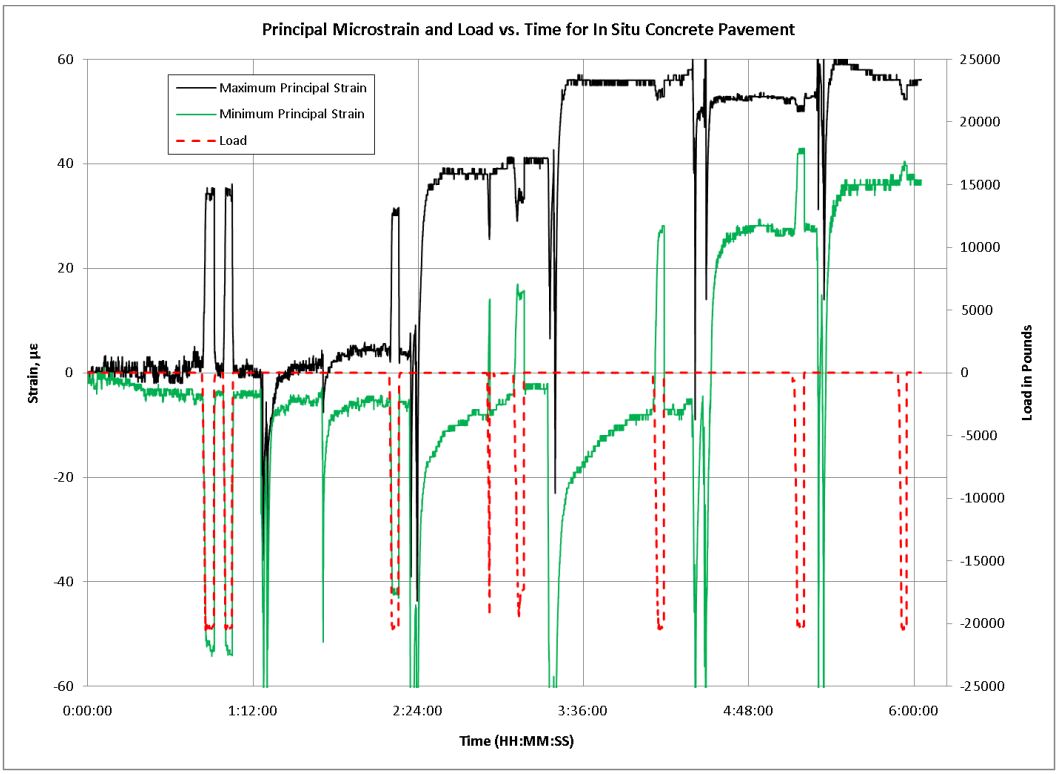

Figure 3.10 Principal strains for Slab 2N where the strain rosette is located 2 feet from applied load and isolated with notches spaced 3 inches apart

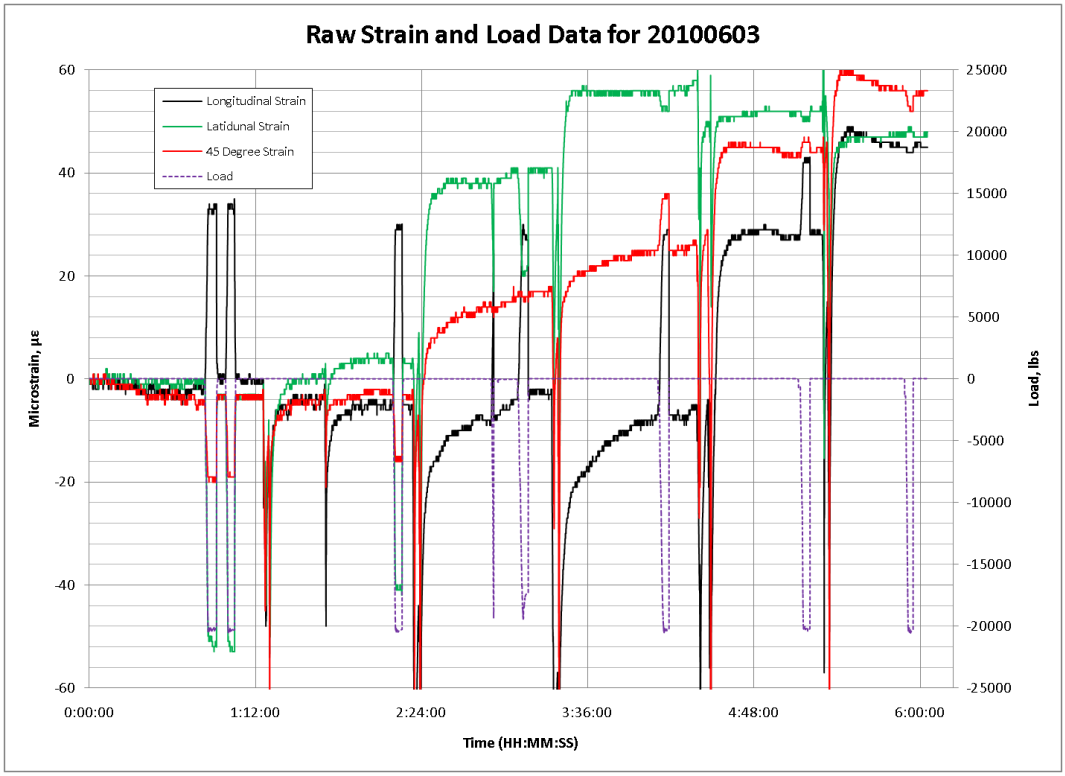

Figure 3.11 Strain and load data for Slab 2N where the strain rosette is spaced 2 feet from applied load and is isolated with notches spaced 3 inches apart

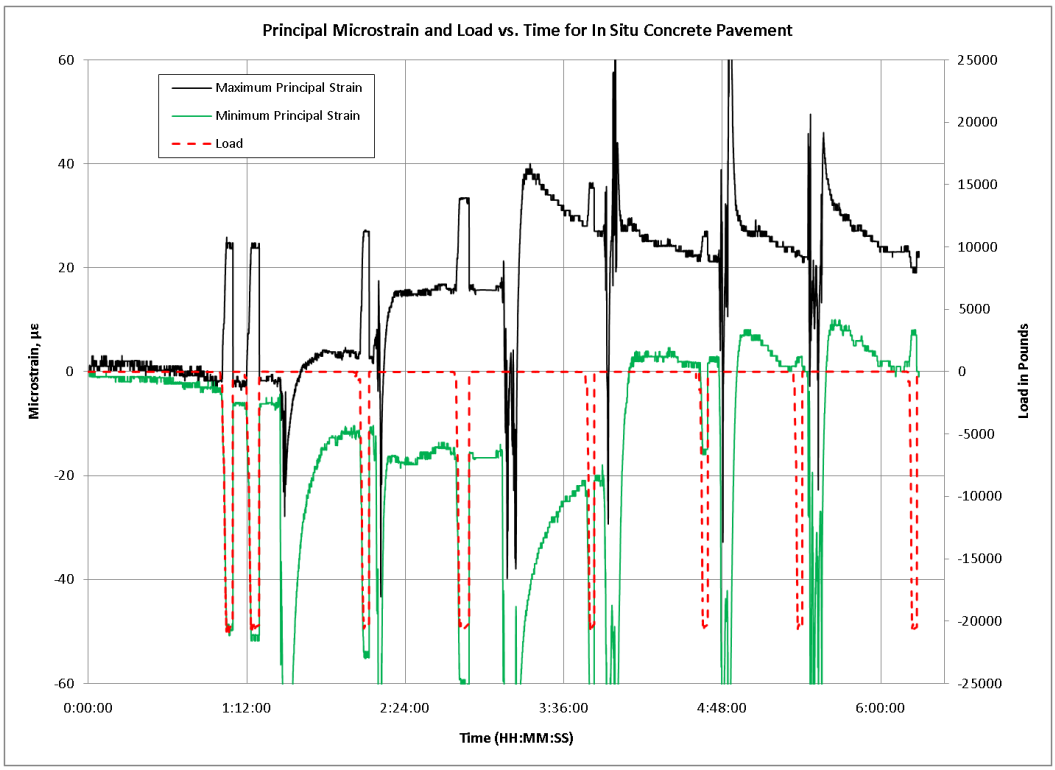

Figure 3.12 Principal strains for Slab 2S where the strain rosette is spaced 2 feet from an applied load and isolated with notches spaced 3 inches apart

Figure 3.13 Strain and load data for Slab 2S where the strain rosette is spaced 2 feet from applied load and isolated with notches spaced 3 inches apart

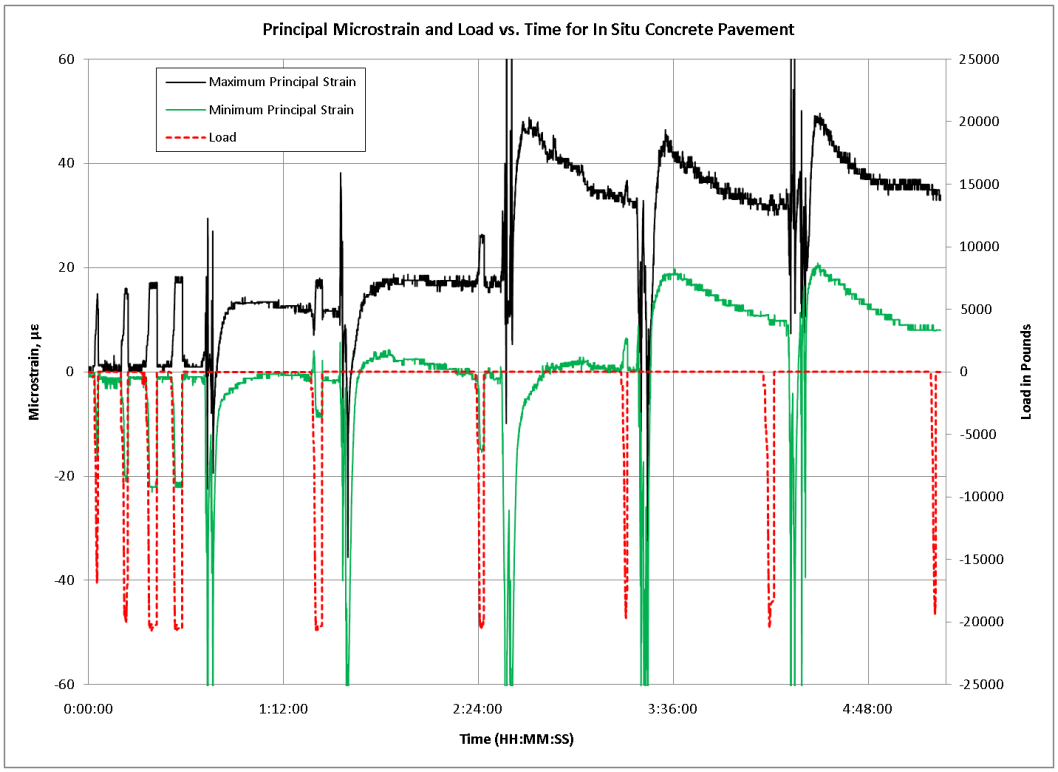

Figure 3.14 Principal strains for Slab 3S where the rosette is spaced 3 feet from an applied load and isolated with notches spaced 3 inches apart

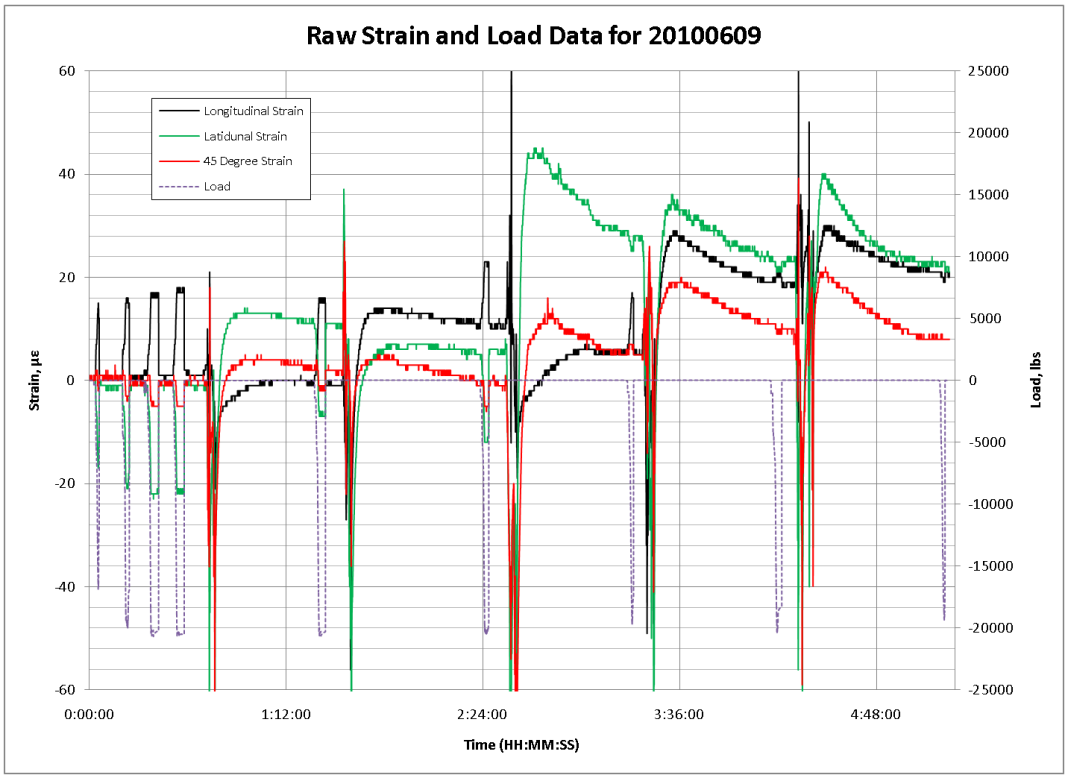

Figure 3.15 Strain and load data for Slab 3S where the strain rosette is spaced 3 feet from applied load and isolated with notches spaced 3 inches apart

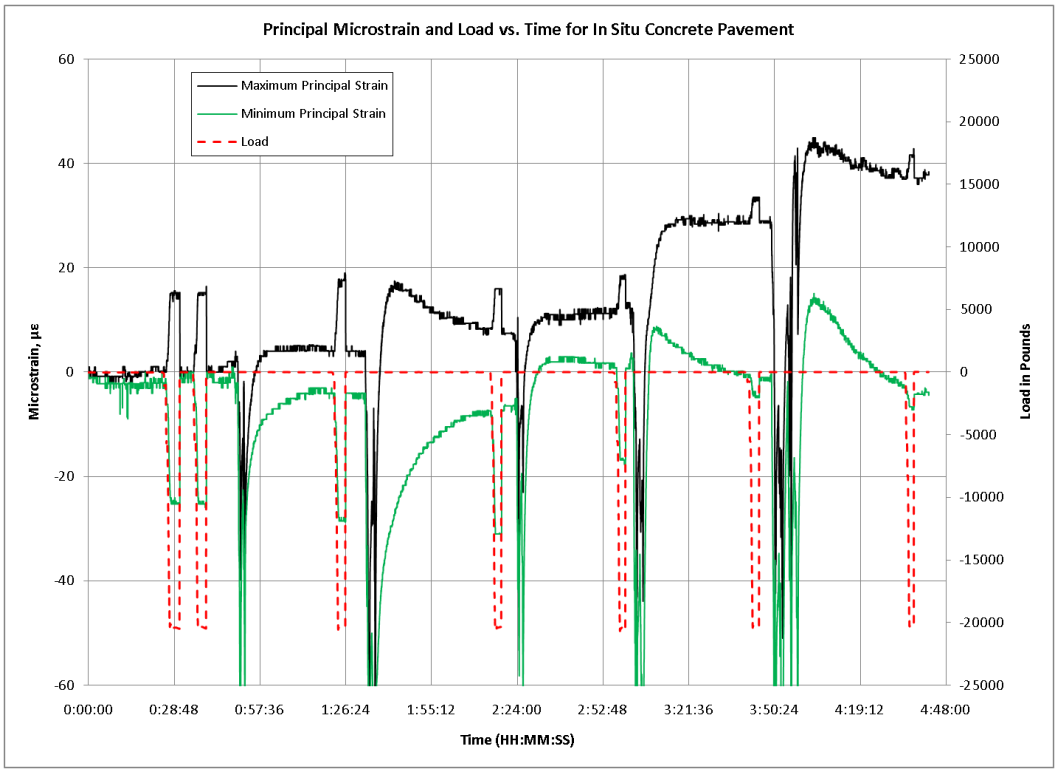

Figure 3.16 Principal strains for Slab 4N where the rosette is spaced 3 feet from an applied load and isolated with notches spaced 3 inches apart

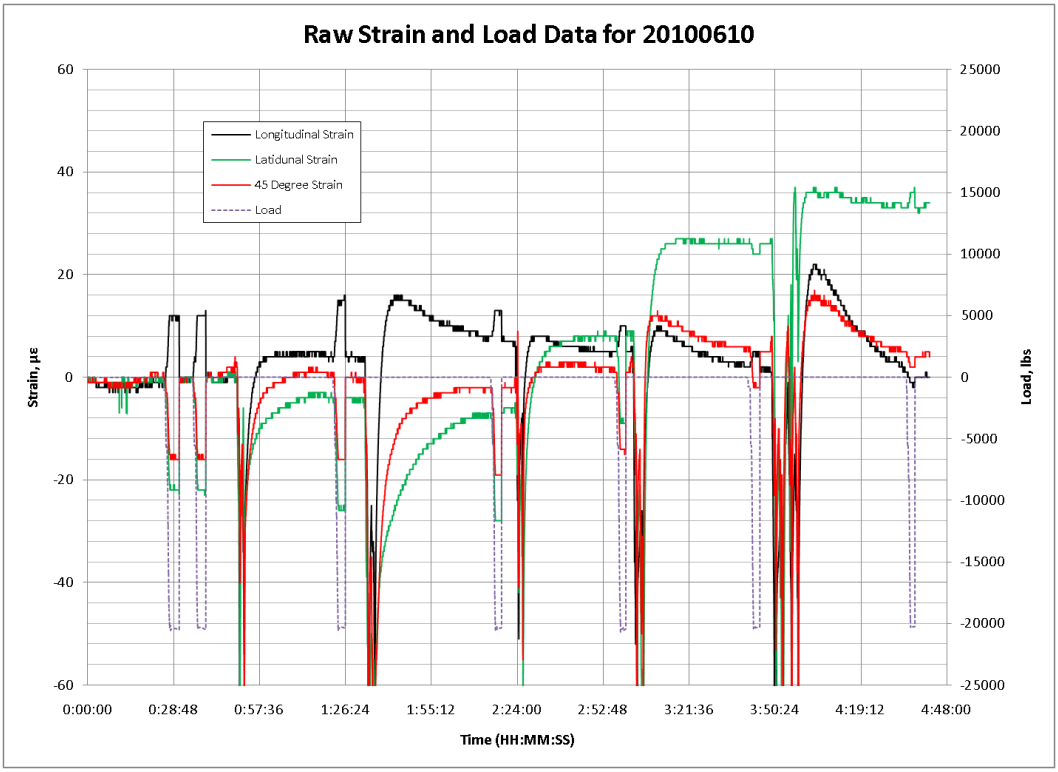

Figure 3.17 Strain and load data for Slab 4N where the strain rosette is spaced 3 feet from applied load and isolated with notches spaced 3 inches apart

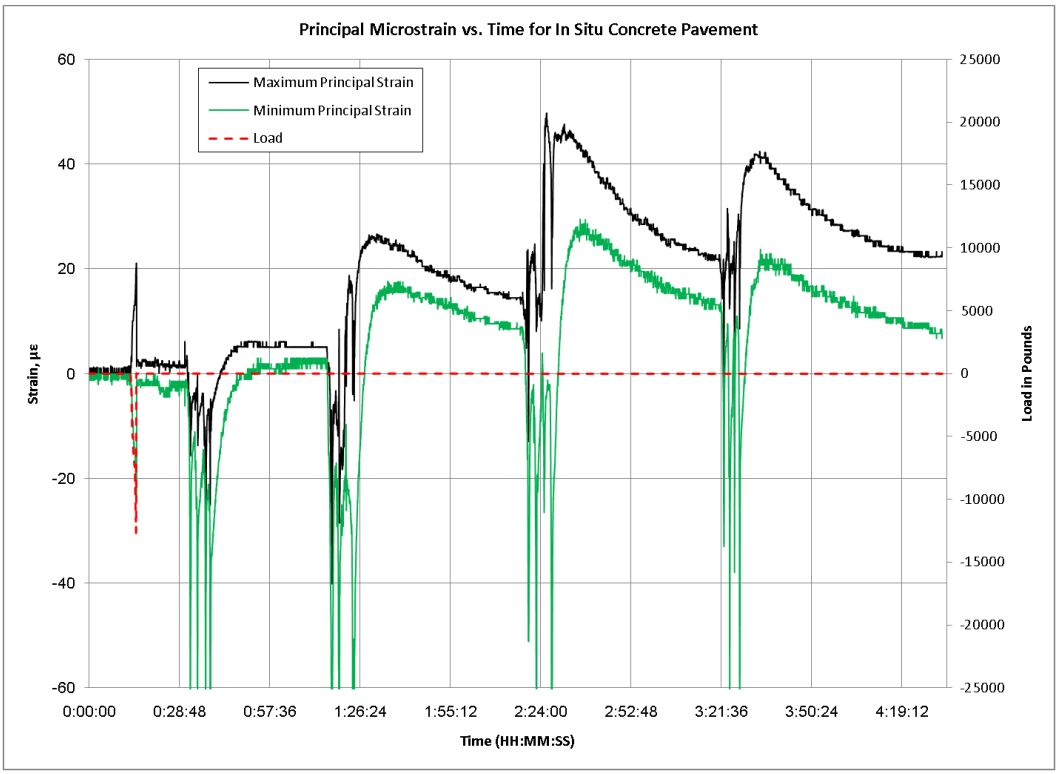

Figure 3.18 Principal strains for Slab 1N where the strain rosette is spaced 2 feet from an applied load and isolated with notches spaced 4 inches apart

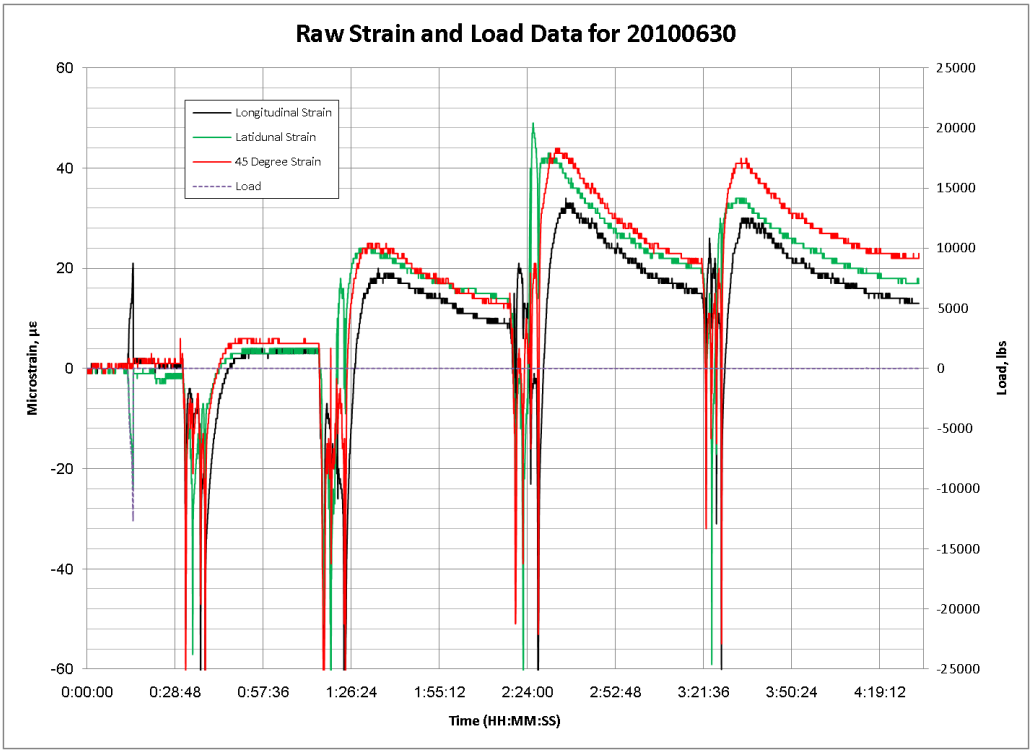

Figure 3.19 Strain and load data for Slab 1N where the strain rosette is spaced 2 feet from applied load and isolated with notches spaced 4 inches apart

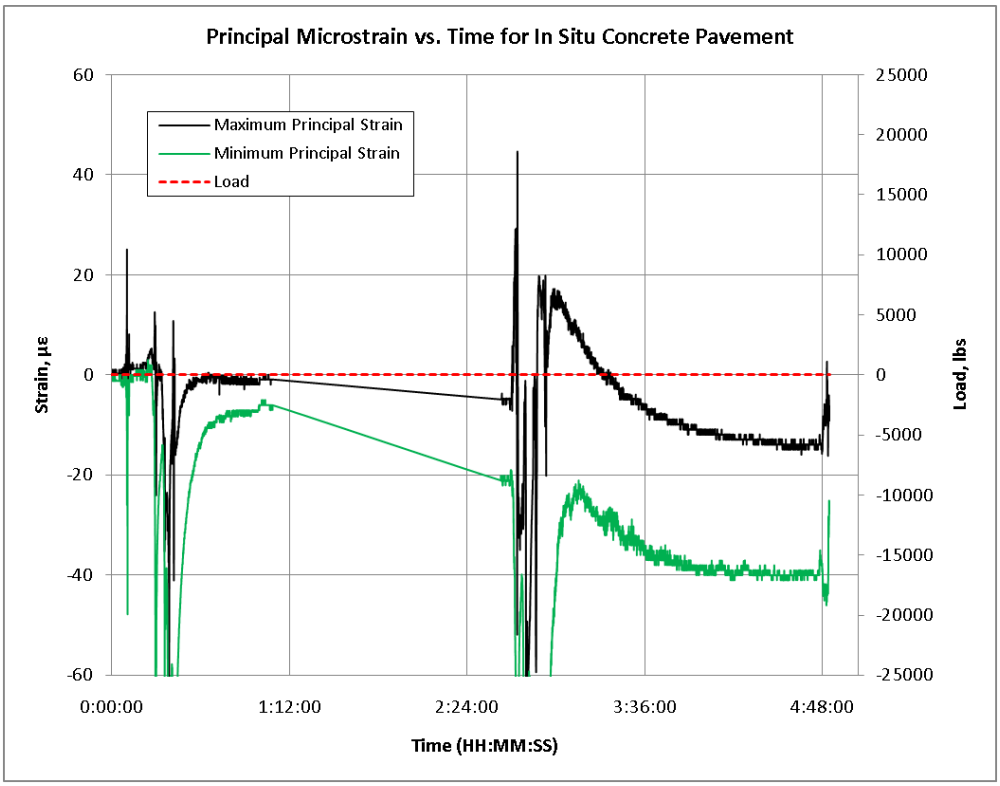

Figure 3.20 Principal strains for Slab 5S where the strain rosette is spaced 3 feet from an applied load and isolated with notches spaced 4 inches apart

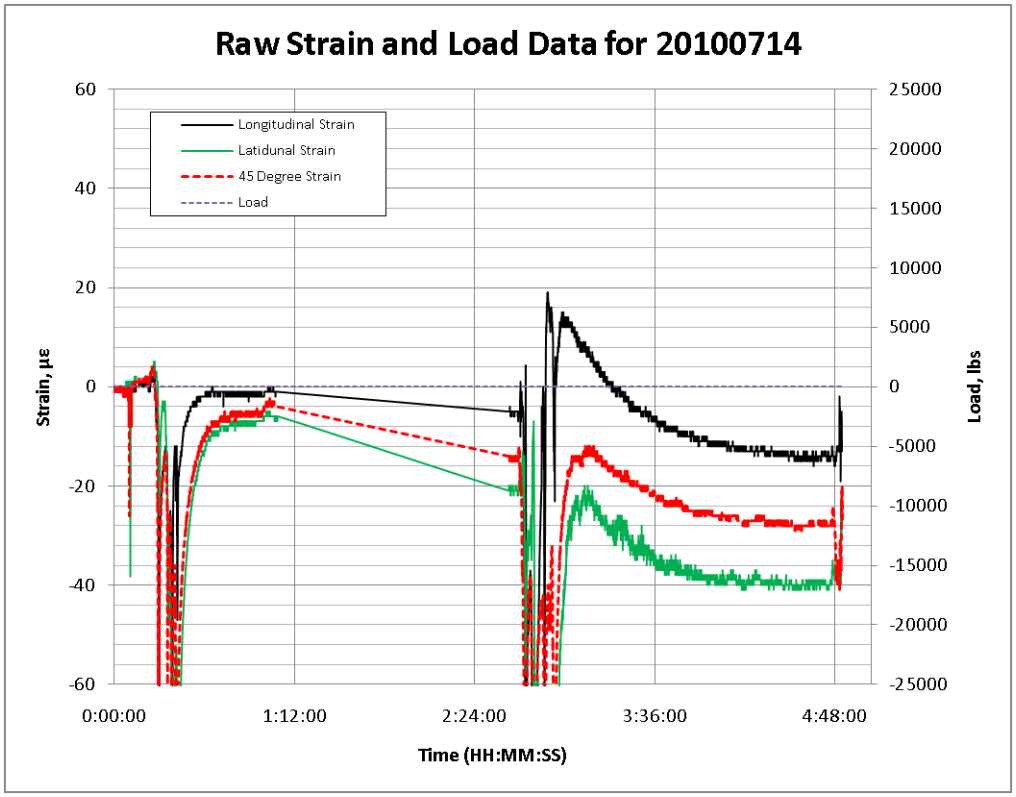

Figure 3.21 Strain and load data for Slab 5S where the strain rosette is spaced 3 feet from applied load and isolated with notches spaced 4 inches apart

CHAPTER 4: RESIDUAL STRESS TESTING ON NAPTF SLAB

4.1 Introduction

In addition to the availability of concrete slabs at ATREL, a 15 foot x 15 foot x 12 inch concrete slab cast at the FAA's NAPTF was available for residual stress testing. This slab was situated in an enclosed environment where live wheel loads could be readily applied. The slab sits atop a granular base with an approximate stiffness value of 30,000 psi. Testing was conducted where the relieved strain for a single notch depth-to-spacing ratio of 0.40 was maintained. This ratio had been determined by previous experimental observation that the majority of residual stresses could be identified at this geometric ratio.

Strain rosettes were affixed at six locations atop the surface of a plain concrete pavement located within the NAPTF on August 17th, 2010. The location of the six rosettes provided a testing matrix which included two midline responses from two center-edge loads, a center-edge response from a corner-edge load, a midline response from a corner-edge load and two in-situ responses.

4.2 Procedure

The preparation of the surface and application of the strain rosettes was the same across all strain rosettes. A center-mark was drawn at six locations and a 2x2 inch square area centered about that center-mark was drawn. Efflorescence and other surface debris were removed by hand by using medium-coarse sandpaper (grit 60) and sanding the area contained within the 2x2 inch square. Moist cotton was used to absorb fine dust and other particulates from the smoothed surface. This was followed by the application of acid and base solutions to neutralize the surface of the concrete per the epoxy manufacturer's recommendation. The moisture from the water, acid and base solutions was allowed to dry before a layer of epoxy was applied to the 2x2 inch square. This first layer of epoxy was thinned with the edge of a zip-tie and its primary purpose was to fill in divots and other small cavities along the surface of the concrete. After initially curing, a second layer of epoxy was applied whose purpose was to create as smooth and even a surface as possible for the application of strain foil gages. This second epoxy layer was treated with acid and base solutions to additionally neutralize the epoxy surface.

Surface strain gages 30 millimeters in length (1.18 inches) were prepared by separating the sheathing holding the two individual lead wires together in order to allow for flexible mobility later during testing. The gages were placed along a smooth, glass surface where a

cellophane tape was affixed along the backing and the gage lifted back. A two-chemical activated glue solution was applied to the exposed underside of the strain gage. This cellophane tape backed strain gage was removed from the glass surface and affixed to the prepared epoxy surface. The rectangular dimensions of the strain gages were contained wholly within the 2x2 inch squared area and overlap of gages (and lead-wires) was prevented. The gage was held in place with three fingers pressing down until the activated glue solution had adequately hardened. The cellophane tape was then carefully removed leaving the gage firmly affixed to the epoxy surface. This process was repeated 18 times as to produce six strain rosettes each containing a reference strain gage, a gage perpendicular to the reference strain gage and a gage at 45 degrees from the reference gage counter-clockwise to the reference strain gage. The orientation of the strain rosettes were all the same such that all reference strain gages were aligned in the East-West direction, all perpendicular gages were aligned in the North-South direction and all gages set at 45 degrees were oriented in the Northeast-Southwest direction.

The lead wires of the gages were aligned so that they split and double-backed towards either side of the strain gage. This was done so that the distance between the lead wires and the passing saw cut would be sufficient in ensuring no damage the strain gage during testing. To further protect these exposed lead wires and gages, an abundant layer of polyurethane was added atop the rosette. The six arrangements of epoxy-prepared and polyurethane-protected strain rosettes were allowed to cure overnight.

4.3 Results for Unloaded Tests

Test A1 comprised the testing of a rosette spaced 10 feet eastward and 5 feet southward from the Northwest corner of the slab. The spacing of the notches to be cut was 3 inches resulting in a 3x3 inch squared area centered about the previously drawn center-mark for the 2x2 inch square. At this designed notch-spacing, the designed notch-depth to isolate the strain rosette from stresses was estimated at 1.2 inches.

Alternatively, Test A2 comprised the testing of a rosette spaced 10 feet eastward and 10 feet southward from the same Northwest corner of the slab. The spacing of the notches was 4 inches which would result in a 4x4 inch squared area. This, too, was centered about the previously drawn center-mark for the 2x2 inch square. At a spacing of 4 inches, the approximate design depth in order to isolate the strain rosette from stresses was estimated at 1.6 inches.

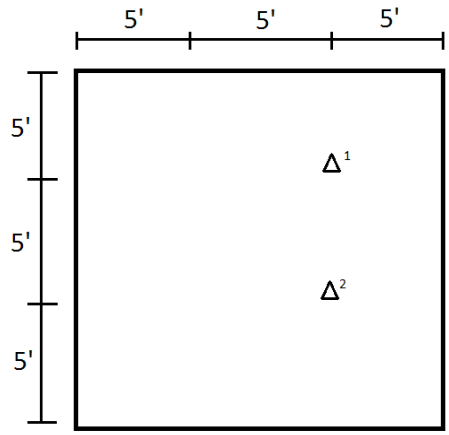

Figure 4.1 Location of Strain Rosettes A1 and A2

Strain rosette A1 was isolated with notch depths averaging 1.3 inches. This resulted in an actual notch depth-to-spacing ratio of 0.42. The final strain readings and measured surface temperatures were:

Table 4.1 Initial and Final Strain Readings for Test A1

	E-W Strain (με)	45° Strain (με)	N-S Strain (με)	Temp (°F)
Initial	0	0	0	77.5
Final	-19	-14	-20	78

For an estimated E-Modulus of 5,000 ksi and Poisson's ratio of 0.15, the approximate measured total stress is 140 psi in tension. The direction of this stress is 43 degrees counter-clockwise from the reference gage.

Strain rosette A2 was surrounded with notches which measured an average depth of 1.4 inches . This resulted in an actual notch depth-to-spacing ratio of 0.35. The final strain readings and measured surface temperatures were:

Table 4.2 Initial and Final Strain Readings for Test A2

	E-W Strain (με)	45° Strain (με)	N-S Strain (με)	Temp (°F)
Initial	0	0	0	77
Final	-195	-155	-59	81

For an estimated E-Modulus of 5,000 ksi and Poisson's ratio of 0.15, the approximate measured in-situ stress is 1,070 psi in tension. The direction of this stress is 12 degrees counter-clockwise from the reference gage.

The magnitudes of the measured stresses between tests A1 and A2 vary approximately tenfold, and there is some cause for concern for the validity of test A2. The diamond saw blade suffered over-heating during the testing of A2 while the saw teeth showed visible signs of cracking. This slowed the rate of cutting and subsequently increased the amount of heat generated in this test. Measured temperature readings upwards of 200^{o}F were observed along the surface of the concrete in the vicinity of the notching. The operating temperature of the strain gages used range from -4^{o}F to 140^{o}F. As a result of this excessive heating in the concrete, the strain gages themselves likely over-heated leading to erroneous strain measurements.

Additionally, Figure 4.16 shows the raw strain data collected for Test A2. This reveals that after saw cutting, the strain measurements did not stabilize to expected values for this type of test. Personnel at the NAPTF noted that this value of tensile strain and calculated stress in the concrete exceeds the modulus of rupture meaning that cracks would have materialized before testing had begun. Cracking was not visible suggesting that this was not the case, further suggesting that test A2 is erroneous. The test was concluded when the strain readings had stabilized while the temperature had not fully returned to its original magnitude.

While the calculated stress of 1,070 psi at A2 is questionable due to the excess time and heat generated during testing, there are some noteworthy observations worth highlighting. Firstly, the calculated stress state of Test D1 is 660 psi. The distance separating test A2 and D1 is no more than 2.5 feet. This suggests that there is a region in the concrete pavement which may have higher localized stresses than other areas. Additionally, a stress of 730 psi was calculated at the location of Test B2 suggesting that these high magnitudes of stresses can possibly and validly exist in the concrete.

It should also be noted that the diamond-edge saw blade used was new and was not expected to suffer the damage it did during testing of A2. The saw blade had successfully notched 1.2 inches in the testing of A1, however could not successfully notch the 0.8 inch incremental cut performed at A2. Both technicians conducting the test, Castaneda and Gonzales, took turns operating the circular saw and noted that the concrete was “harder” than material that has been worked with before. This notion was later supported in that high-strength quartzite aggregates had in fact been used in the concrete mix. Lastly, the range of strains measured across the pavement surface suggests that there can be a gradient of built-in stresses existing in the

material. Localized areas of high and low stiffness caused by varying vibratory/compaction techniques may exist.

4.4 Results for Corner-Edge Loaded Tests

Test B1 comprised the testing of a rosette spaced 7.5 feet eastward and 2 inches southward from the Northwest corner of the slab. The spacing of the notches to be cut was 4 inches resulting in a 4x4 inch squared area centered about the previously drawn center-mark for the 2x2 inch square. The location of this strain rosette used the North free edge of the slab necessitating only three notches. At this designed notch-spacing, the designed notch-depth to isolate the strain rosette from stresses was estimated at 1.6 inches.

Test B2 comprised the testing of a rosette spaced 5 feet eastward and 33 inches southward from the Northwest corner of the slab. The spacing of the notches to be cut was 3 inches resulting in a 3x3 inch squared area centered about the previously drawn center-mark for the 2x2 inch square. At this designed notch-spacing, the designed notch-depth to isolate the strain rosette from stresses was estimated at 1.2 inches.

In both test scenarios, a load was designed to be placed along the West edge of the slab and loaded in increments before and after testing. The 52 inch diameter Michelin tires were positioned such that the center of the northern tire was 21.5 inches eastward while displaced 12 inches southward. The southern tire was similarly positioned 21.5 inches eastward and 66 inches southward. When loaded, the tires remained entirely upon the top surface of the slab and did not contour around the slab edges.

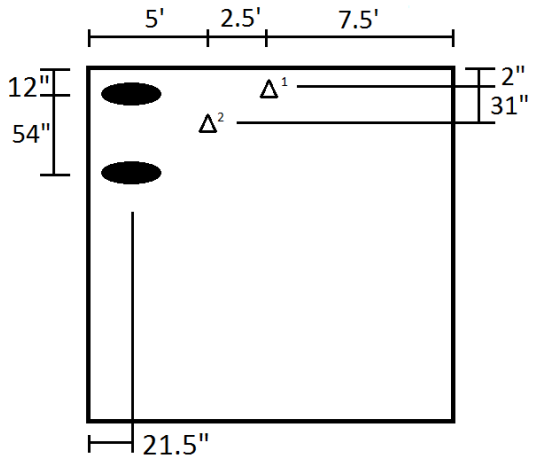

Figure 4.2 Location of Strain Rosettes B1, B2 and Wheel Loads

Strain rosette B1 was isolated with notches of an average depth of 1.6 inches resulting in a notch depth-to-spacing ratio of 0.41. The final strain readings and surface temperatures were:

Table 4.3 Initial and Final Strain Readings for Test B1

	E-W Strain (με)	45° Strain (με)	N-S Strain (με)	Temp (°F)
Initial	0	0	0	78
Final	-139	-93	10	77.5

For an estimated E-Modulus of 5,000 ksi and Poisson's ratio of 0.15, the approximate measured in-situ stress is 730 psi in tension. The direction of this stress is 10 degrees counter-clockwise from the reference line.

Test B1 was the first location to be loaded before and after testing to ascertain the strain response due to incremented loads. This effort was performed in order to determine whether the stresses due to an applied load had been isolated sufficiently and whether the response varies linearly or elsewise. The total load applied was incremented from 10 kips to 20 kips, 40 kips, 60 kips, 80 kips, 60 kips, 40 kips, 20 kips and lastly 10 kips. This was performed in a stepwise function and the magnitude of the strain responses compared before and after.

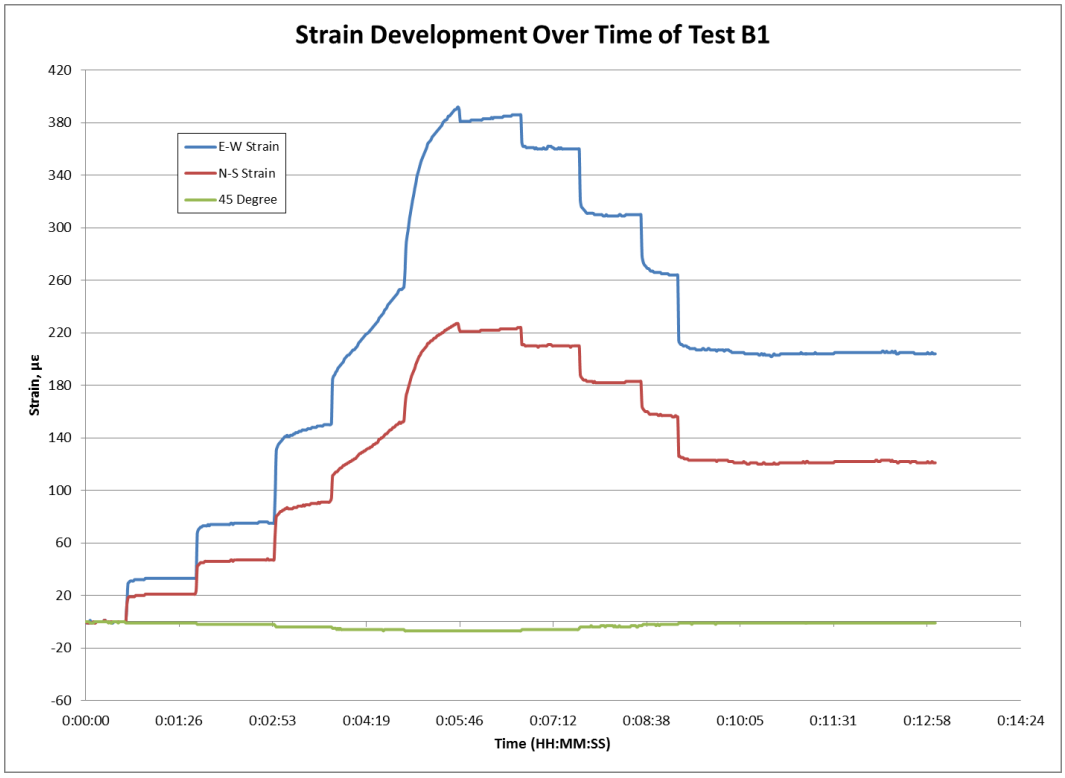

Figure 4.3 Strain Response of B1 Due to Applied Load Before Notches

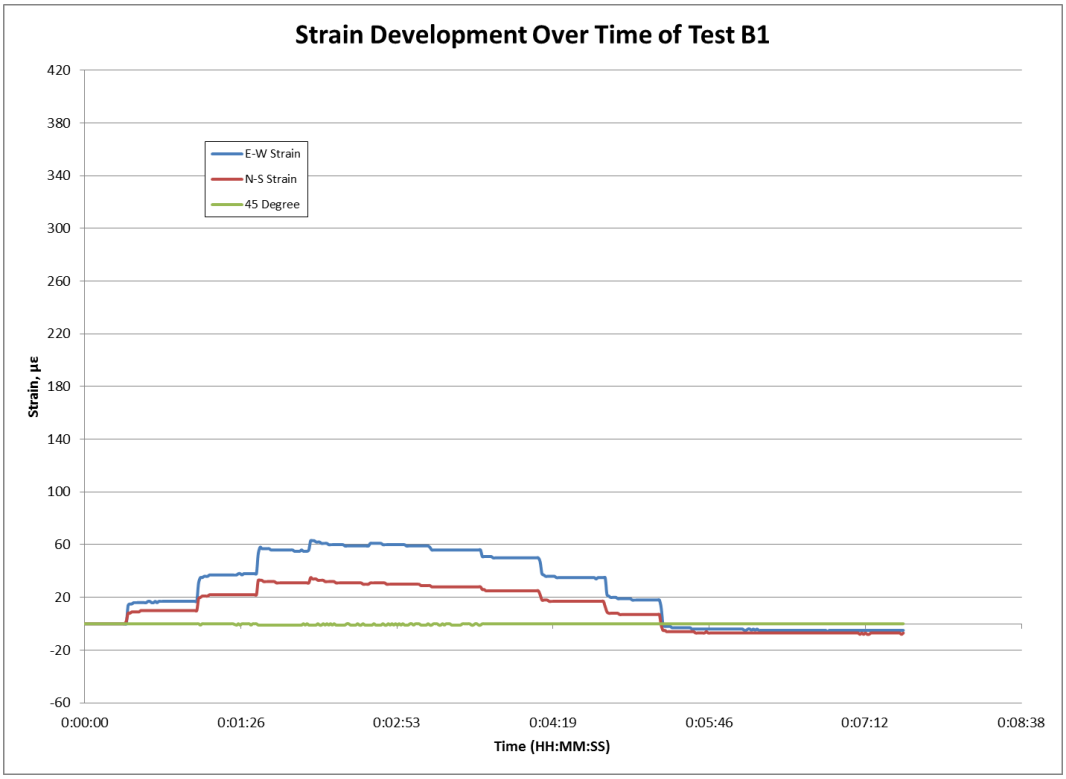

Figure 4.4 Strain Response of B1 Due to Applied Load After Notches

Table 4.4 Percent Change of Diminished Strain Response of B1 Before and After Notches

Test B1	% Change		
Load (kips)	E-W Strain (με)	45° Strain (με)	N-S Strain (με)
0	0%	0%	0%
10	52%	48%	0%
20	50%	48%	50%
40	38%	34%	25%
60	n/a	n/a	n/a
80	n/a	n/a	n/a
60	15%	14%	14%
40	14%	12%	0%
20	12%	9%	0%
10	8%	5%	0%
0	1%	5%	0%

Table 4.5 Revised Percent Change of Diminished Strain Response of B1 Before and After Notches

Test B1	% Change		
Load (kips)	E-W Strain (με)	45° Strain (με)	N-S Strain (με)
0	0%	0%	0%
10	52%	48%	0%
20	50%	48%	50%
40	38%	34%	25%
60	n/a	n/a	n/a
80	n/a	n/a	n/a
60	33%	35%	17%
40	34%	29%	0%
20	36%	29%	0%
10	36%	24%	0%
0	0%	0%	0%

The initial loading sequence was unstable largely due to the fact that slab had not been previously loaded since its construction. Settling of the base along with other seating phenomenon likely occurred when this slab was loaded upwards of 80 kips. This makes comparison of the loading sequences before and after saw notching beyond the first load of 20 kips difficult as the strain value is not stabilized. The strain magnitudes particularly drift at loads of 40, 60 and 80 kips. However, the latter portion of the initial load where the load is incrementally lessened can be compared since its values are stable and presumably symmetric with the initial loading sequence. The magnitude change in this latter portion was used to revise the percent change of the three strain directions. The strain values of the latter portion are used as the point of comparison for the loading sequence after the notches are made. Doing so results in Table 4.5 where it appears that the strain response is limited to approximately one third of its original magnitude for a notch depth-to-spacing ratio of 0.40 along the edge of the slab.

4.5 Results for Center-Edge Loaded Tests

Test C1 comprised the testing of a rosette spaced 5 feet eastward and 7.5 feet southward from the Northwest corner of the slab. The spacing of the notches to be cut was 4 inches resulting in a 4x4 inch squared area centered about the previously drawn center-mark for the 2x2 inch square. At this designed notch-spacing, the designed notch-depth to isolate the strain rosette from stresses was estimated at 1.6 inches.

Test D1 comprised the testing of a rosette spaced 10 feet eastward and 7.5 feet southward from the Northwest corner of the slab. The spacing of the notches to be cut was 3 inches resulting in a 3x3 inch squared area centered about the previously drawn center-mark for the 2x2 inch square. At this designed notch-spacing, the designed notch-depth to isolate the strain rosette from stresses was estimated at 1.2 inches.

Both locations were contrived in order to place a load along both the West and East edges of the slab and produce strain responses that, by symmetry, should be similar in magnitude. The 52 inch diameter tires were positioned such that the center of the northern tire was positioned 21.5 inches eastward and 63 inches southward while the southern tire was positioned 21.5 inches eastward and 117 inches southward. When loaded, the tires remained entirely upon the top surface of the slab and did not wrap around the slab edges.

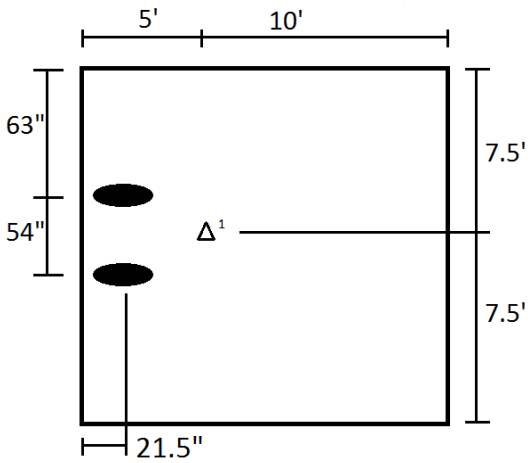

Figure 4.5 Location of C1 and Wheel Loads

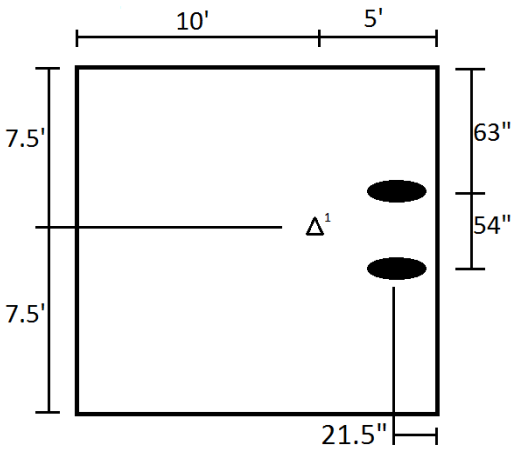

Figure 4.6 Location of D1 and Wheel Loads

Strain rosette C1 was notched to an average depth of 1.7 inches resulting in a notch depth-to-spacing ratio of 0.41. The final strain readings and surface temperatures were:

Table 4.6 Initial and Final Strain Readings for Test C1

	E-W Strain (με)	45° Strain (με)	N-S Strain (με)	Temp (°F)
Initial	0	0	0	77.5
Final	-28	-35	-23	78

For an estimated E-Modulus of 5,000 ksi and Poisson's ratio of 0.15, the approximate measured in-situ stress is 190 psi in tension. The direction of this stress is 37 degrees counter-clockwise from the reference line.

Strain rosette D1 was notched to an average depth of 1.2 inches resulting in a notch depth-to-spacing ratio of 0.41. The final strain readings and temperatures were:

Table 4.7 Initial and Final Strain Readings for Test D1

	E-W Strain (με)	45° Strain (με)	N-S Strain (με)	Temp (°F)
Initial	0	0	0	78
Final	-111	-16	-14	80*

*Temperature does not coincide with final strain measurements. Instead, it is the last measured temperature observed 10 minutes prior to the end of testing.

For an estimated E-Modulus of 5,000 ksi and Poisson's ratio of 0.15, the approximate measured in-situ stress is 660 psi in tension. The direction of this stress is 22 degrees counter-clockwise from the reference line.

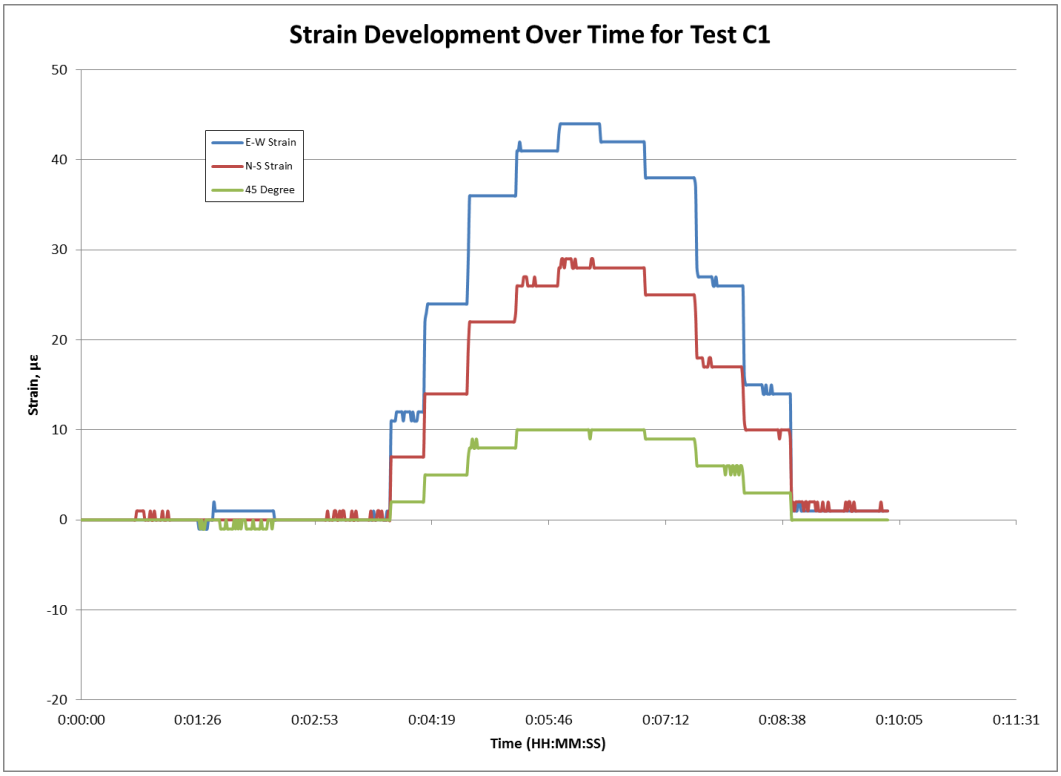

Figure 4.7 Strain Response of C1 Due to Applied Load Before Notches

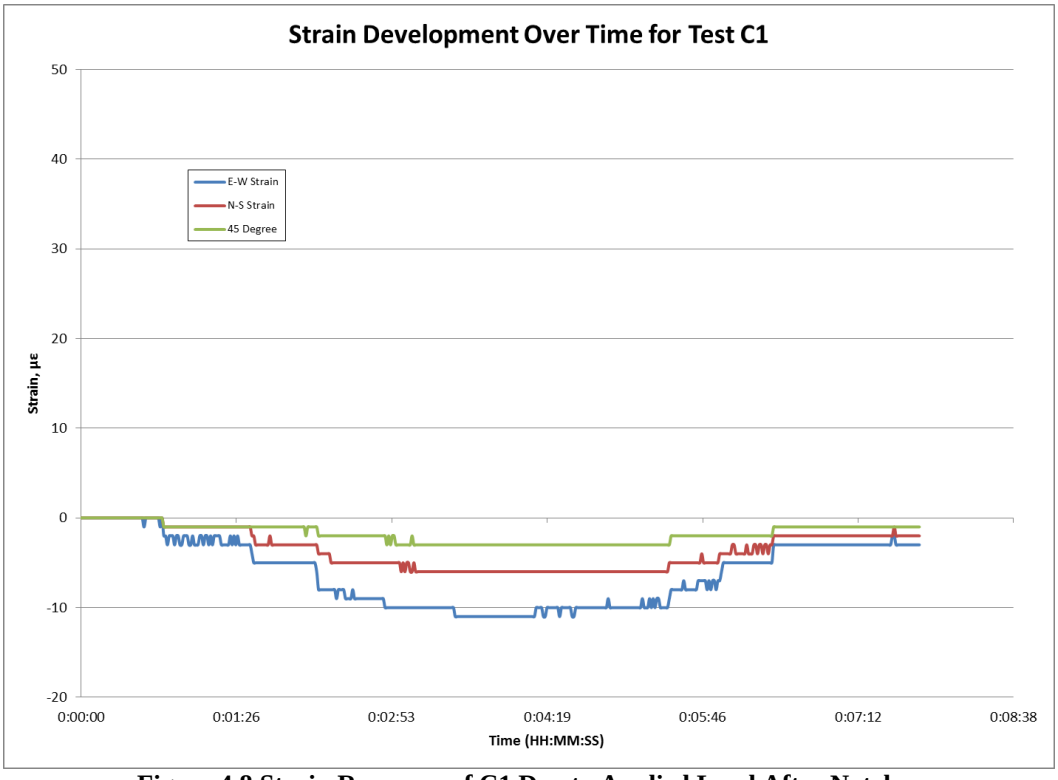

Figure 4.8 Strain Response of C1 Due to Applied Load After Notches

Table 4.8 Percent Change of Strain Response of C1 Before and After Notches

Test C1	% Change		
Load (kips)	E-W Strain (με)	45° Strain (με)	N-S Strain (με)
0	0%	0%	0%
10	-27%	-14%	-50%
20	-21%	-21%	-20%
40	-22%	-23%	-25%
60	-24%	-19%	-20%
80	-25%	-21%	-30%
60	-26%	-16%	-30%
40	-26%	-24%	-33%
20	-30%	-29%	-33%
10	-33%	-40%	-67%
0	0%	0%	0%

Test C1 occurs within the interior of the slab away from edges unlike Test B1 which is located at a free edge. At a notch depth to spacing ratio of 0.41, the strain response after loading is negative in value, as expected. This is indicative that progressive, deepening saw cuts would have resulted in strain magnitudes whose values are diminished from their original values. The reversal in the sign of the strain values indicates that over-relaxation of the material has occurred in a phenomenon nicknamed as a "pinching effect." This effect has been observed in previous testing wherein the effect of the applied stress is not only diminished but reversed. This likely occurs because the confining stress of the material near the surface is more readily relieved than the induced stress from an applied load. Moreover, the newly formed notches act as flaws and intensify the induced stresses into radially-acting crack stresses. These crack stresses can act upwards into the isolated 3x3 inch squared area and reverse the observed strain measurements. As such additional saw cutting is needed to fully relieve the artificial applied stresses, but the observed pinching effect is an indication that the surface stresses have been appropriately isolated and the final strain response is of the total stress present in the material. When the strain response is plotted against the applied load, it becomes evident that the strain assumes non-linear behavior both before and after notching.

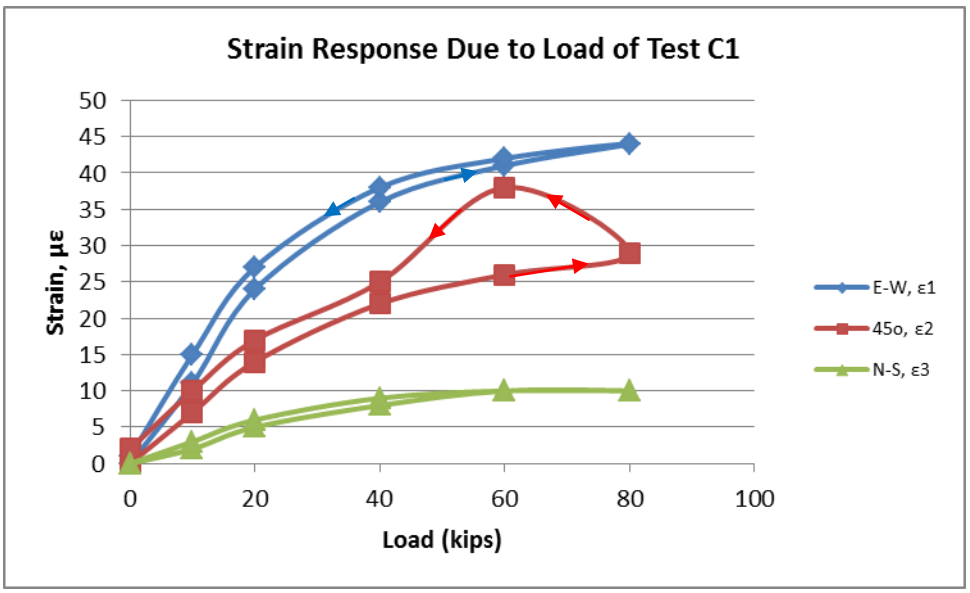

Figure 4.9 Strain Response of C1 Due to Applied Load Before Notches

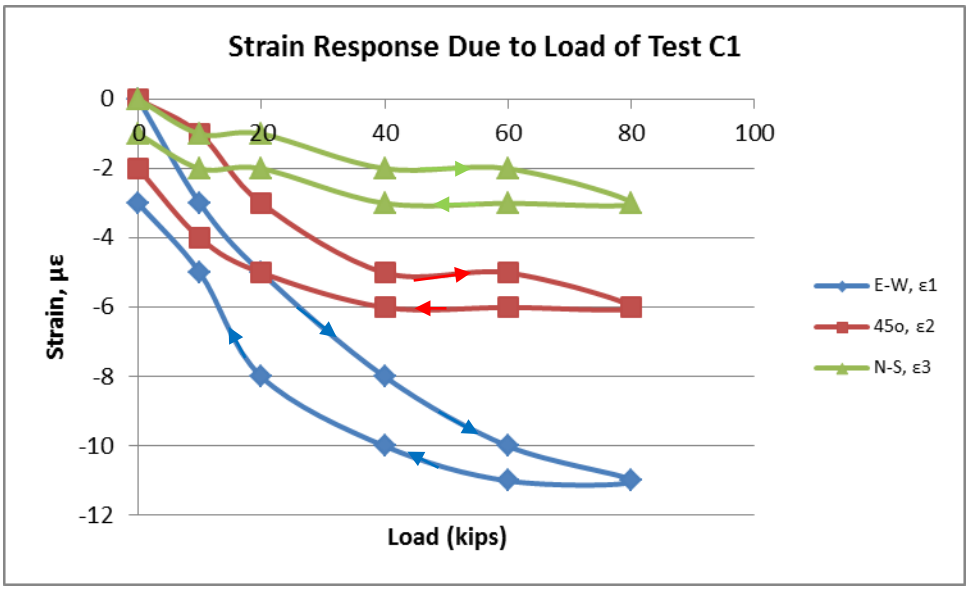

Figure 4.10 Strain Response of C1 Due to Applied Load After Notches

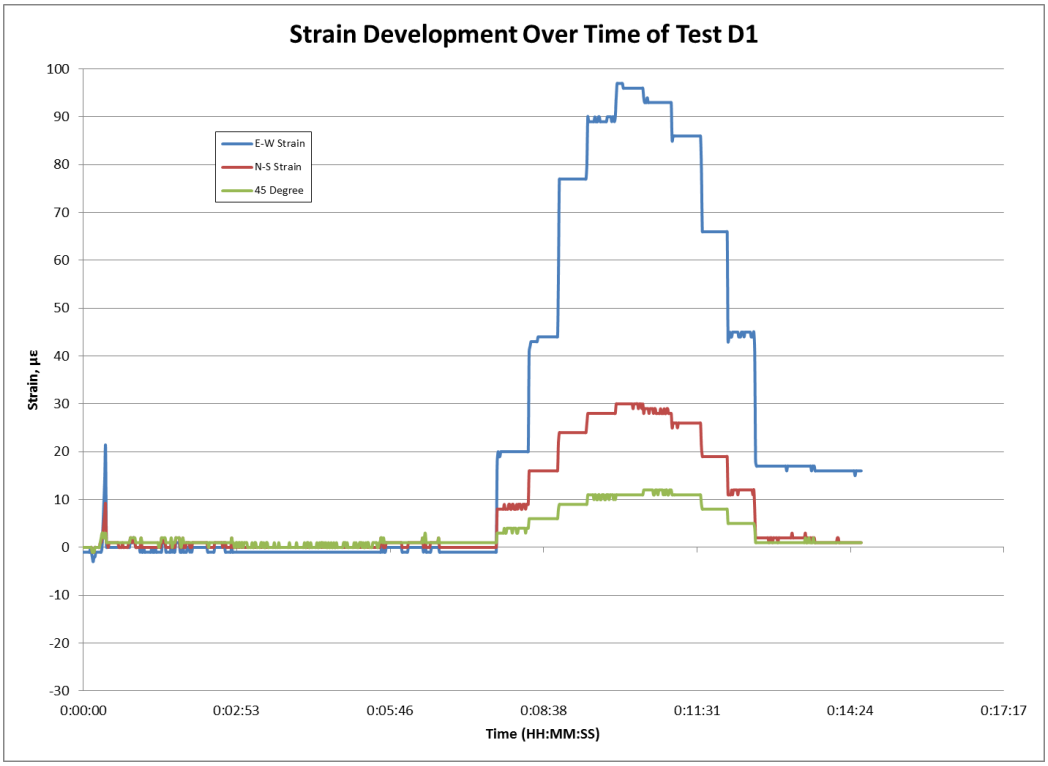

Figure 4.11 Strain Response of D1 Due to Applied Load Before Notches

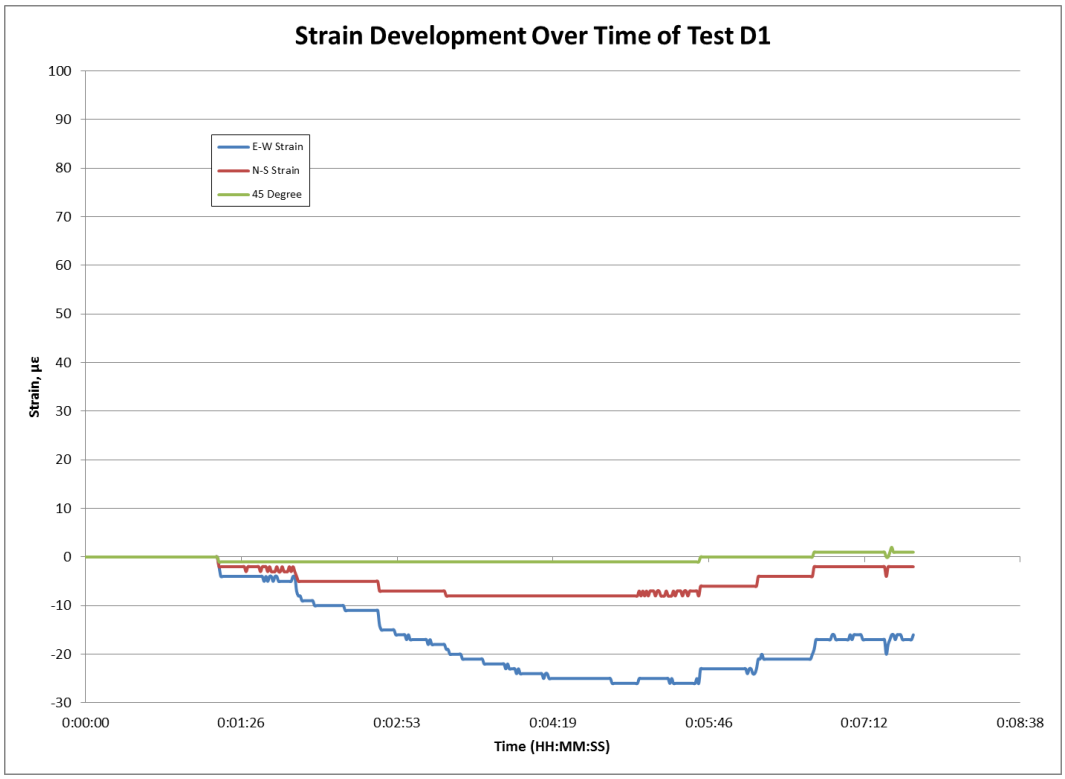

Figure 4.12 Strain Response of D1 Due to Applied Load After Notches

Test D1 similarly occurs within the interior of the slab, and is done so symmetrically with Test C1 in order to draw a comparison and determine repeatability of the testing procedure. The magnitude of the calculated total stresses varies approximately threefold from 190 psi and 660 psi. Similarly the strain measurements during loading and unloading do not equal. The principal strain magnitudes of Test D1 by loading are approximately 30-60% larger than those of test C1. This behavior is unexpected since the concrete material and underlying granular base support are not expected to vary enough to yield these results. It is also possible that the latitudinal strain gage was faulty since its behavior during testing was unexpected. Its stabilization over time is starkly lower than previous tests. Because it was the latitudinal strain gage, alternative latitudinal and longitudinal strain calculations cannot be made. A plot of the strain response is attached at the end of this chapter.

While the magnitude of the strain readings due to the applied loads varies unexpectedly between the two tests, the magnitude of the stress isolated is similarly negated suggesting that the 3x3 inch squared area has been adequately isolated at a depth of 1.2 inches.

Table 4.9 Percent Change of Strain Response of D1 Before and After Notches

Test C1	% Change		
Load (kips)	E-W Strain (με)	45° Strain (με)	N-S Strain (με)
0	0%	0%	0%
10	-20%	-22%	-25%
20	-21%	-31%	-17%
40	-21%	-29%	-11%
60	-22%	-29%	-9%
80	-24%	-27%	-9%
60	-27%	-29%	-8%
40	-29%	-31%	-9%
20	-35%	-42%	0%
10	-47%	-36%	0%
0	0%	0%	0%

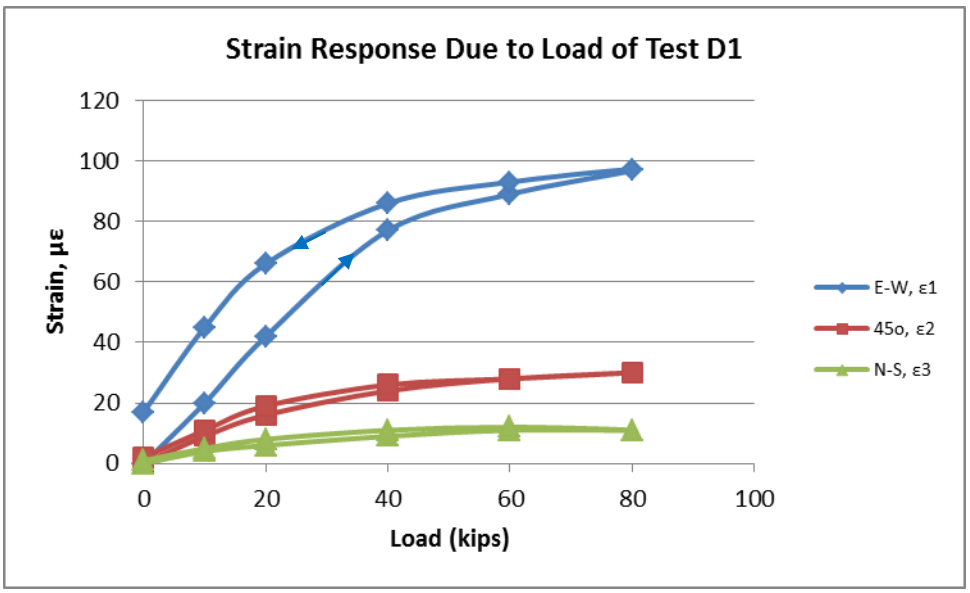

Figure 4.13 Strain Response of D1 Due to Applied Load Before Notches

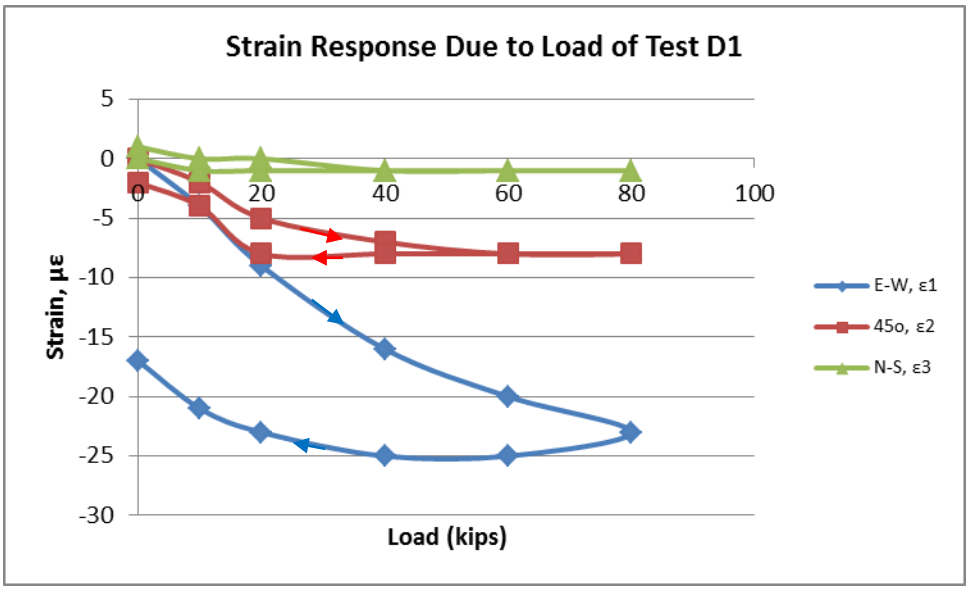

Figure 4.14 Strain Response of D1 Due to Applied Load After Notches

4.6 Figures and Graphs

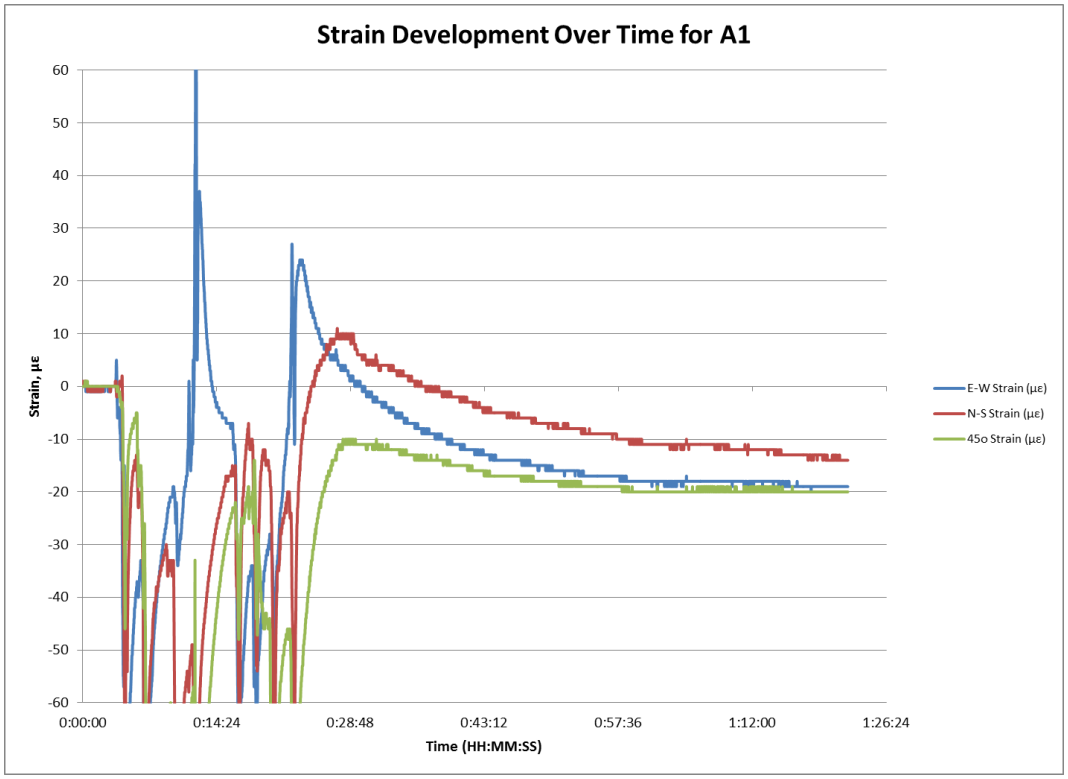

Figure 4.15 Strain Response of A1 During Testing

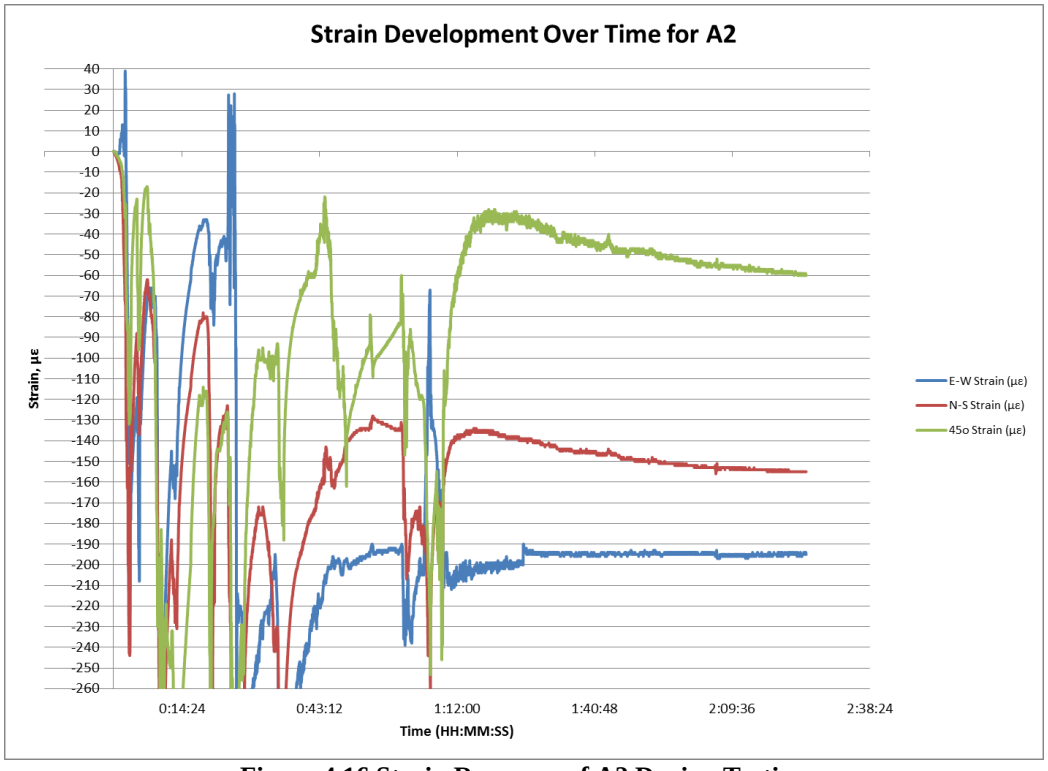

Figure 4.16 Strain Response of A2 During Testing

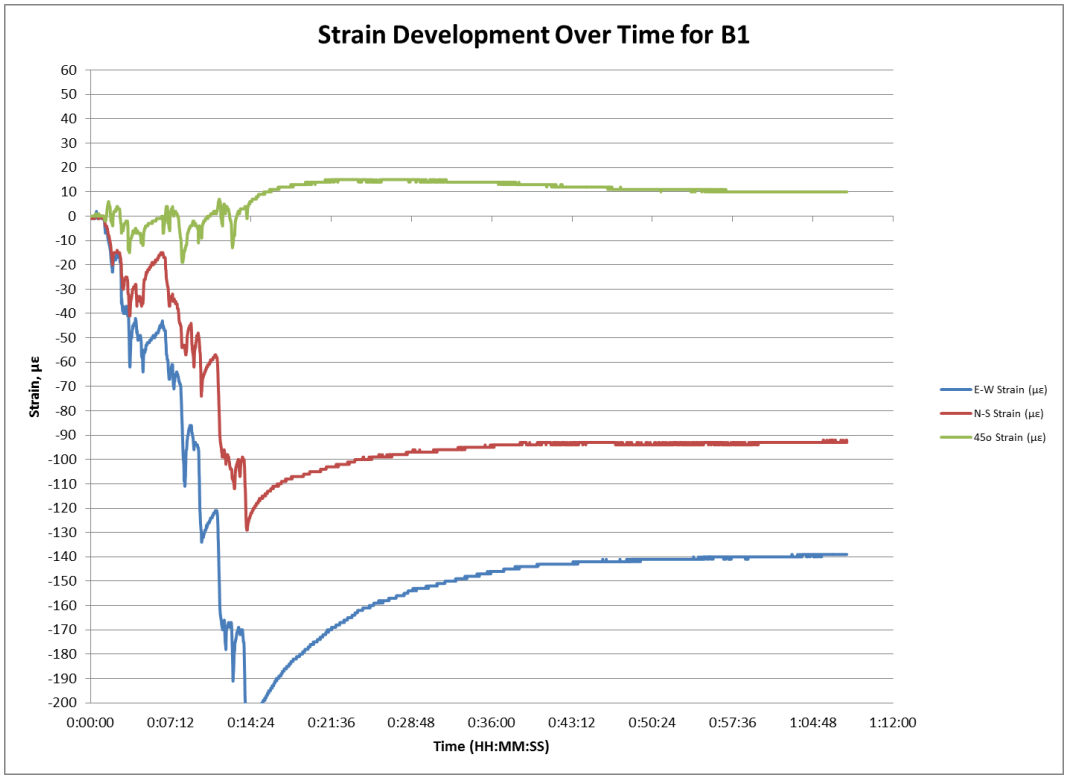

Figure 4.17 Strain Response of B1 During Testing

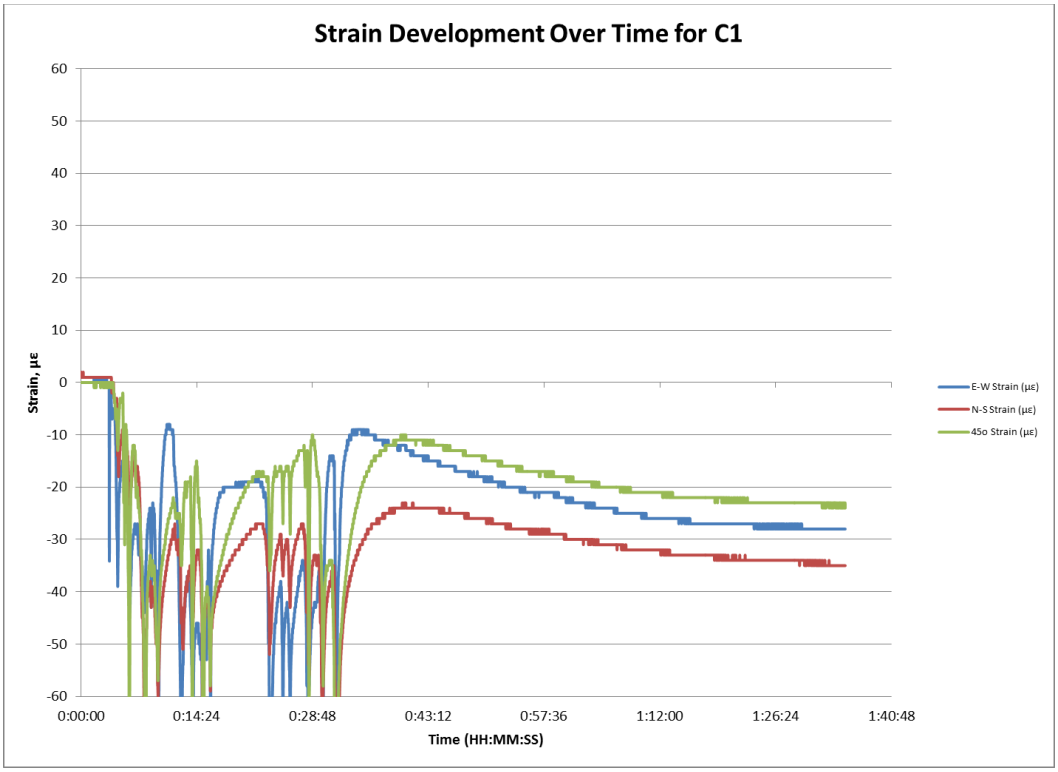

Figure 4.18 Strain Response of C1 During Testing

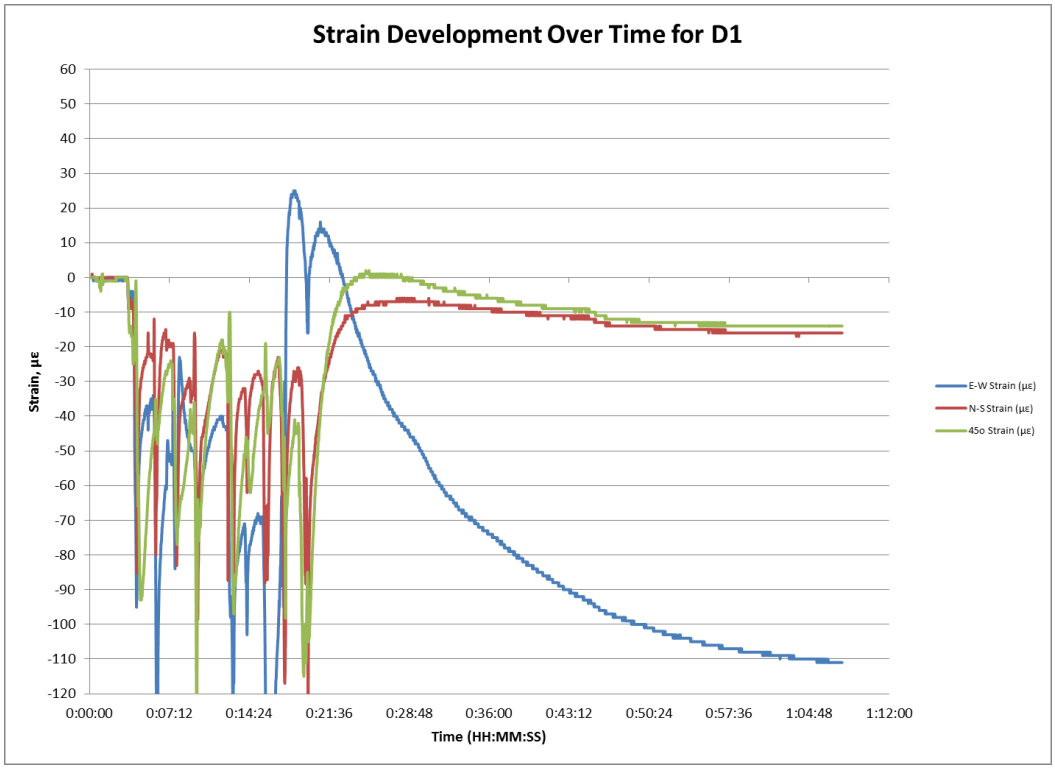

Figure 4.19 Strain Response of D1 During Testing

Figure 4.20 Overview of six strain rosettes attached to 15' squared slab

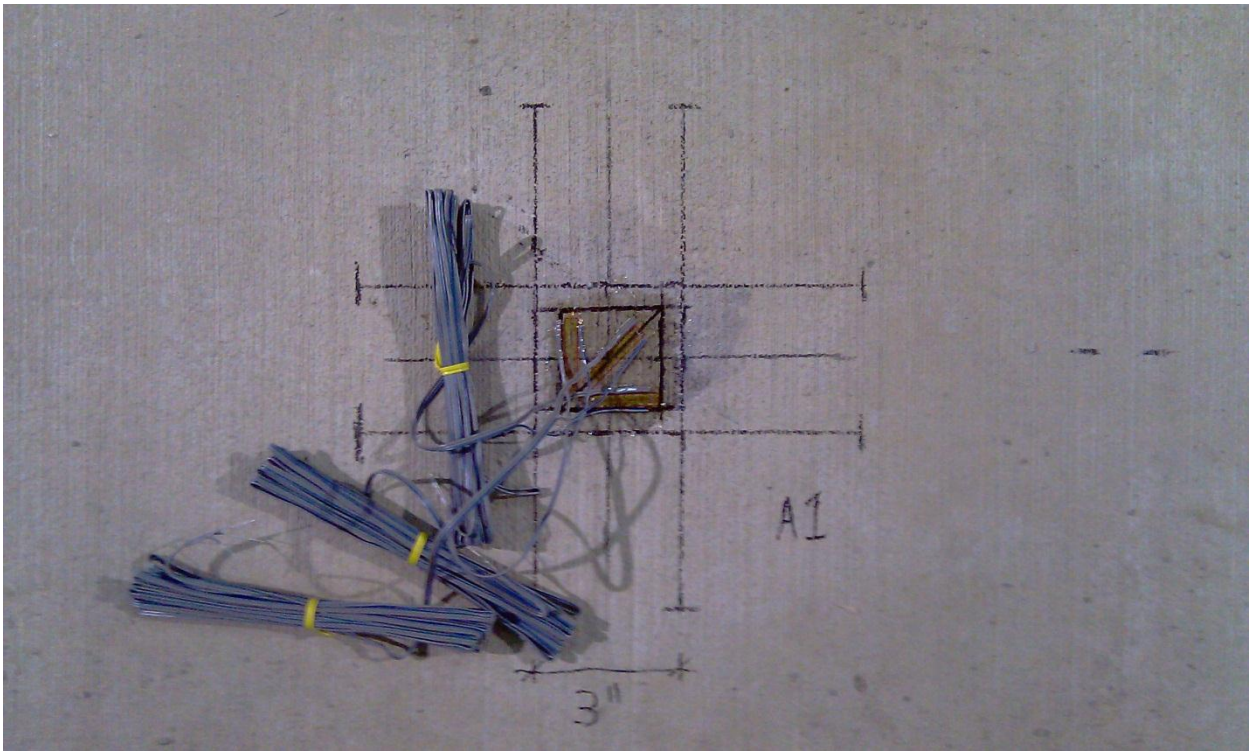

Figure 4.21 Strain rosette A1 with 3 inch spacing

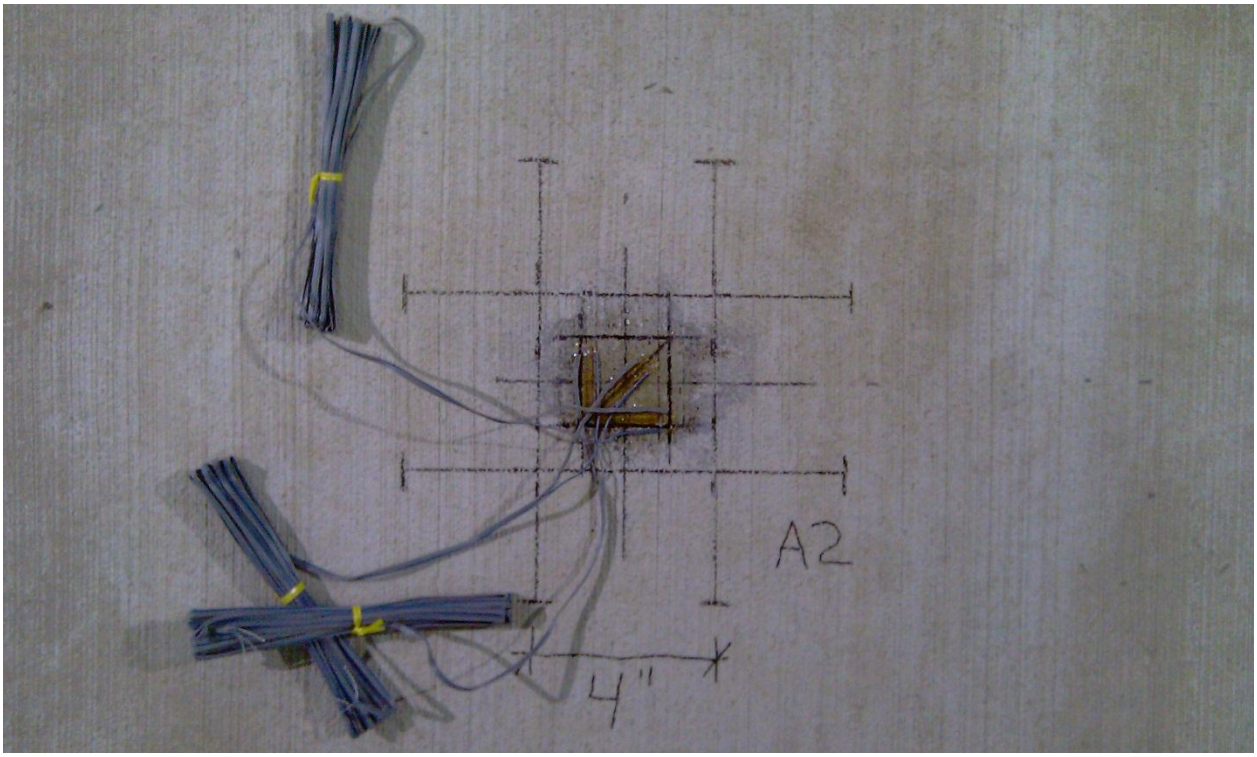

Figure 4.22 Strain rosette A2 with 4 inch spacing

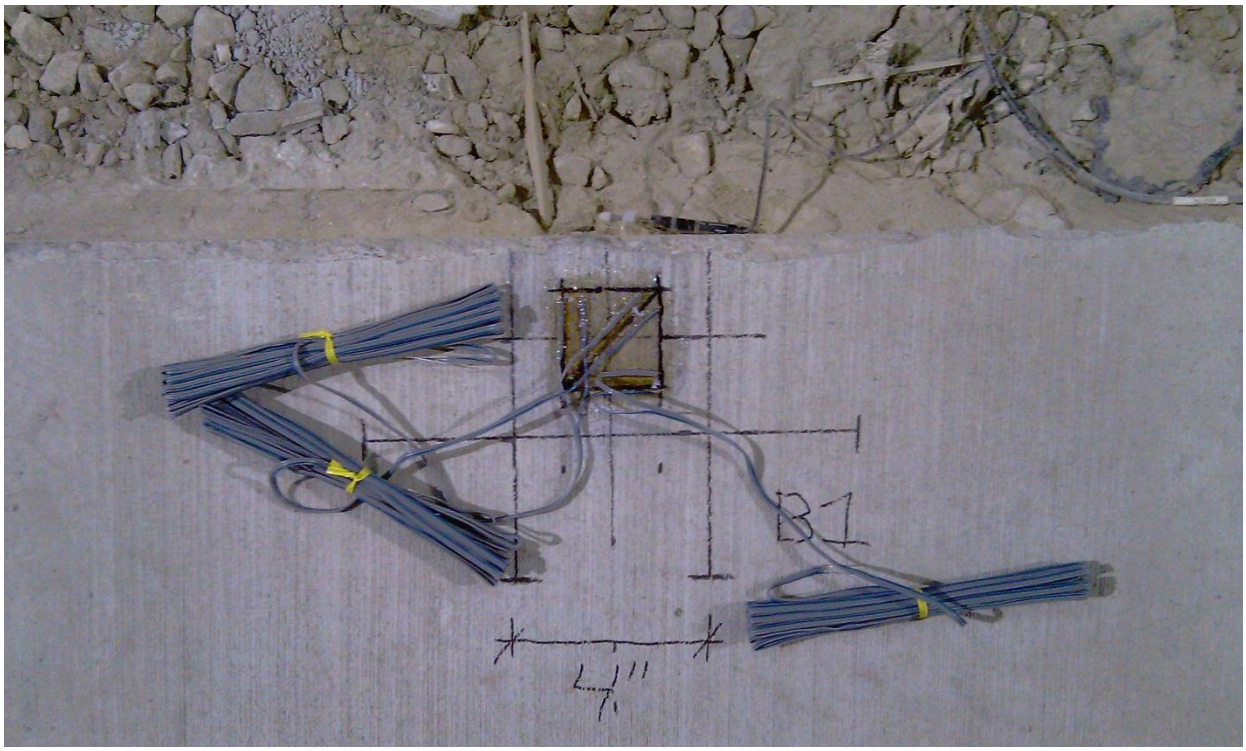

Figure 4.23 Strain rosette B1 with 4 inch spacing

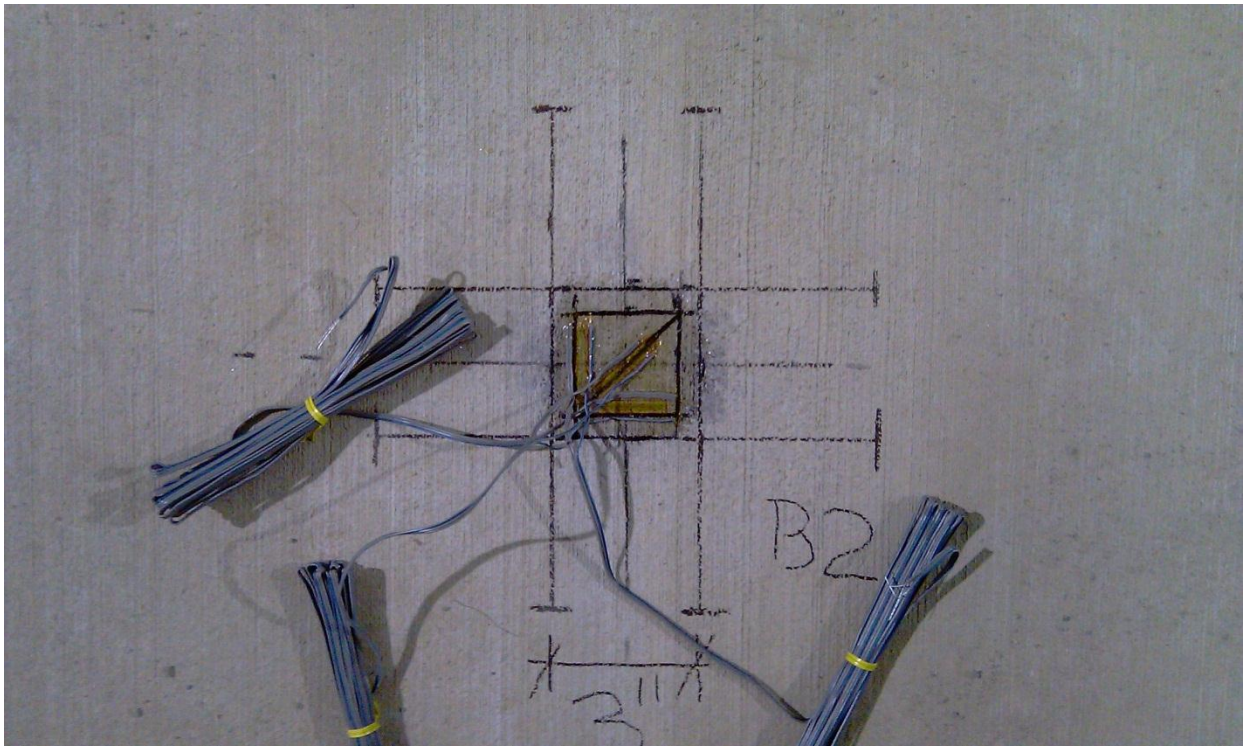

Figure 4.24 Strain rosette B2 with 3 inch spacing

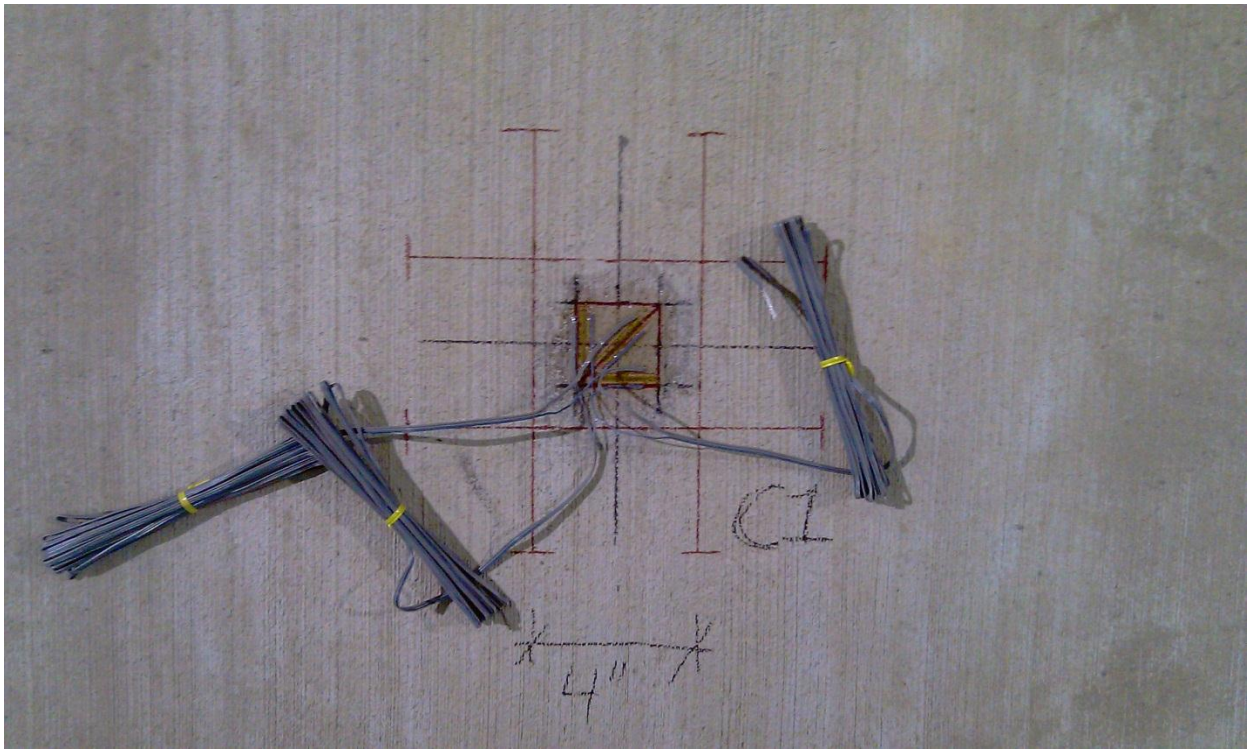

Figure 4.25 Strain rosette C1 with 4 inch spacing

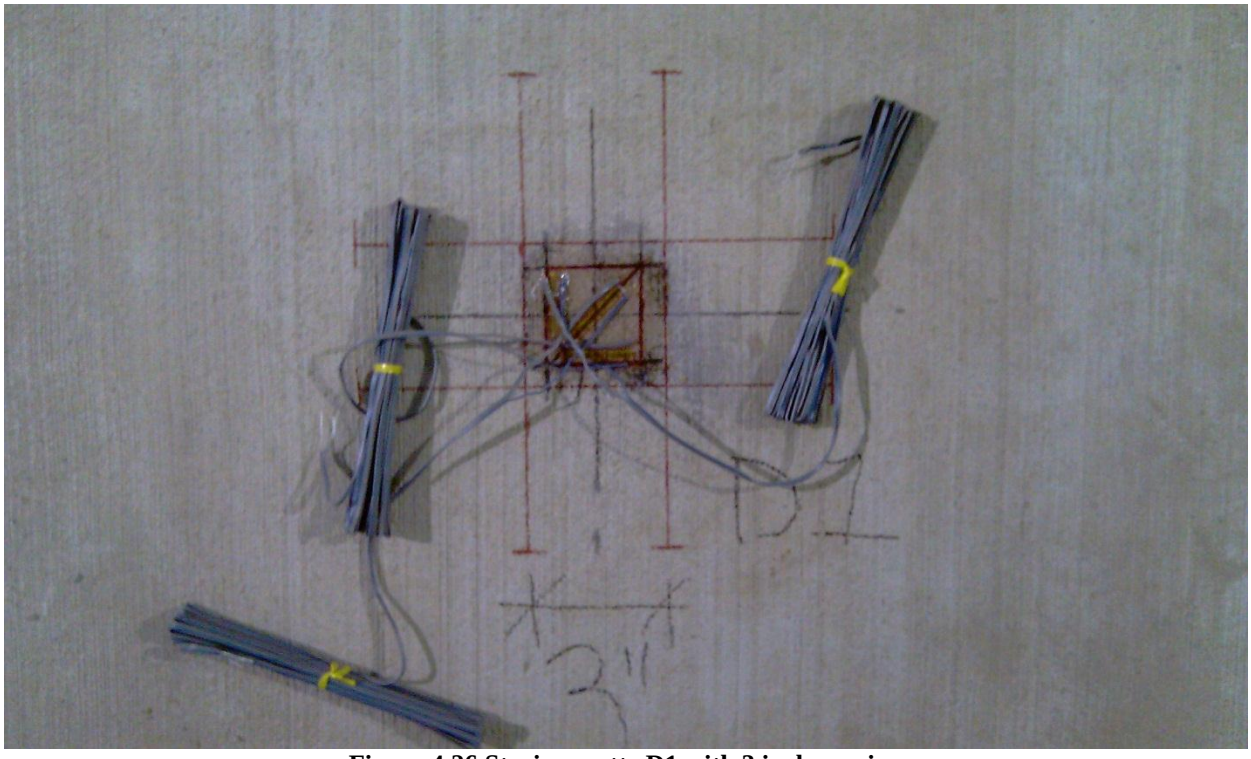

Figure 4.26 Strain rosette D1 with 3 inch spacing

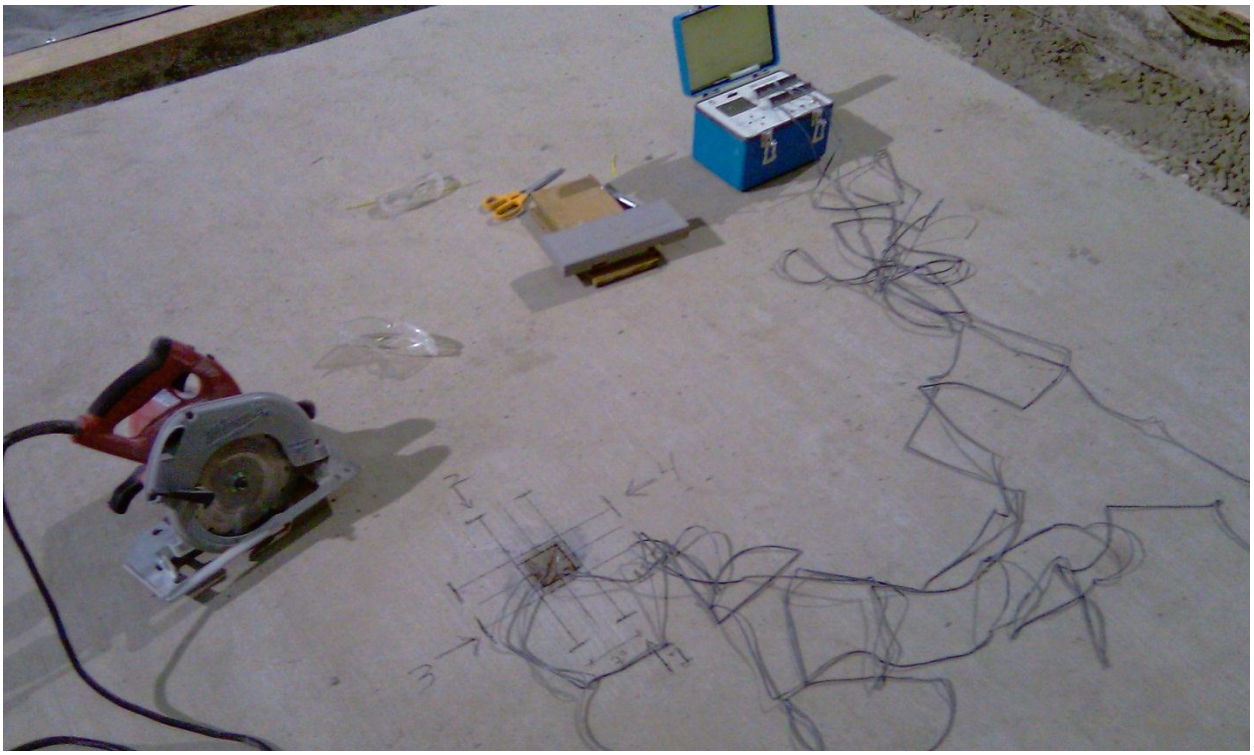

Figure 4.27 Testing of A1, typical testing layout

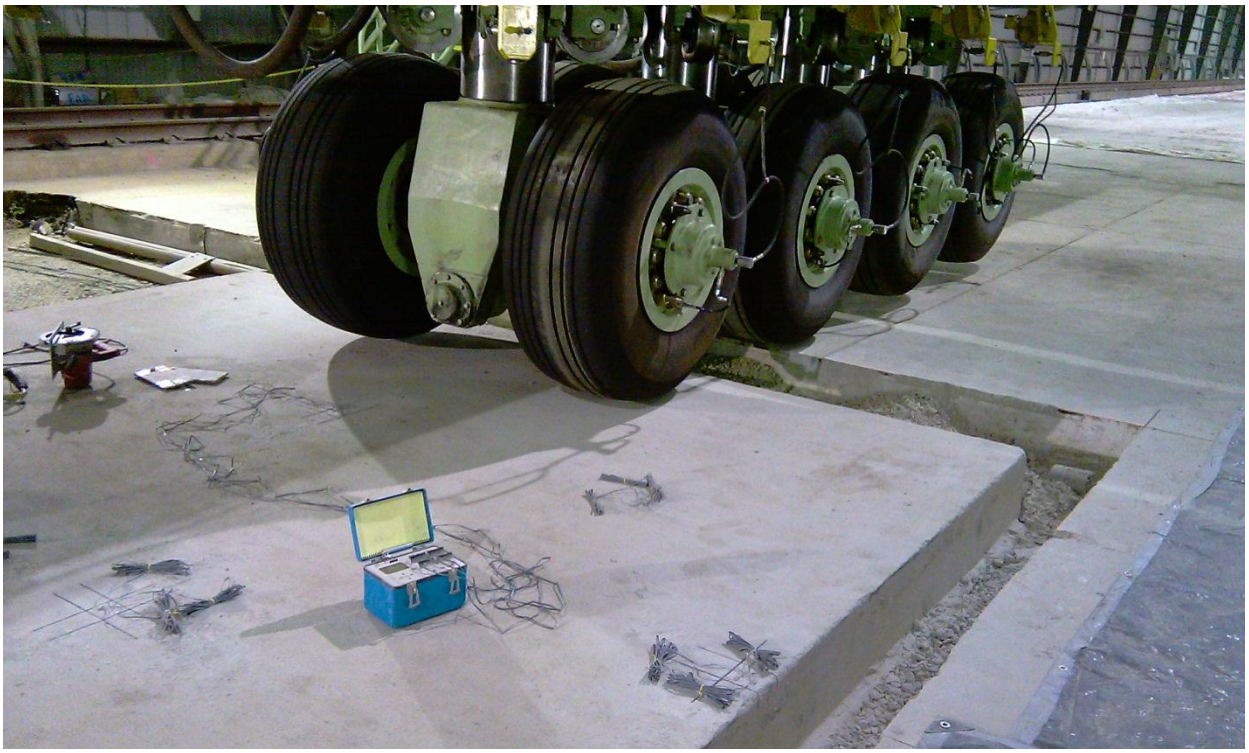

Figure 4.28 Wheel loads positioned along center-edge for test C1

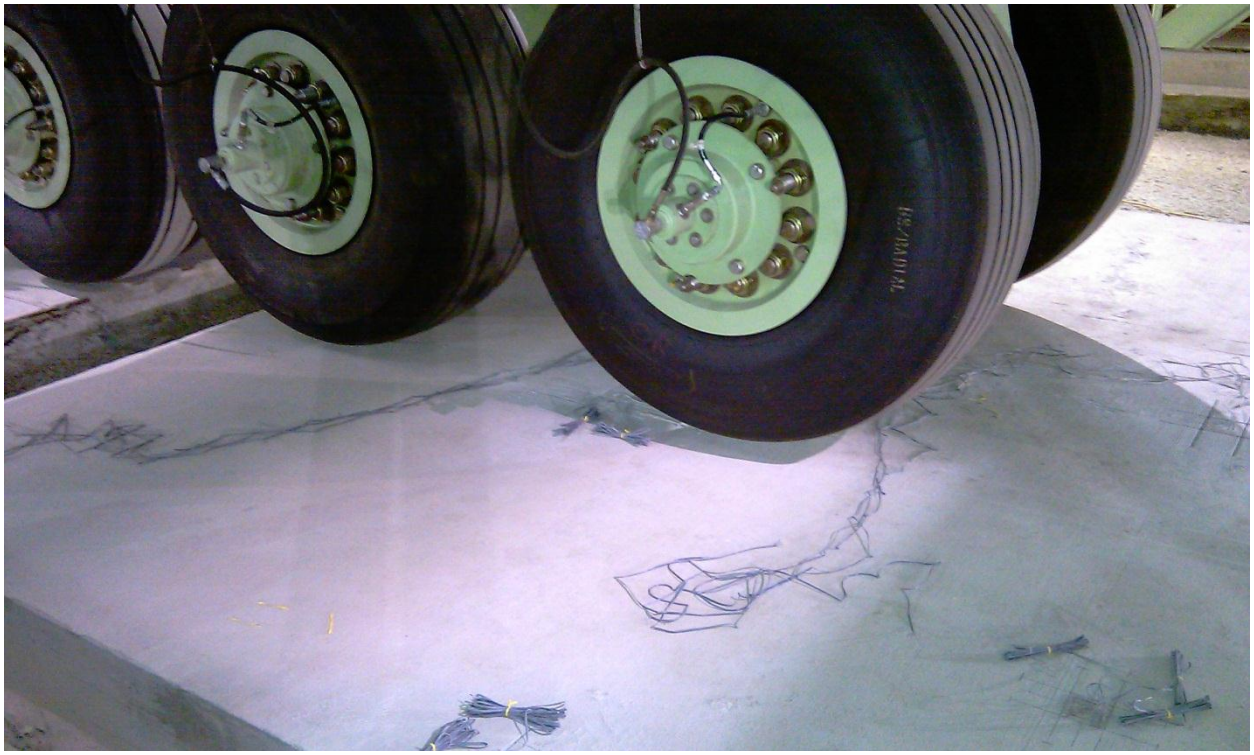

Figure 4.29 Wheel loads positioned along opposite center-edge for test D1 (2nd axle used)

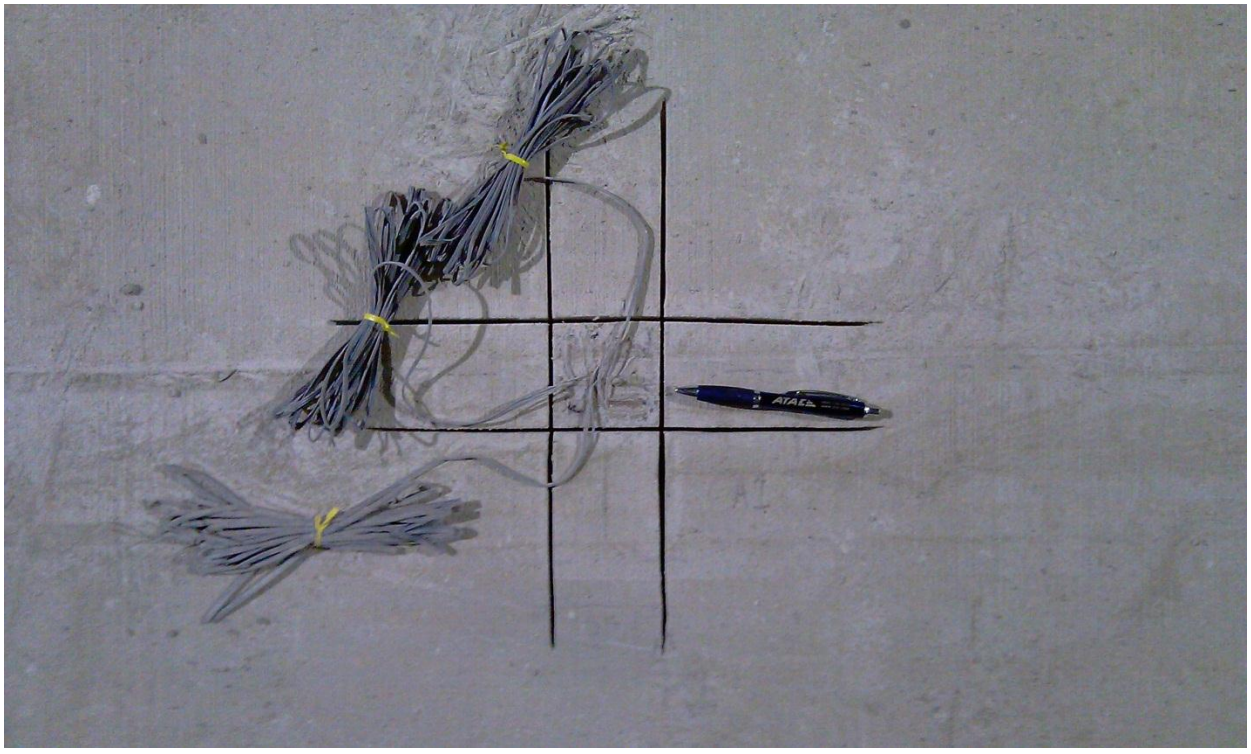

Figure 4.30 Strain rosette A1 after testing

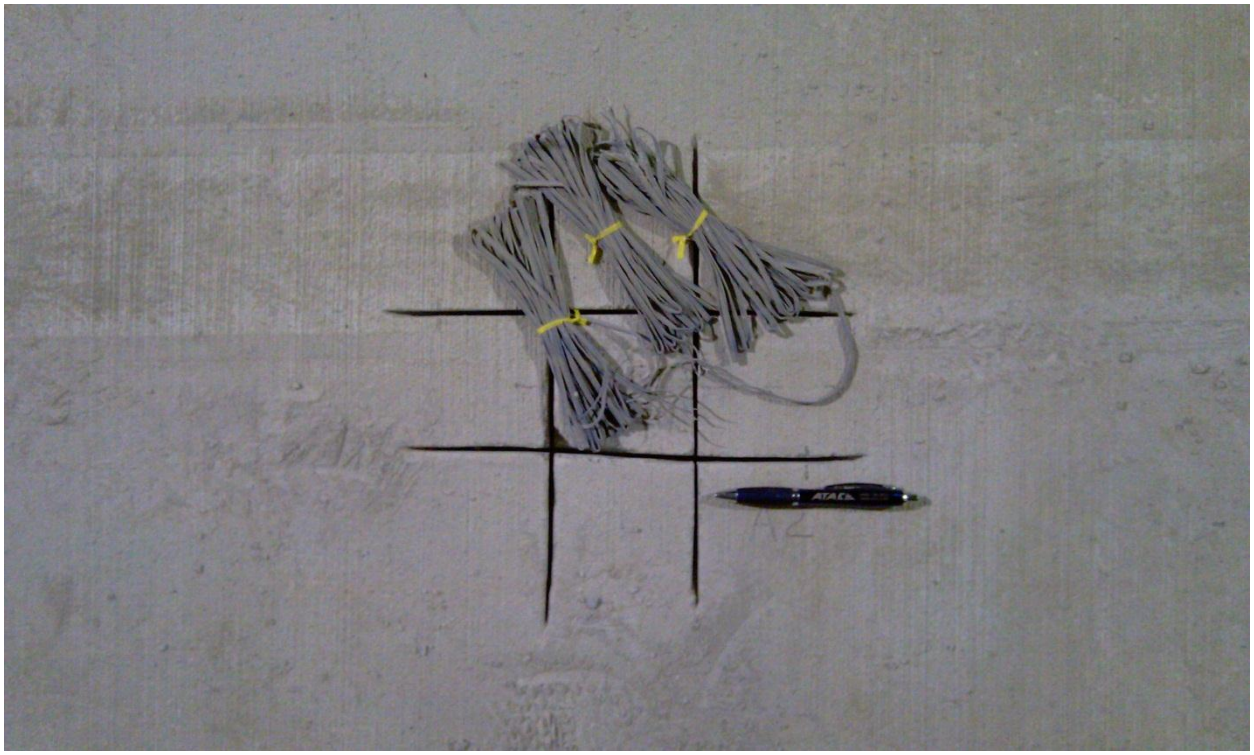

Figure 4.31 Strain rosette A2 after testing

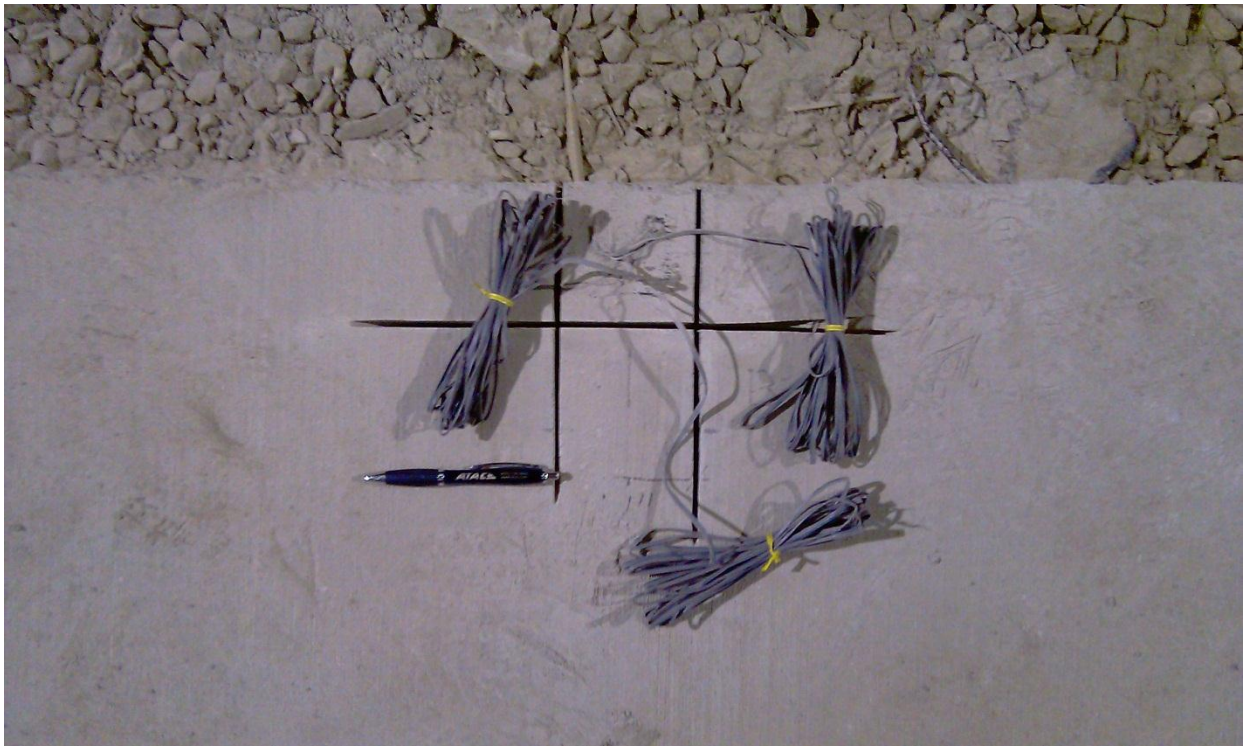

Figure 4.32 Strain rosette B1 after testing

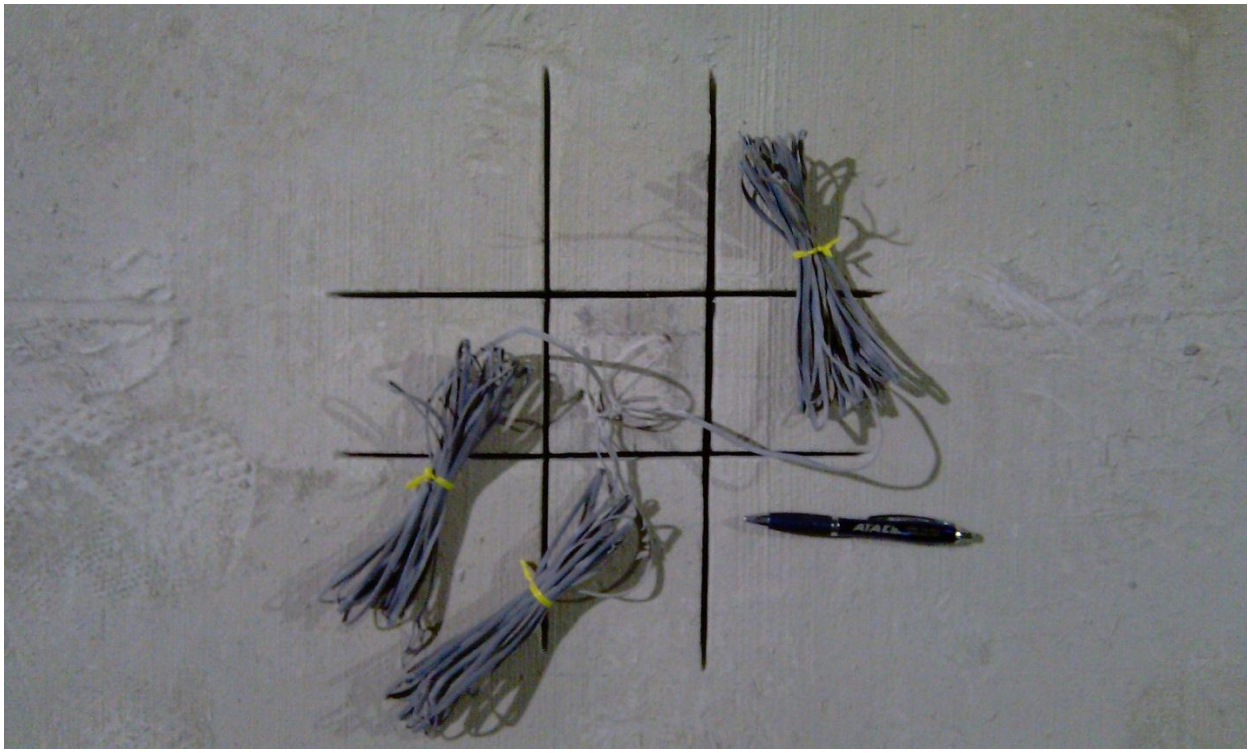

Figure 4.33 Strain rosette C1 after testing

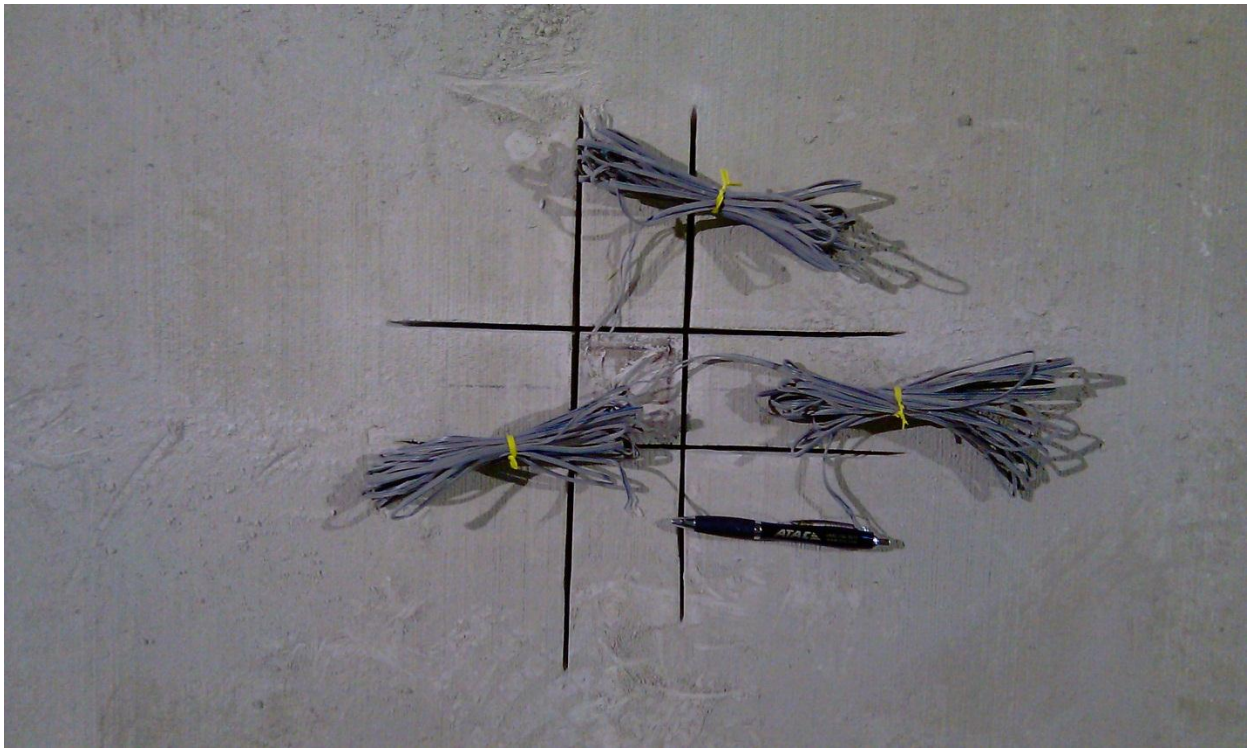

Figure 4.34 Strain rosette D1 after testing

Figure 4.35 Cardboard guides used to protect gages during saw passes

Figure 4.36 Lowering the saw blade at one end of the guide line

Figure 4.37 Center of saw blade advanced 10 inches forward to the end of the guide line

Figure 4.38 Revised notching geometry for test B1. Note the battery powered circular saw in use.

Figure 4.39 Wheel loads positioned at the corner-edge for test B1

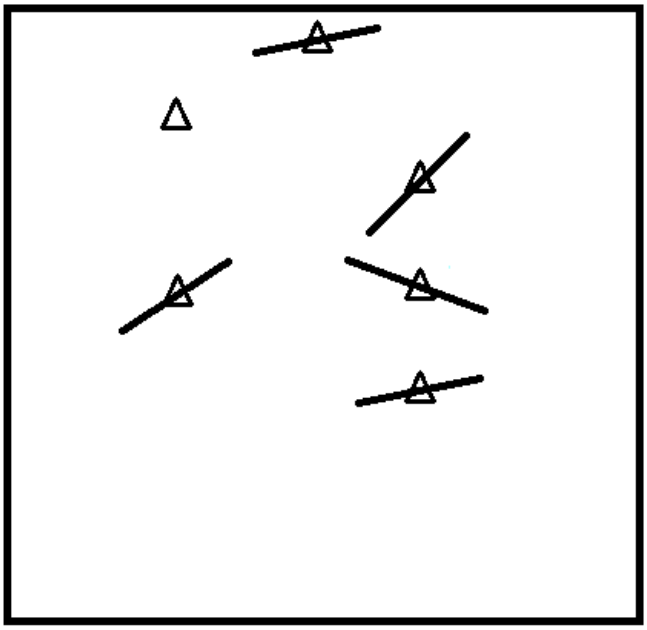

Figure 4.40 Depiction of direction of calculated maximum principal stress

CHAPTER 5: RESIDUAL STRESS TESTING ON MISCELLANEOUS CONCRETE

5.1 Introduction

Additional field testing was carried out on miscellaneous concrete in varying conditions in an effort to ascertain a larger database of information. Under supervision of the author, testing was carried out over the summer of 2010 by Gustavo Gonzales-Justo, a visiting student from *La Universidad de Málaga* in Spain. This testing identified concrete used in typical locations such as pedestrian walkways and airport airfields. The notch spacing varied across tests from 3 inches, 4 inches and 5 inches. Varying saw cut depths were made and the amount of relieved strain was observed. This testing by a second individual was also important in fine-tuning a testing procedure that can be used by persons unfamiliar with this testing method.

5.2 Results for Additional Testing of ATREL and NSEL Concrete

Additional testing of available slabs at ATREL was performed where the notch geometries were varied. However, unlike previous active testing – that is testing which incorporated an applied load – only passive testing was performed. This passive testing is merely the observance of the relief of strain for deepening saw cuts. Testing is complete when the change in stabilized strain between two cutting sequences varied less than 1 με from its previous stabilized magnitude.

A concrete walkway between two buildings on the UIUC campus was identified as being available for testing, as well. This concrete walkway was jointed into 10 foot x 7 foot segments, many of which were free from surface damage. Each slab was immediately adjacent to the building leading to potentially high constraining stresses, however. Thus this site could lead to potentially interesting results.

A variety of notching geometries was performed at these two locations and their results are summarized in the table below. These 8 tests were performed across three slabs and their locations are depicted in Figure 5.1. While each test was performed independent of the others, it was decided that Test NSEL #6 would re-test the previously tested strain rosette at Test NSEL #5 by deepening the cut to a depth of 2.0 inches. Theoretically, this calculated residual stress is thusly in addition to the previously quantified stress found in NSEL #5. However, the superposition of this result is an approximation since daily temperatures and moisture conditions can induce moderate alterations to the stress state of concrete.

Table 5.1 Residual stress calculations for numerous tests with varying notch geometries

Date	Location	ID	Notch Spacing (in)	Notch Depth (in)	E-W Strain (με)	45o Strain (με)	N-S Strain (με)	Max Stress (psi)	Min Stress (psi)	Residual Stress (psi)
20100731	NSEL	#1	5	0.5	30	39	28	171.4	101.5	171
20100803	NSEL	#2	5	1.0	8	42	21	166.5	-30.1	167
20100803	NSEL	#3	5	1.0	-1	6	-1	19.6	-29.1	-29
20100804	NSEL	#4	5	1.1	-7	0	-8	-9.1	-61.4	-61
20100804	NSEL	#5	5	1.1	-1	-4	-13	-9.6	-56.3	-56
20100805	NSEL	#6	5	2.2	-10	-11	-9	-39.2	-50.2	-50
20100806	NSEL	#7	3	2.1	5	3	-4	20.3	-15.6	20
20100807	NSEL	#8	3	2.2	-7	-14	-13	-29.7	-64.5	-64
20100816	ATREL	#1	4	1.9	-25	-1	15	47.4	-94.5	-94
20100816	ATREL	#2	4	1.8	-17	0	11	35.7	-63.9	-64

The corresponding graphs of the strain development are included at the end of this chapter. It is interesting to note the unclear variability for tests conducted with a notch spacing of 5 inches. These tests, while moderately successful in identifying a stabilized strain value, do not offer confidence in having identified the residual stress. This is because the strain magnitudes tend to show continuous drifting and require longer times to stabilize. This is likely due to the need of the saw cut heat to dissipate through a larger volume of isolated material.

Additionally, it is expected that deeper notches are needed in order to fully alleviate the stresses in a larger-sized isolated square based on experimental observations of a notch depth-to-spacing ratio of 0.40. However, the increasing size of the square material also suggests that the relieved stress is a very local measurement of its underlying concrete. An alternate experiment making use of larger-sized strain gages may reveal altered results, but this is not a desirable option as increasing the notch spacing necessitates deepening the saw cuts.

5.3 Results for Rantoul General Airport Test

A testing opportunity was made available at the Rantoul General Airport on a decommissioned taxiway. The plain concrete slab measured 40 feet by 12.5 feet and was situated in the interior of a taxiway that had been inoperable for a number of years. The surface of the

concrete was largely undamaged, yet was roughly grooved and weathered. Severe data fluctuations during testing hindered an appropriate analysis for this slab; however, lessons were learned in order to proceed with future field testing.

Firstly, heating due to direct sunlight will hinder results in two ways. Heating of concrete will cause thermal expansion while heating of the strain gages themselves will alter their resistivity and further affect the strain readings. Secondly, appropriate equipment must be used such that the testing procedure is continuous. Results from this test were incomplete since the fourth cut was unable to be complete due to a drained battery in the hand-held circular saw. However, the availability of strain gages normal and perpendicular to the available cuts allowed for an approximation of the residual stress in the longitudinal and latitudinal directions. Either interpretation, however, could not be made due to the extensive fluctuation in the strain gage measurements as evident in Figure 5.12.

5.4 Results for O'Hare Airport Fuel Depot Test

An instrumented recycled aggregate concrete slab at the Chicago O'Hare airport was made available to be tested. This slab had been cast 2 months prior and was not expected to have suffered appreciable stress development. However, cracking had formed along an adjacent curb in a geometry suggesting that the slab had expanded beyond its designed limits and was pulling the concrete curb along with it.

The center of the 15 foot by 9 foot concrete slab was identified as a suitable area to test. Previous knowledge of the slab provided that there was no underlying steel reinforcement beneath the surface of the concrete which would have altered expected results. The site of testing also necessitated supervisory personnel, so it was desired that testing be performed as quickly as possible. As such, quick-setting epoxies were employed in order to rapidly adhere the strain rosette onto the concrete surface. Additionally, it was decided that a smaller notch-spacing of 3 inches would be suitable considering its ability to release heat more rapidly due to its smaller volume. Lastly, modest wind and shade barriers were erected in order to diminish strain data fluctuations as they were observed in previous testing at the Rantoul General Airport.

Unlike the previous test conducted at the Rantoul General Airport, the results for this test were viable and a calculated residual stress was made other than for a damaged strain gage angled 45 degrees from the latitudinal and longitudinal strain gages. Assuming a stiffness of 4,000 ksi in the material, the stabilized strain readings suggest a residual stress of 67 psi in

compression when saw cuts at a depth of 1.2 inches are made. Figure 5.13 shows that the use of modest wind and shade barriers (comprised of buckets and cardboard) can adequately maintain the integrity of the test results. These barriers were erected at the onset of surface preparation in order to ensure that no active cooling of the concrete material would occur during testing.

5.5 Figures and Graphs

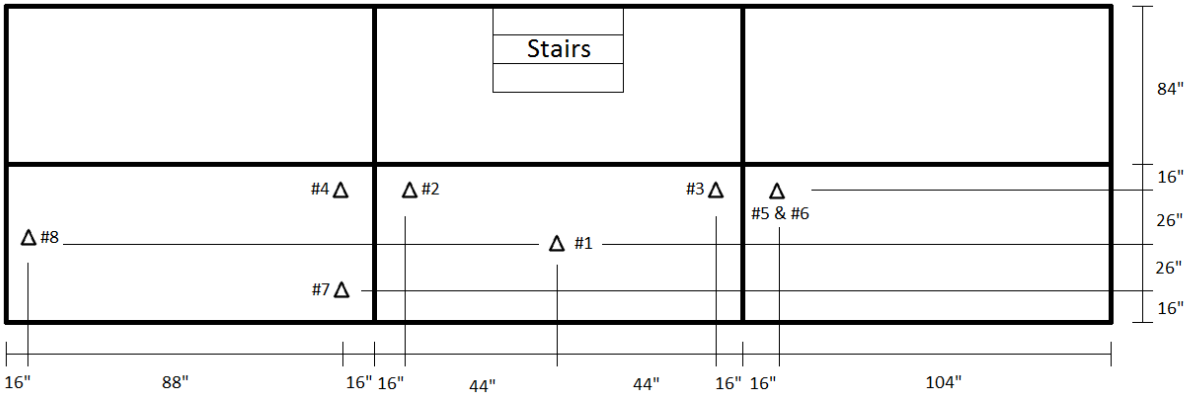

Figure 5.1 Location of 8 NSEL testing locations along concrete walkway

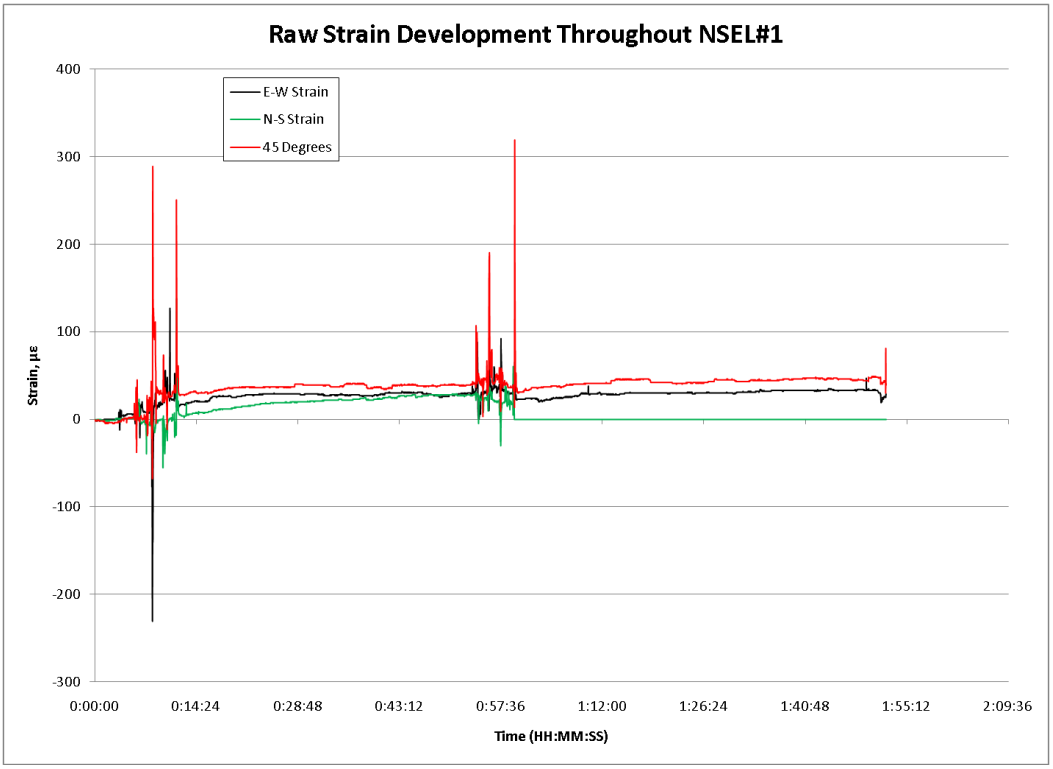

Figure 5.2 Strain development of NSEL #1 throughout testing

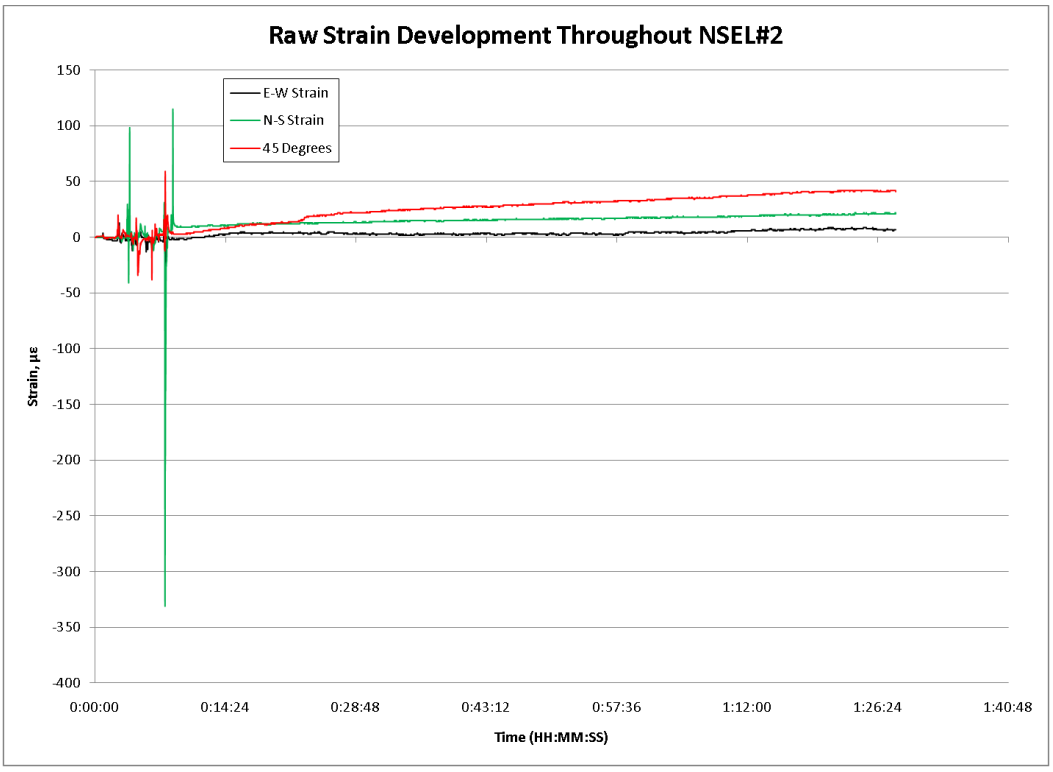

Figure 5.3 Strain development of NSEL #2 throughout testing

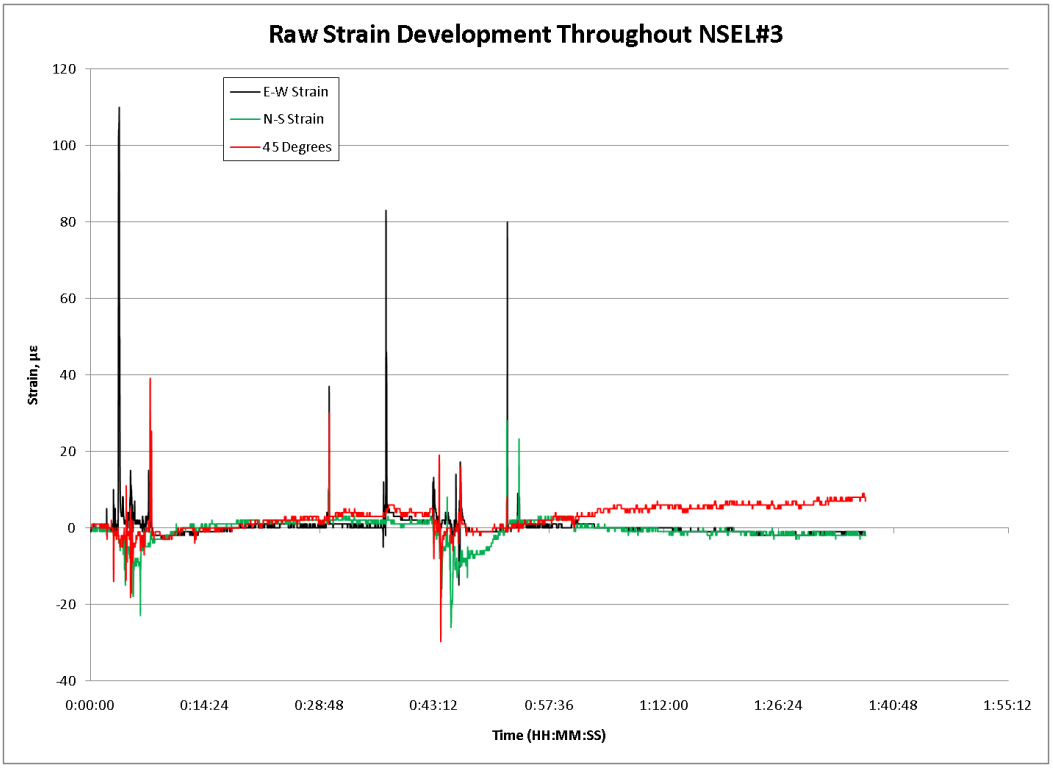

Figure 5.4 Strain development of NSEL #3 throughout testing

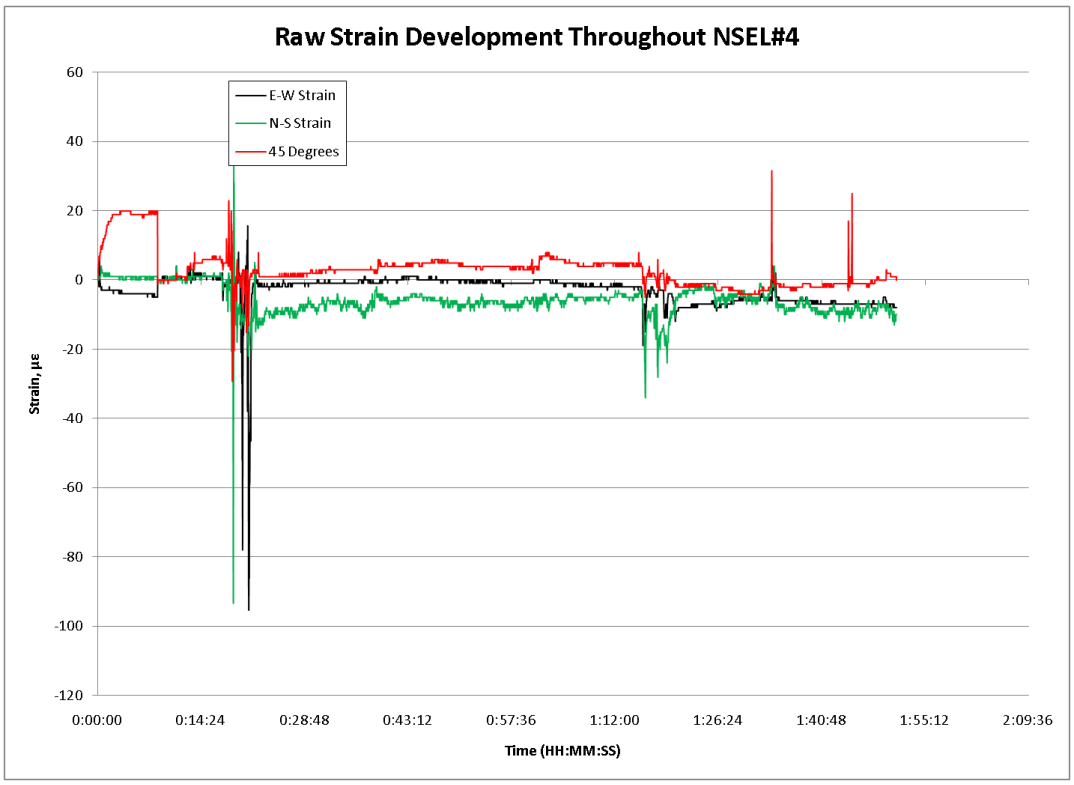

Figure 5.5 Strain development of NSEL#4 throughout testing

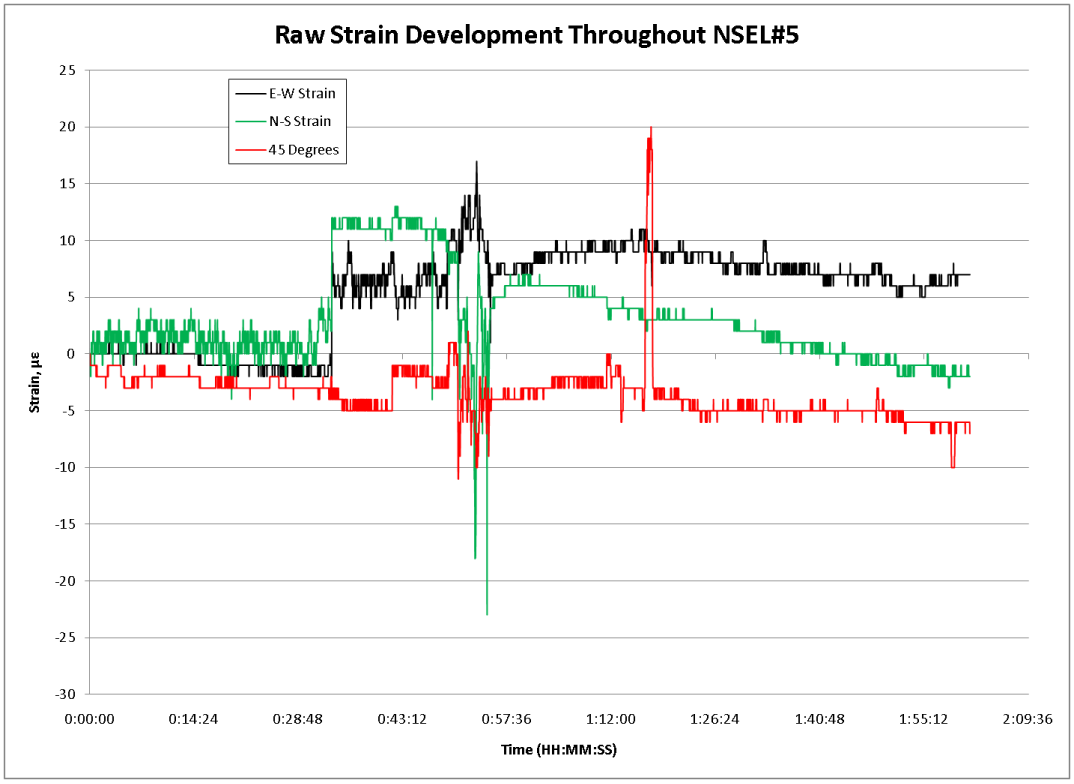

Figure 5.6 Strain development of NSEL #5 throughout testing

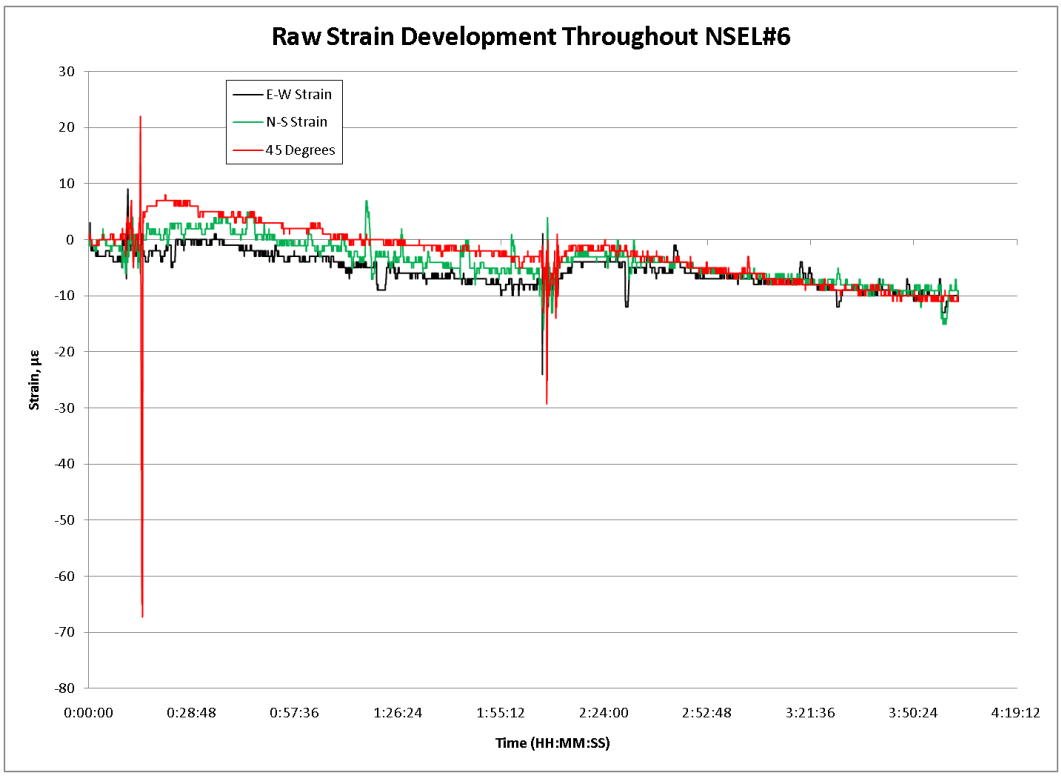

Figure 5.7 Strain development of NSEL #6 throughout testing

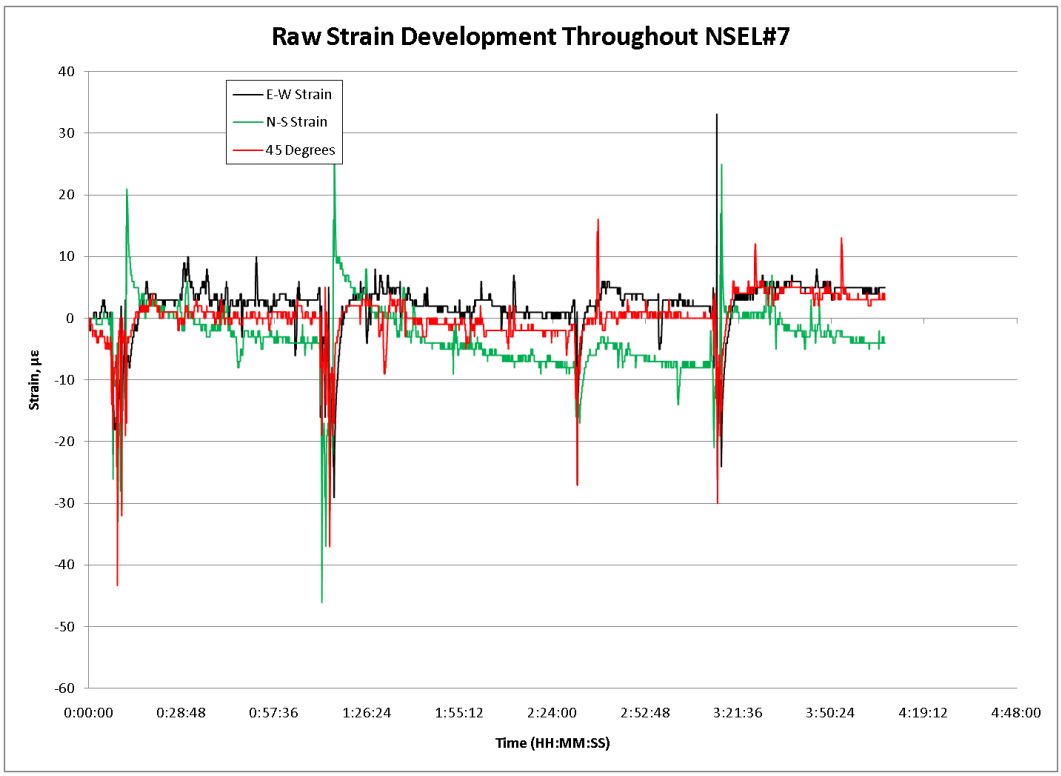

Figure 5.8 Strain development of NSEL #7 throughout testing

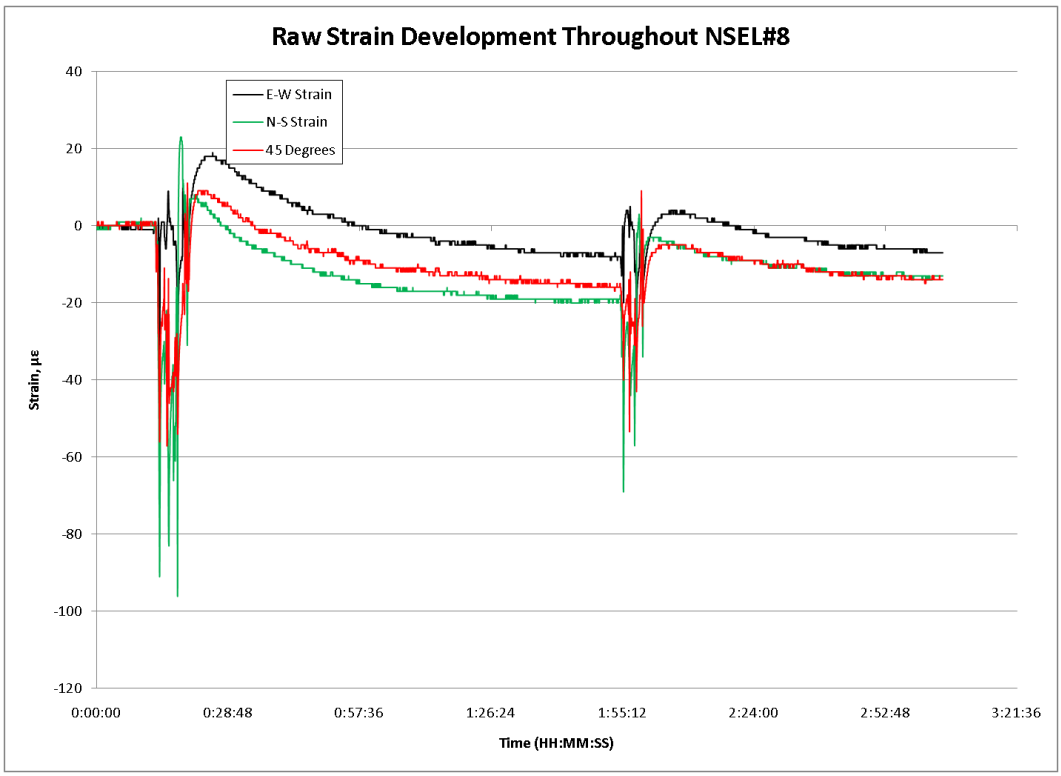

Figure 5.9 Strain development of NSEL #8 throughout testing

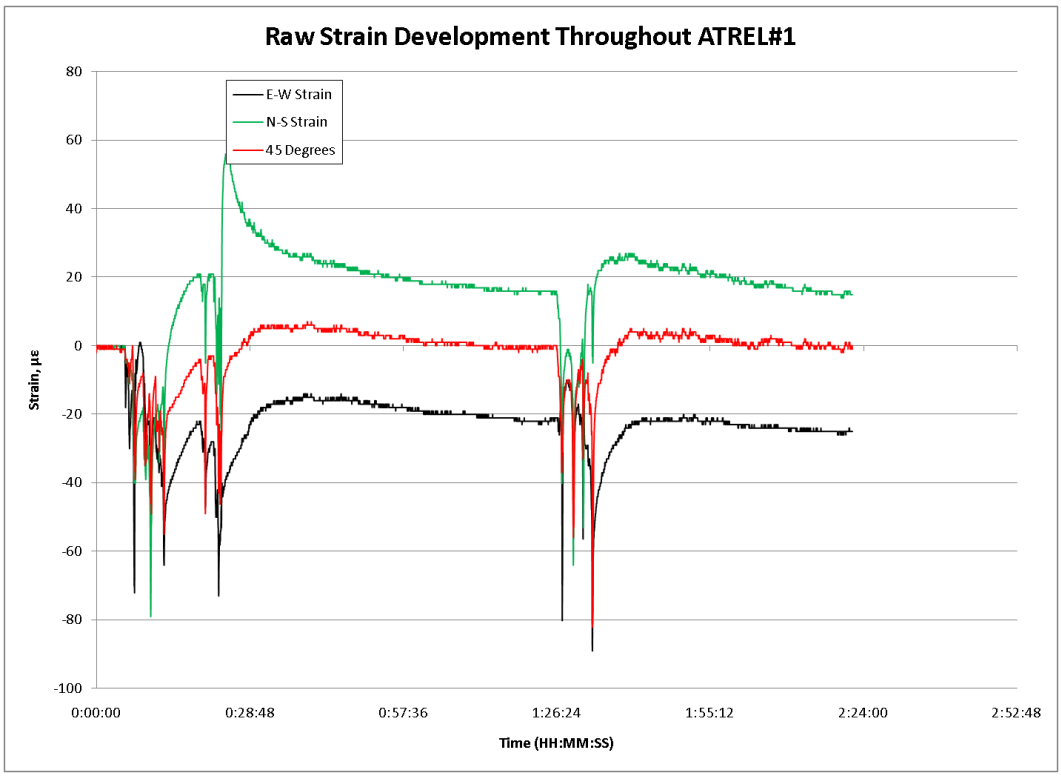

Figure 5.10 Strain development of ATREL #1 throughout testing

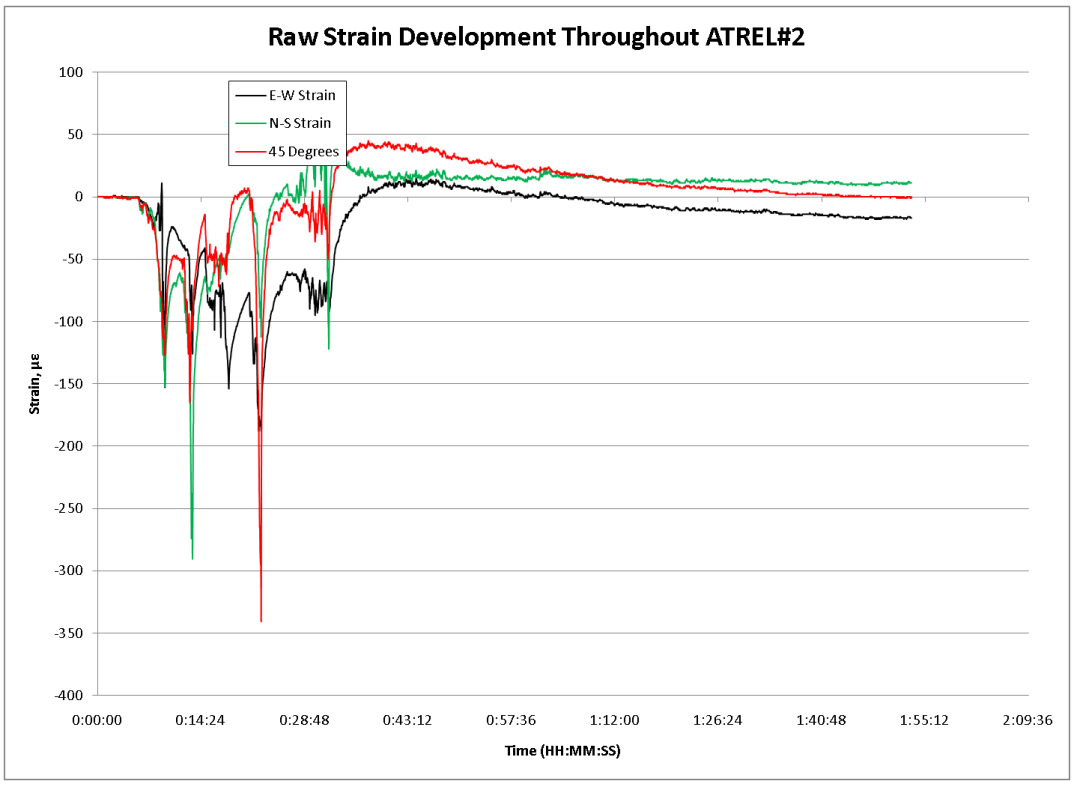

Figure 5.11 Strain development of ATREL #2 throughout testing

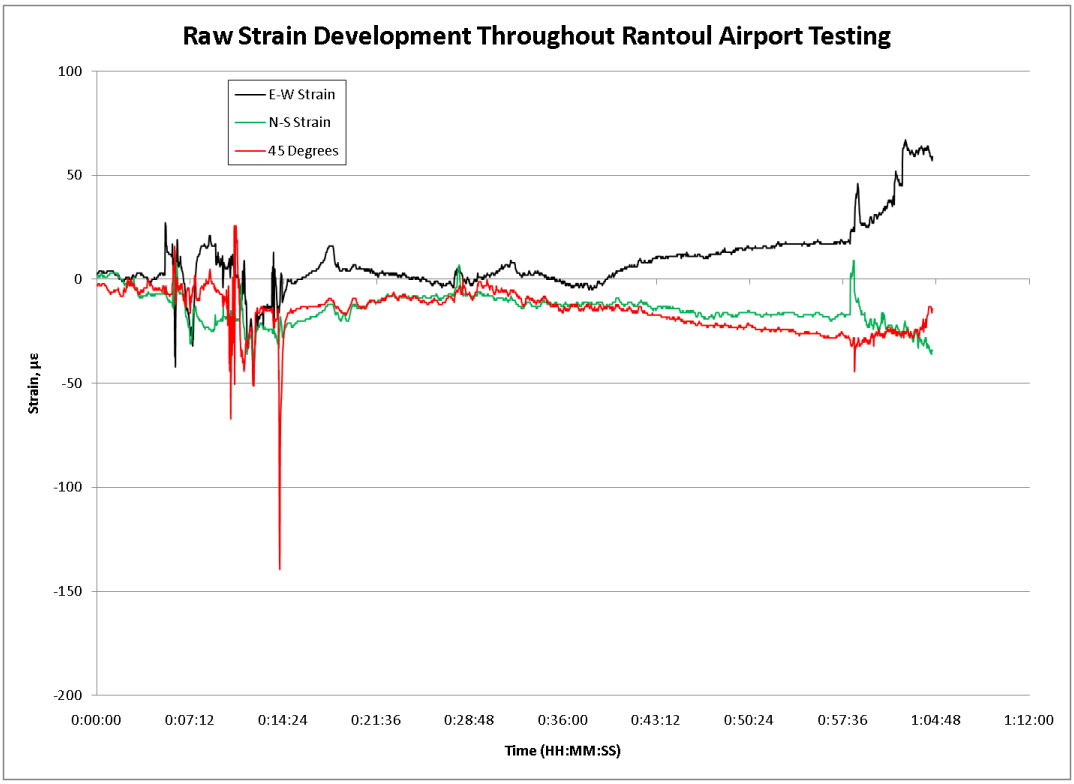

Figure 5.12 Erratic strain development throughout Rantoul Airport Testing

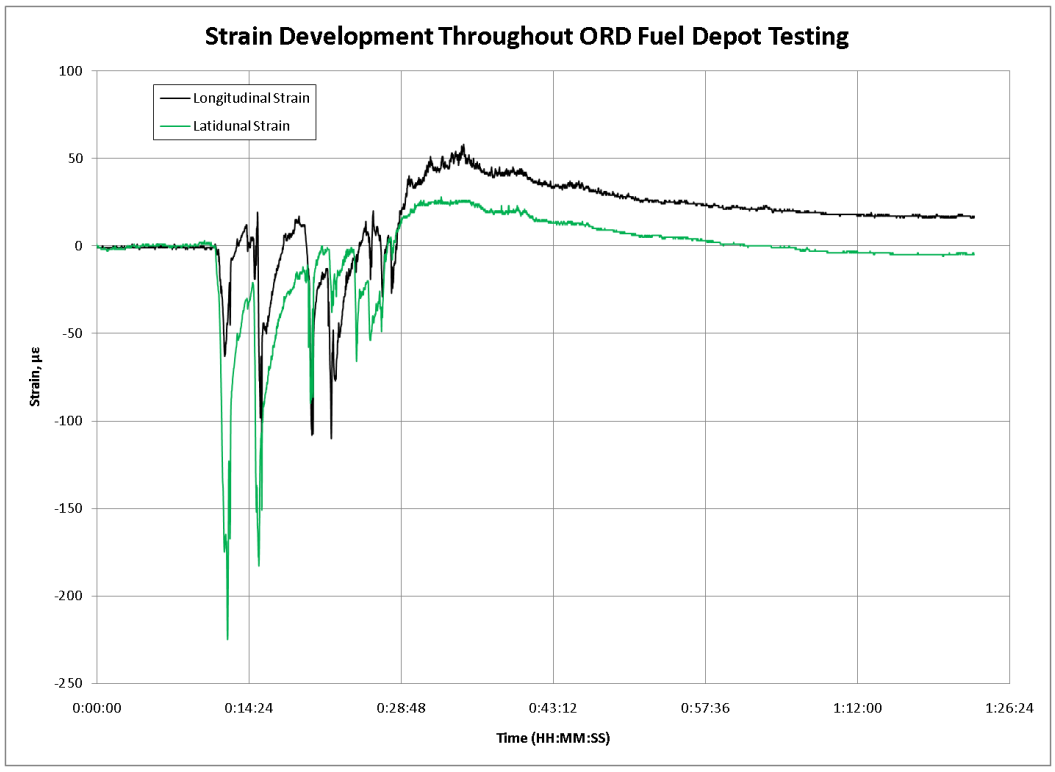

Figure 5.13 Strain development for ORD Fuel Depot test

Figure 5.14 View of NSEL #1

Figure 5.15 View of NSEL #2 (below) and NSEL #3 (above)

Figure 5.16 View of NSEL #2 (left) and NSEL #3 (right)

Figure 5.17 View of NSEL #4 (left)

Figure 5.18 View of NSEL #5 (with strain gages)

Figure 5.19 View of NSEL #6 (lower left)

Figure 5.20 View of NSEL #7

Figure 5.21 View NSEL #8 before testing (lower center)

Figure 5.22 View of Rantoul Airport slab to be tested

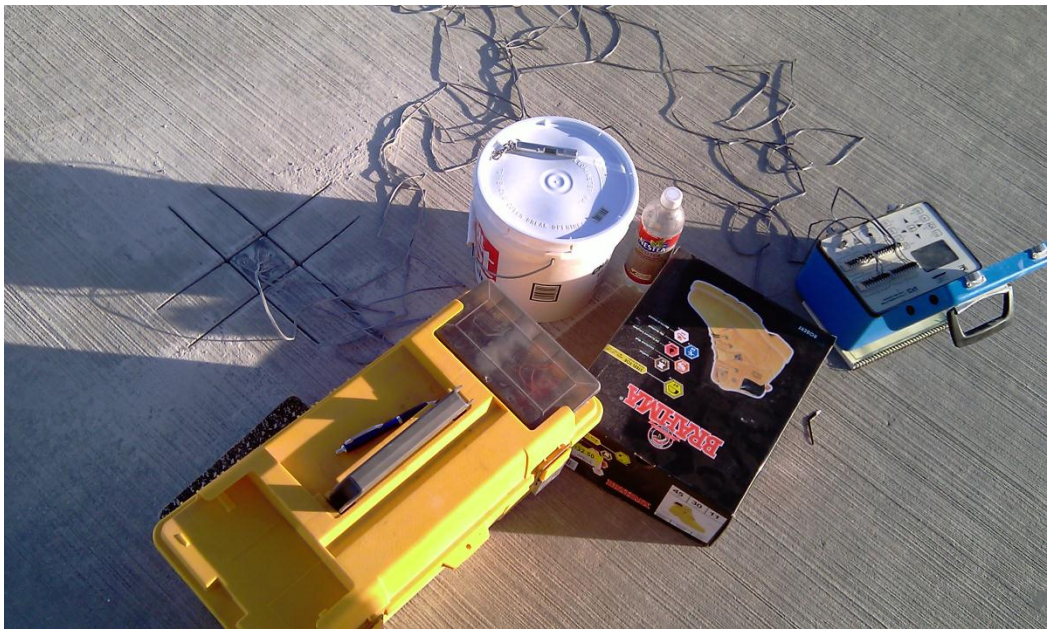

Figure 5.23 Testing at ORD Fuel Depot with bucket providing shade to testing location.

CHAPTER 6: FINITE ELEMENT MODELING

6.1 Introduction

The simple geometry pursued during testing lent itself to eventual FEM analysis. Two major analyses were performed: one for the slabs tested at ATREL with an applied load and another for the multiple tests performed at the NAPTF. The results from these analyses could be used to compare the experimental results and the theoretical results to provide credence for the testing procedure as a viable testing method. Patran 2008 was used to construct the slab models while ABAQUS was used as a processor.

6.2 Modeling of ATREL Slabs

The slabs at ATREL were modeled in Patran as Hex8 elements with 0.5 inch element lengths. A total static load of 20.28 kips was applied as discrete point loads of 30 lbs across 676 nodes at the center edge of the modeled slab in a geometry in accordance with past testing. The stiffness of the concrete material was estimated at 4.5×10^6 psi with a Poisson's ratio of 0.15 and a density of 0.0833 pci. The Winkler foundation was modeled as grounded non-linear springs with a stiffness of 10.7 lb/in in compression and 0 lb/in in tension. This support allows for the modeled slab to undergo vertical lift-off as is typical in most pavement systems.

The width of the notches was established at 0.15 inches and used to construct the isolated square area of material. This square area was modeled in two locations: centered 2 feet from the edge of the slab with the load and 3 feet from the edge of the slab with the load. At either of these locations, four notch geometries were modeled: 2 inch spacing, 3 inch spacing, 4 inch spacing and 5 inch spacing. Each of these notch geometries was deepened in its material in 0.5 inch increments to an ultimate depth of 2.0 inches (or 2.5 inches in the case of the isolated square material with notches spaced 5.0 inches apart).

Elements contained within the surface of the isolated square area were flagged in Patran and later extracted from the ABAQUS processed results file. These elements contained calculated stress and stain values in both the longitudinal and latitudinal directions. These modeled results could be graphed in order to ascertain behavior for deepening saw cuts around material. Their graphical results are depicted at the end of this chapter.

Figures 6.3 through 6.8 depict the magnitudes of the Von Mises stresses in the modeled ATREL slabs where the strain rosette is located 2 feet from the midline edge and the isolated square area measures 3x3 inches. The stress of each model element is plotted against the notch

depth-to-spacing ratio in the ensuing graphs. Larger sized isolated squares like those with dimensions of 5 inches by 5 inches contain 100 elements along the top surface since the element lengths are 0.5 inches long. Isolated squares of 4 inches by 4 inches contain 64 elements, 3 inches by 3 inches contain 36 elements and 2 inch by 2 inch contains 16 elements.

The stresses of these model elements are defined in two directions: S11 and S33. These directions coincide with the latitudinal and longitudinal stresses, respectively, during testing. Their magnitudes can vary by differing the stiffness of either the subgrade support or the stiffness of the material used as inputs in the analysis. The stress magnitude for each model element is plotted against the notch depth-to-spacing geometry. A third-order polynomial best-fit line is calculated for these modeled data points.

Superimposing the experimental stress values obtained from test results and comparing them with the best-fit lines of modeled stresses results in Figures 6.9 and 6.10. While the experimental stress values do not necessarily coincide with the modeled curves, they do trend in the same direction. This suggests that the underlying modeled Winkler foundation is too elastic and allows for excess bending and flexure. However, an iterative process can be undertaken to modify the modeled stress values to better coincide with the experimental stress values. Proceeding with this process can lead to the back-calculation of the stiffness of the subgrade support. This effort is unnecessary, however, since Figures 6.11 through 6.14 reveal interesting behavior.

While the Von Mises stress magnitudes differ significantly between the strain rosettes located 2 feet from the slab edge and 3 feet from the slab edge, the percent of applied stress relieved is remarkably similar. This suggests that regardless of the stress state of a concrete pavement or structure, the magnitude of stress can be assuredly relieved if an appropriate saw cut depth is reached. As a consequence, calculations for the residual stress are not affected if the stiffness of the underlying subgrade is unknown.

Based on this observation, an additional model was created where the notch spacing was 2 inches. While no experimental test was performed with this geometry, it allowed for the formation of Figure 6.18. This graph was devised by extracting from each notch spacing graph the minimum notch depth-to-spacing ratio required to relieve 100% of the applied stress. Thusly, a seemingly non-linear relationship was devised which suggests the minimum notch depth-to-

spacing ratio given a notch spacing. The graph also depicts the minimum depth required to achieve that same ratio.

It is interesting to note however that these minimum notch depth-to-spacing ratios do not coincide with the experimentally determined notch depth-to-spacing ratio of 0.40. Figure 6.17 shows the longitudinal and latitudinal calculated stresses from an applied load from strain rosettes spaced either 2 feet or 3 feet from the slab edge. A third-order polynomial fit function reveals that the minimum notch depth-to-spacing ratio is approximately 0.33 to 0.36.

6.3 Modeling of NAPTF Slab

An FEM analysis was created in PATRAN and processed through ABAQUS to characterize the behavior of the loaded concrete slab located at the NAPTF. In Figure 6.19, two wheel loads, demonstrated by P, are positioned along the top-left edge. The 40,000 pound-force individual wheel loads are distributed along an approximate area of 170 in^2 inducing an approximate strain magnitude of $77x10^{-6}$ in the EW-direction (Z-axis) and $-10.8x10^{-6}$ in the NS-direction (X axis) in the vicinity of the notch location. This differs from the experimental strain observations significantly (magnitudes upwards of 350% and 35%, respectively).

The FEM analysis was moderately fine-tuned; it uses an approximate E-modulus of 4,500 ksi, a density of 144 pcf and a Winkler spring foundation with nodal grounded spring supports spaced 1.0 in apart with a stiffness coefficient of 10.7 lb/in acting solely in compression. An iterative process was performed with the spring stiffness in order to achieve a result that is similar in magnitude to the experimental results. Stiffening the Winkler foundation support can decrease the magnitude of the modeled strain magnitudes, but doing so would veer away from the experimental results. The more important observation will be the percentage of the nominal stress alleviated when saw cuts are included.

It should be noted that the modeled strain value (Z-axis) is in the same direction of the strain channel that seemingly recorded permanent creep-like deformations (see Figure 4.3). If the latter portion of Figure 4.3 were isolated, then the modeled strain value deviates from the experimental strain value by approximately 94%, instead.

A similar FEM analysis was performed for a concrete slab with wheel loads positioned about the center-edge of the concrete slab. The strain magnitudes in the EW-direction (Z-axis) and NS-direction (X-axis) were $44.4x10^{-6}$ and $-34.8x10^{-6}$, respectively. This differed from the experimental results by approximately 1% and 440%, respectively, in Test C1 and 120% and

420%, respectively, in Test D1. Similarly, an iterative process needs to be considered in order to more closely match the experimental results with the theoretical results. However, the discrepancy between the experimental, symmetrical tests of C1 and D1 suggests that an exact model will be unable to capture subtle variations in the material and the support. The same Winkler support and material properties were used.

6.4 Figures and Graphs

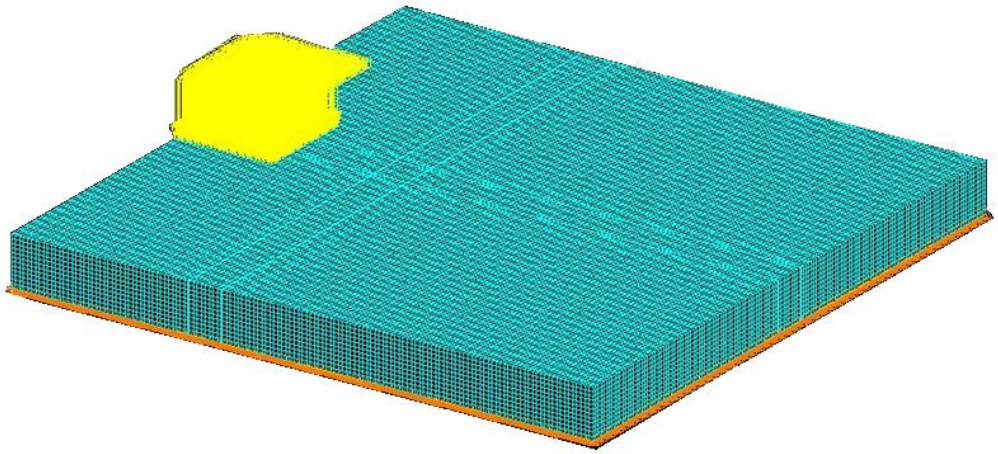

Figure 6.1 Isometric view of 6 foot x 6 foot x 6in modeled slab with spring supports and distributed loading

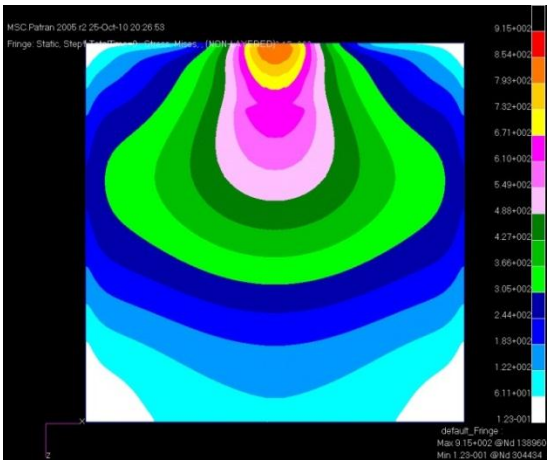

Figure 6.2a Von Mises stress distribution of slab with isolated 3x3 inch squared area located 2 feet from the slab edge cut to 0.0 inch depth.

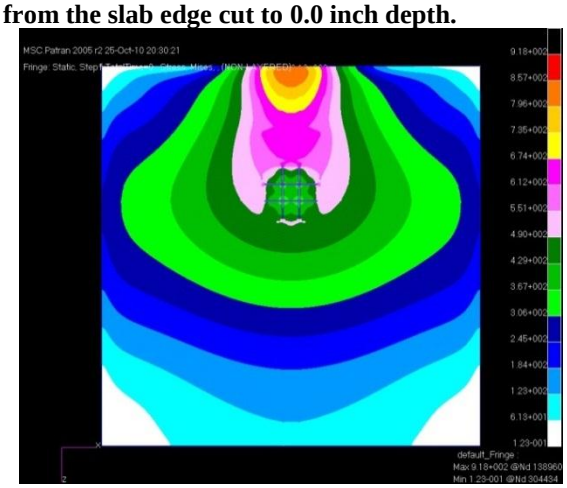

Figure 6.2b Von Mises stress distribution of slab with isolated 3x3 inch squared area located 2 feet from the slab edge cut to 0.5 inch depth.

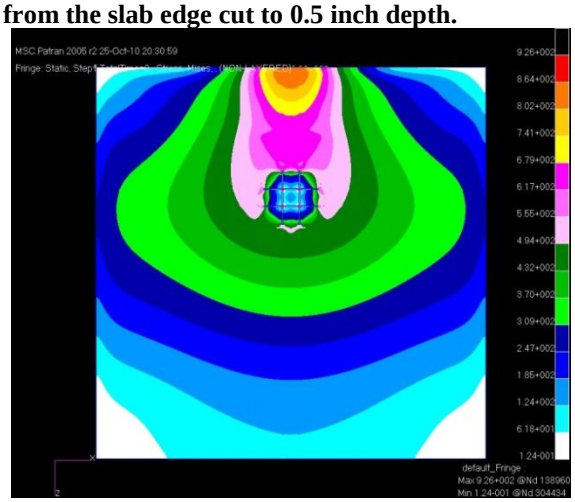

Figure 6.2c Von Mises stress distribution of slab with isolated 3x3 inch squared area located 2 feet from the slab edge cut to 1.0 inch depth.

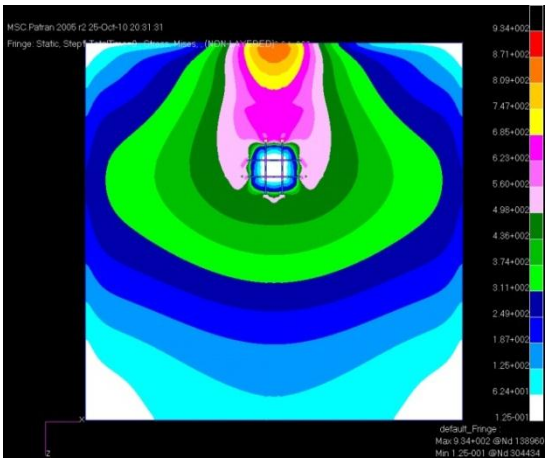

Figure 6.2d Von Mises stress distribution of slab with isolated 3x3 inch squared area located 2 feet from the slab edge cut to 1.5 inch depth.

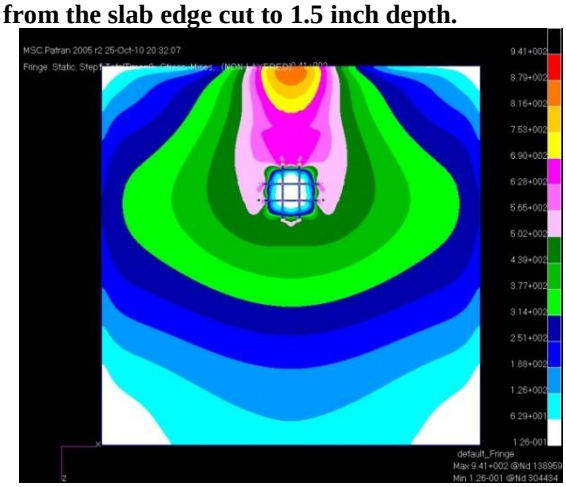

Figure 6.2e Von Mises stress distribution of slab with isolated 3x3 inch squared area located 2 feet from the slab edge cut to 2.0 inch depth.

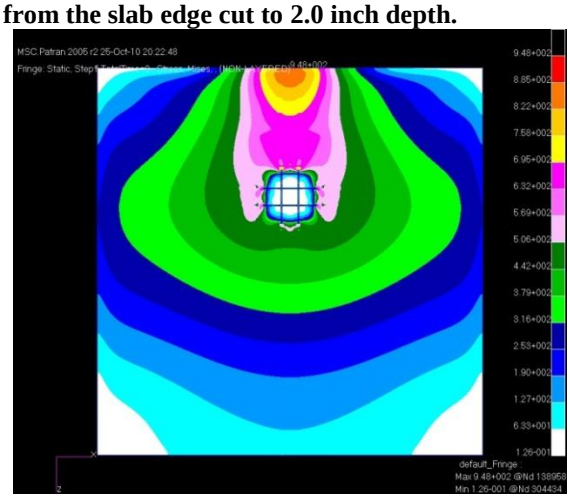

Figure 6.2f Von Mises stress distribution of slab with isolated 3x3 inch squared area located 2 feet from the slab edge cut to 2.5 inch depth.

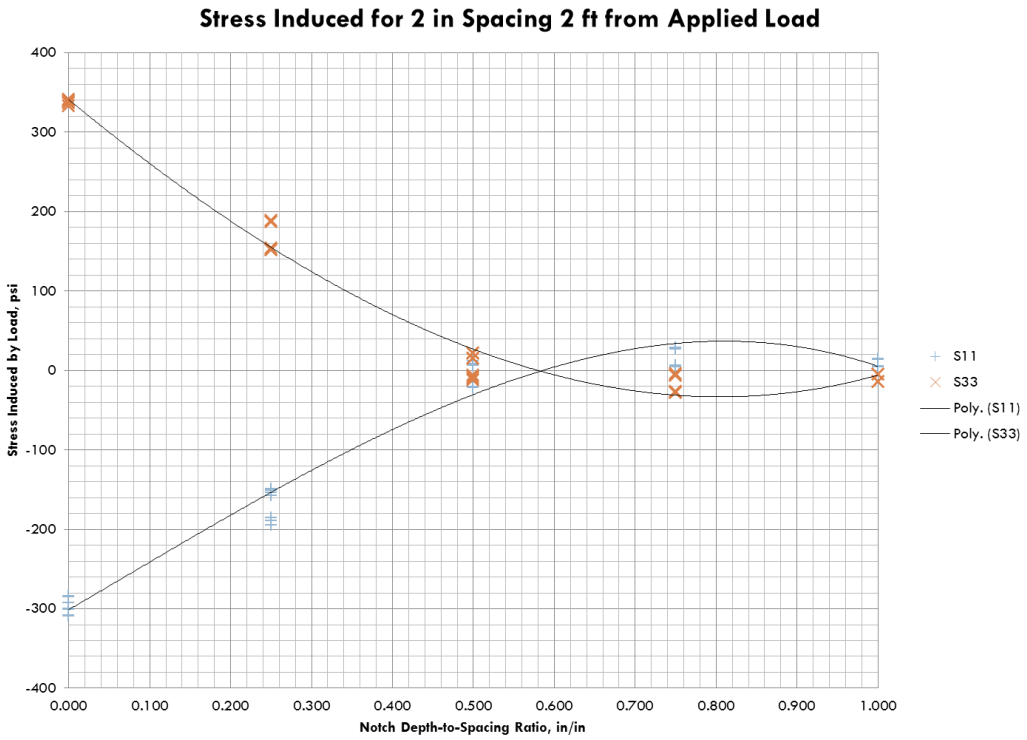

Figure 6.3 Longitudinal and latitudinal Von Mises stress magnitudes for isolated square 2 feet from edge of slab with notch spacing of 2 inches

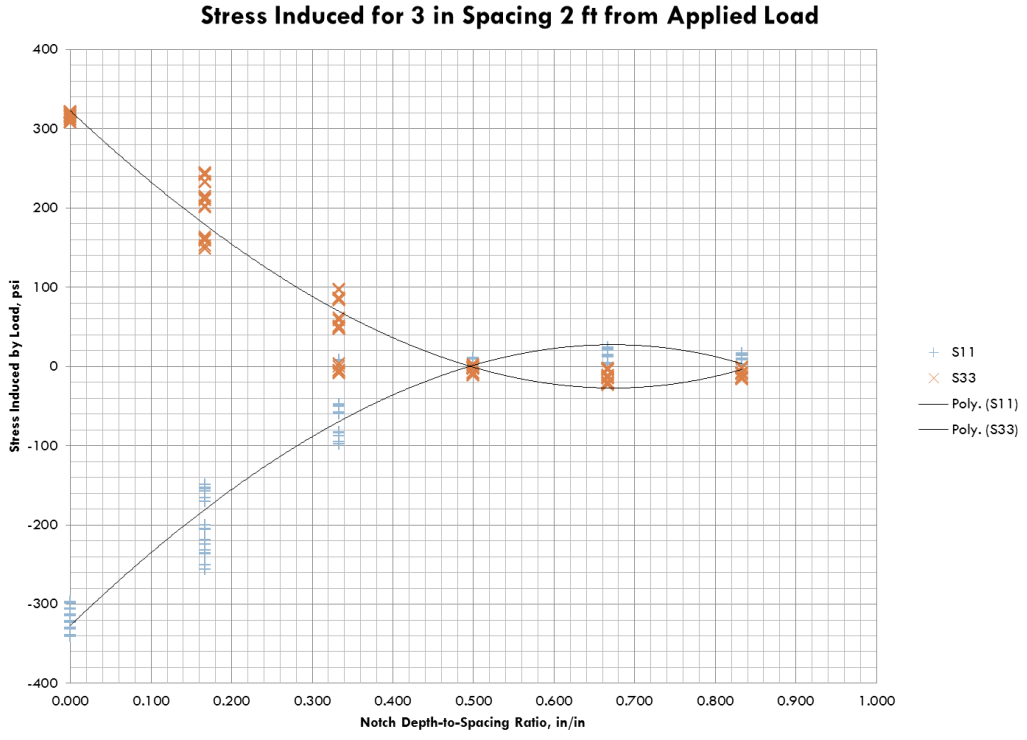

Figure 6.4 Longitudinal and latitudinal Von Mises stress magnitudes for isolated square 2 feet from edge of slab with notch spacing of 3 inches

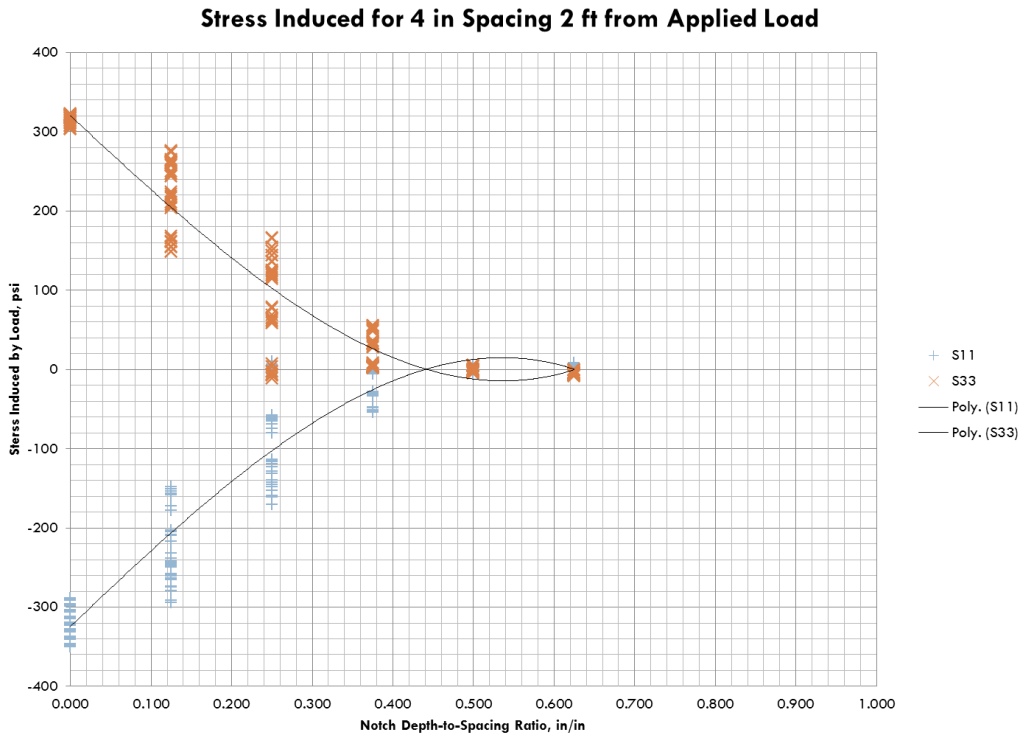

Figure 6.5 Longitudinal and latitudinal Von Mises stress magnitudes for isolated square 2 feet from edge of slab with notch spacing of 4 inches

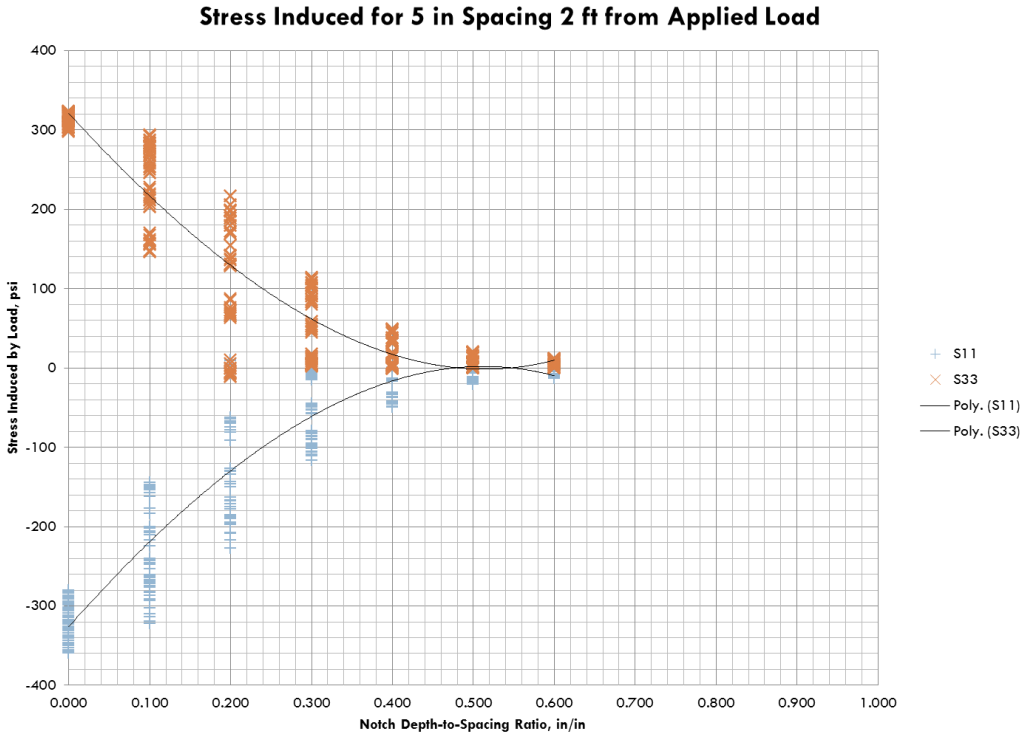

Figure 6.6 Longitudinal and latitudinal Von Mises stress magnitudes for isolated square 2 feet from edge of slab with notch spacing of 5 inches

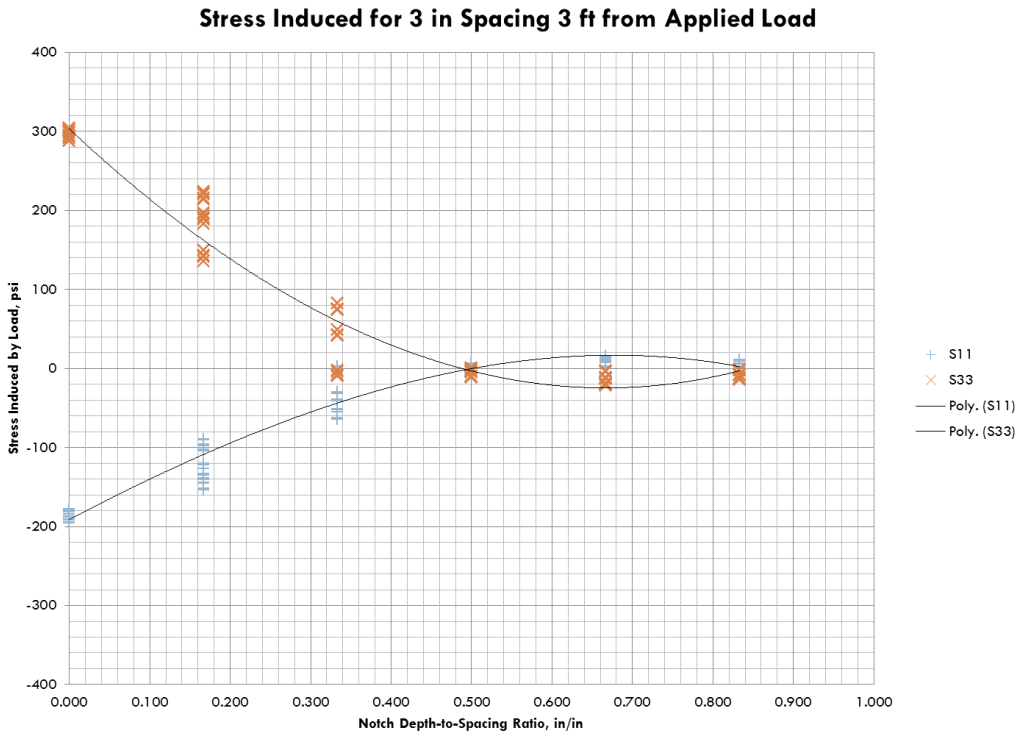

Figure 6.7 Longitudinal and latitudinal Von Mises stress magnitudes for isolated square 3 feet from edge of slab with notch spacing of 3 inches

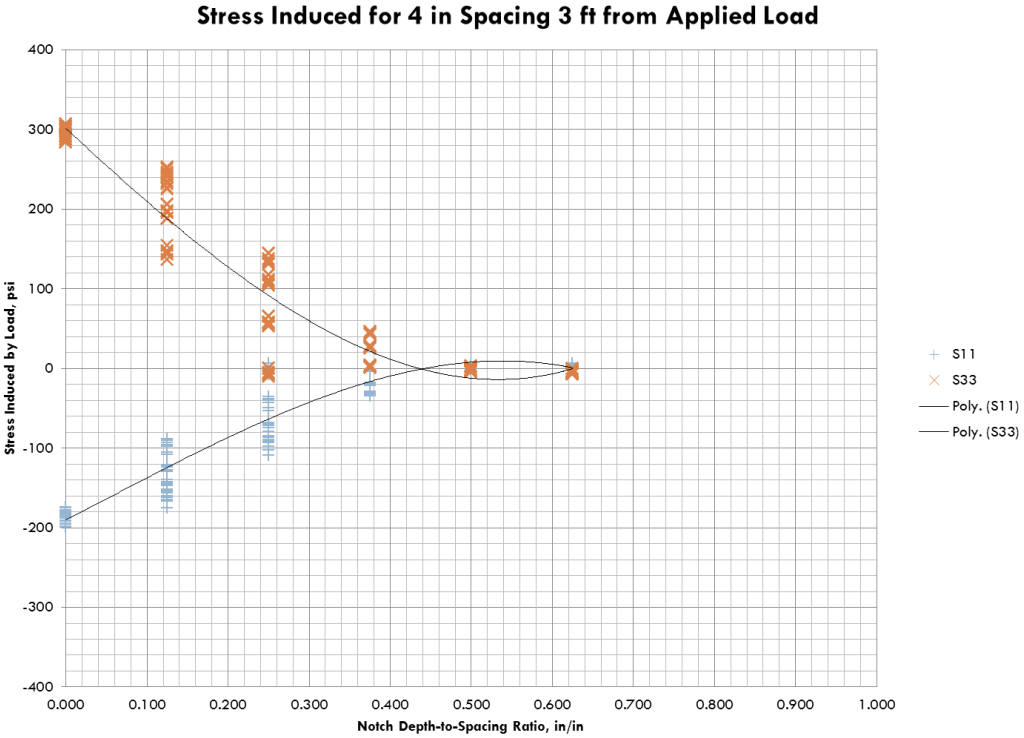

Figure 6.8 Longitudinal and latitudinal Von Mises stress magnitudes for isolated square 3 feet from edge of slab with notch spacing of43 inches

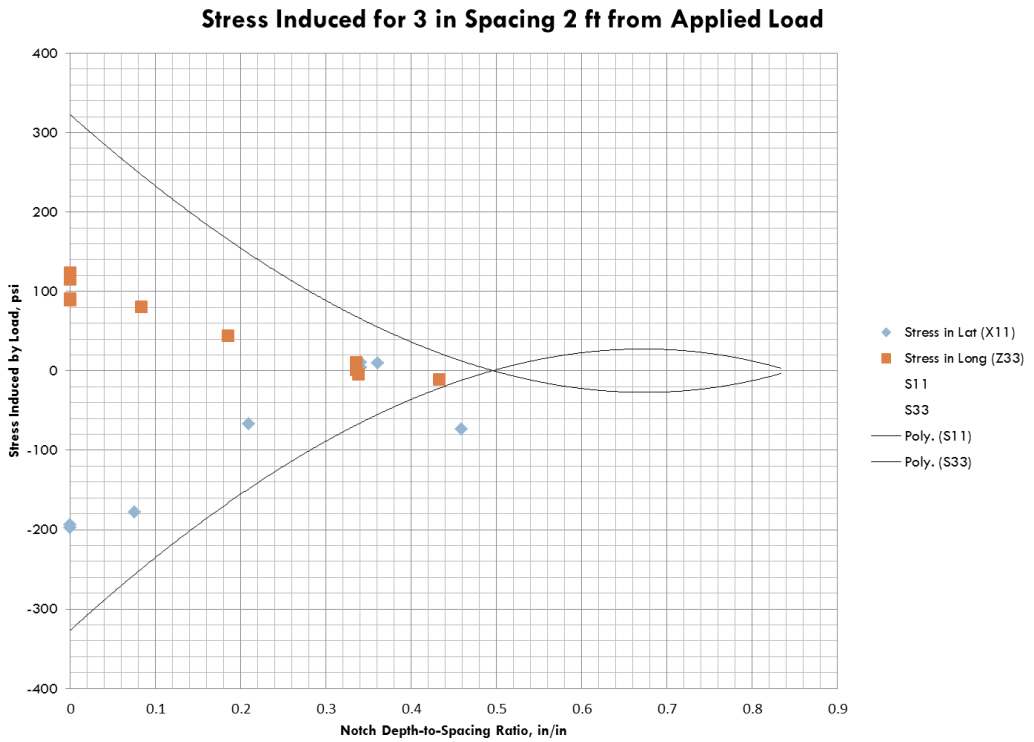

Figure 6.9 Comparison of experimental calculated stresses with modeled trend line for isolated square 2 feet from slab edge and with notch spacings of 3 inches

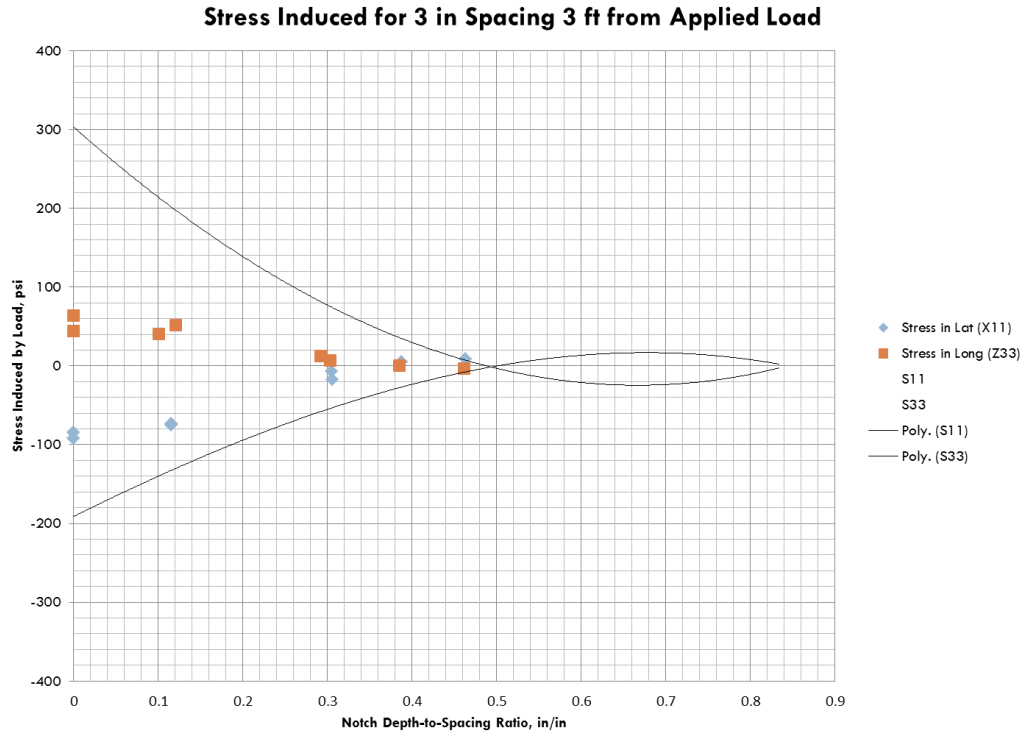

Figure 6.10 Comparison of experimental calculated stresses with modeled trend line for isolated square 3 feet from slab edge and with notch spacings of 3 inches

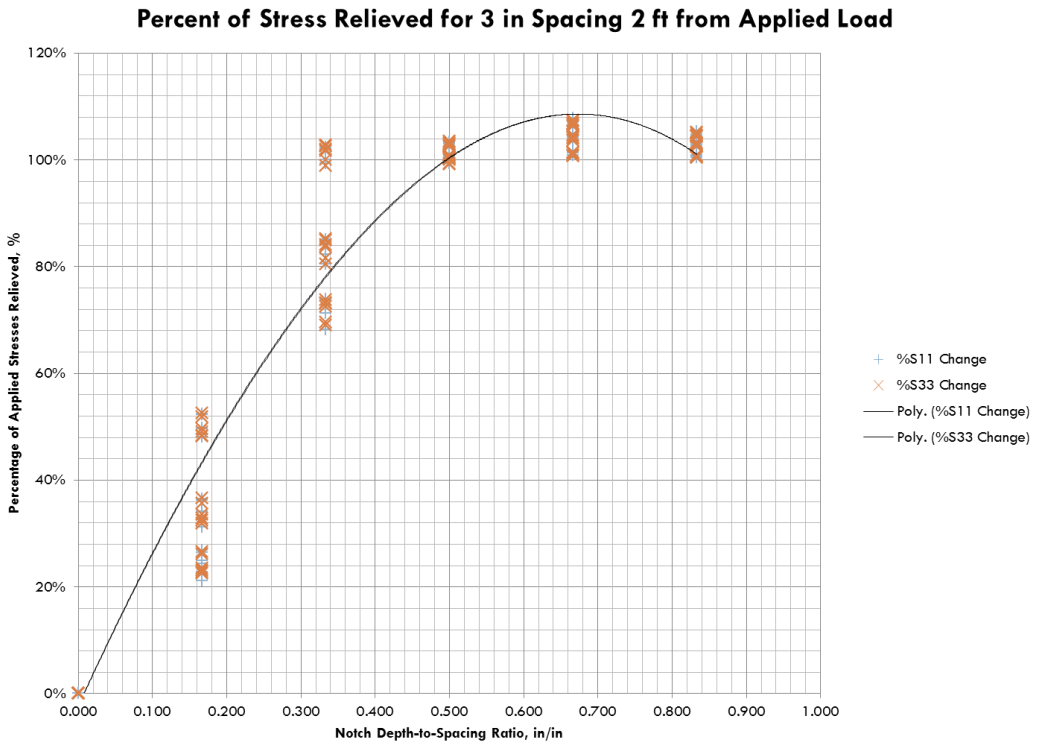

Figure 6.11 Percent of modeled applied stress relieved by increasing notch depth-to-spacing ratio

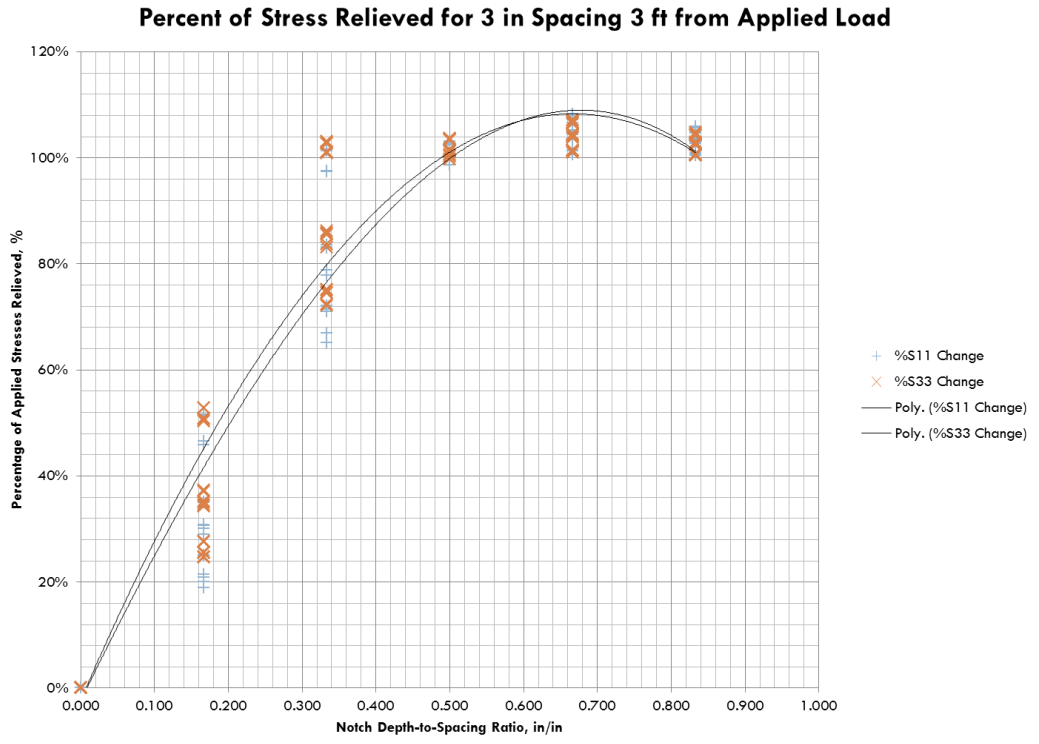

Figure 6.12 Percent of modeled applied stress relieved by increasing notch depth-to-spacing ratio

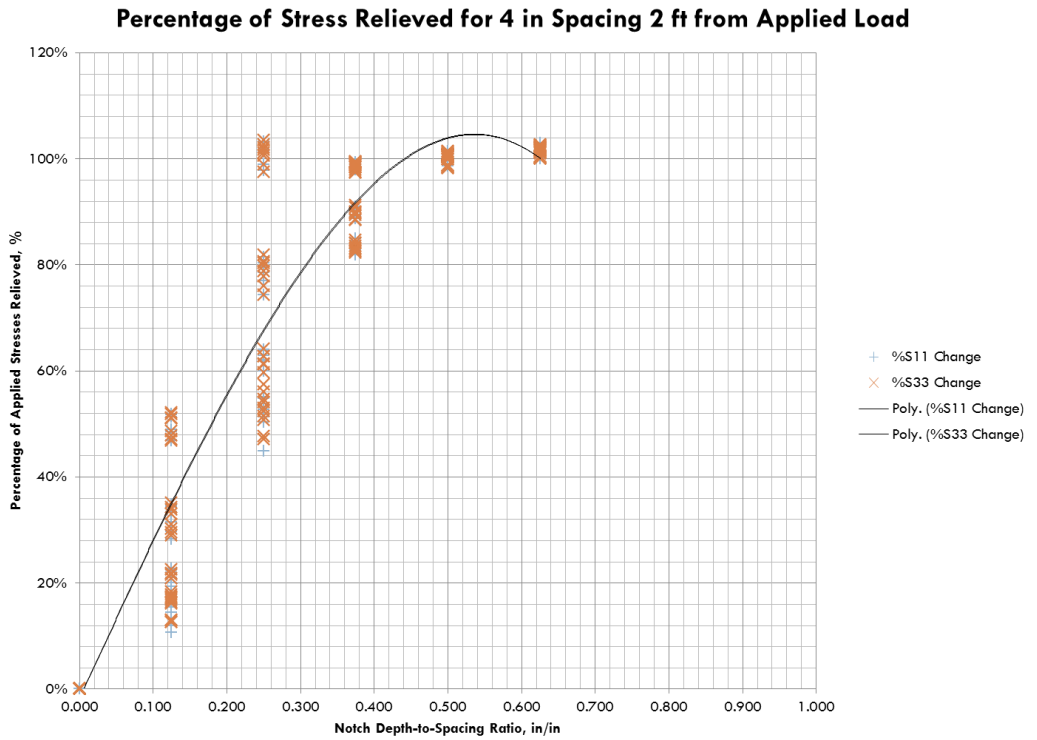

Figure 6.13 Percent of modeled applied stress relieved by increasing notch depth-to-spacing ratio

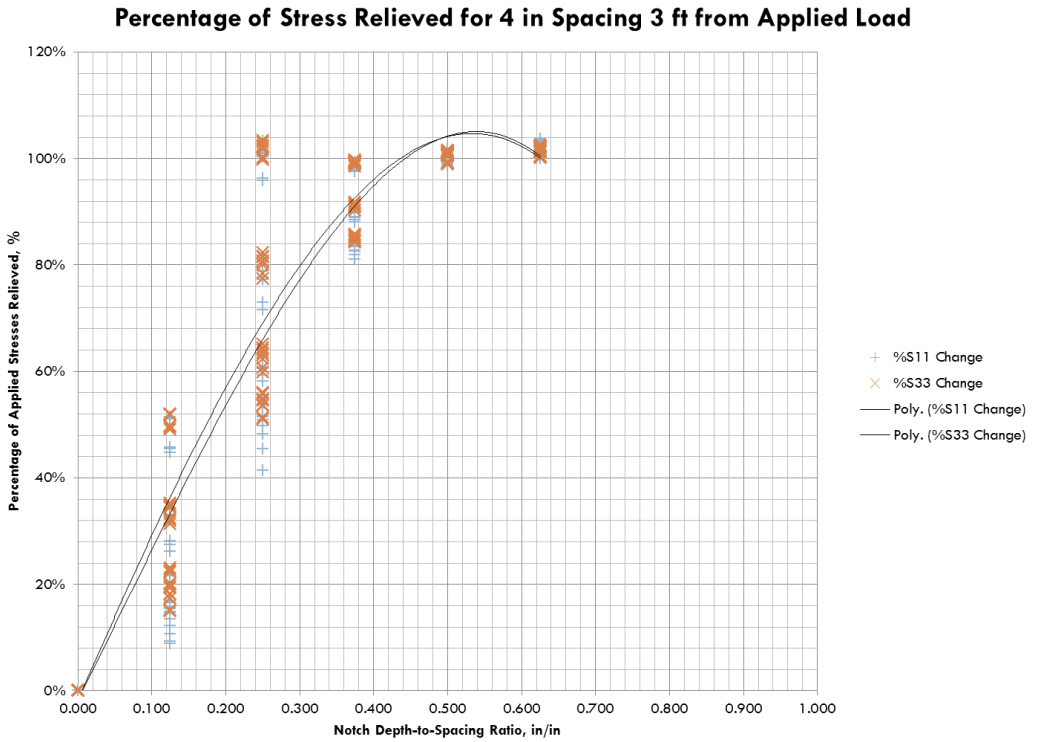

Figure 6.14 Percent of modeled applied stress relieved by increasing notch depth-to-spacing ratio

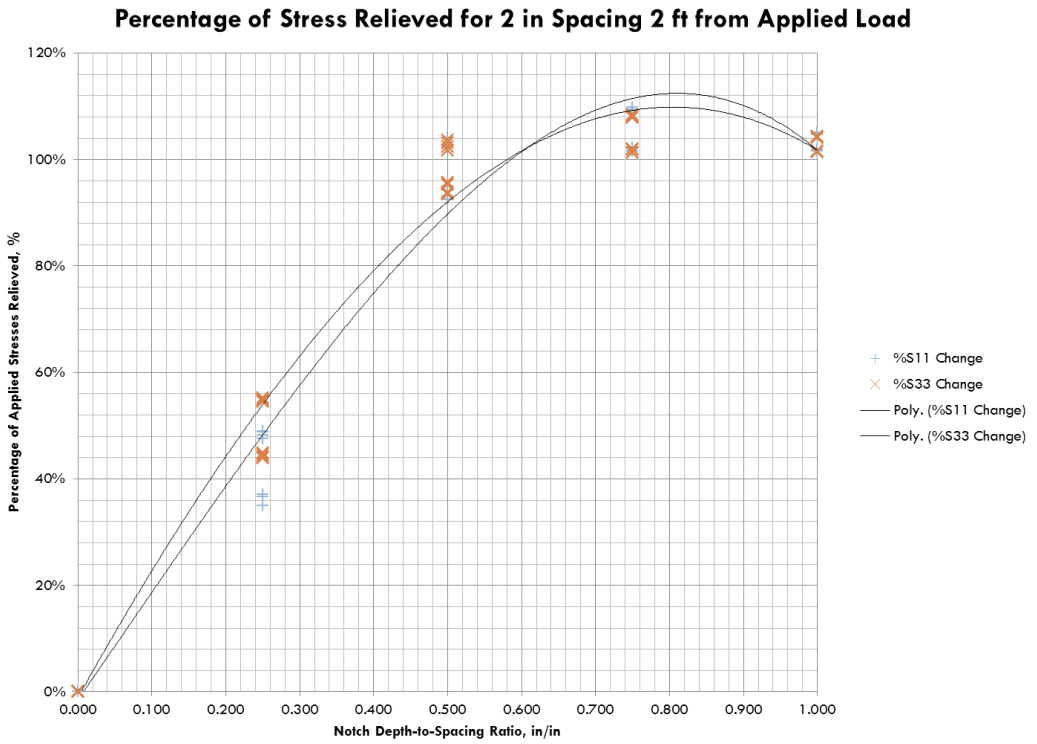

Figure 6.15 Percent of modeled applied stress relieved by increasing notch depth-to-spacing ratio

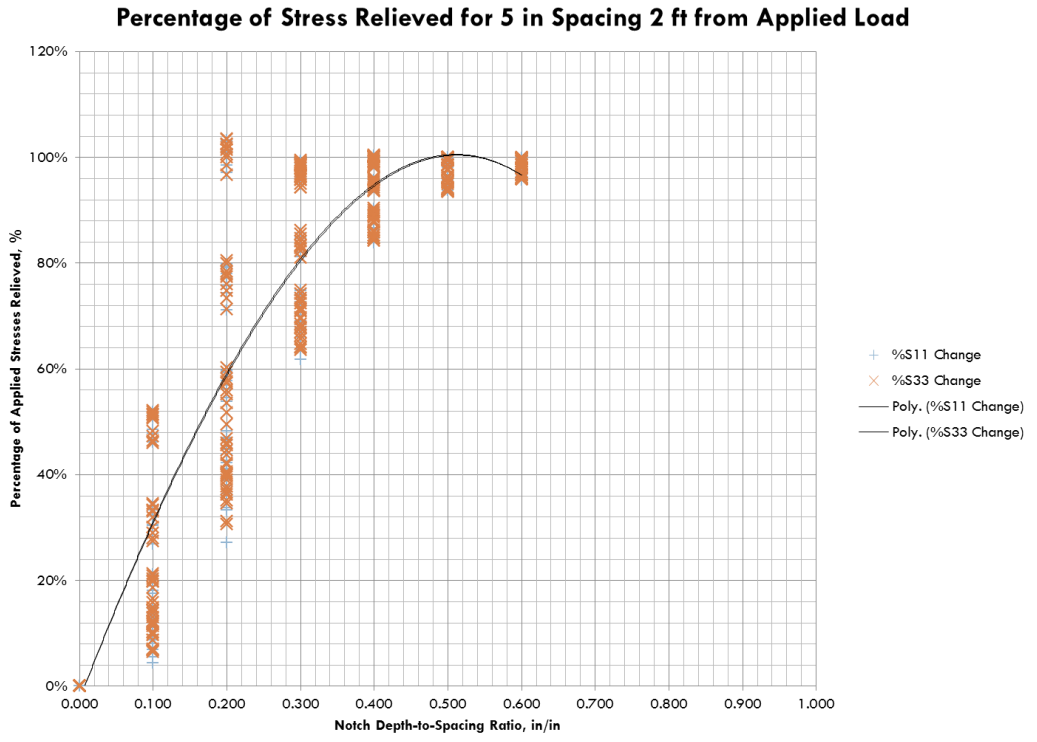

Figure 6.16 Percent of modeled applied stress relieved by increasing notch depth-to-spacing ratio

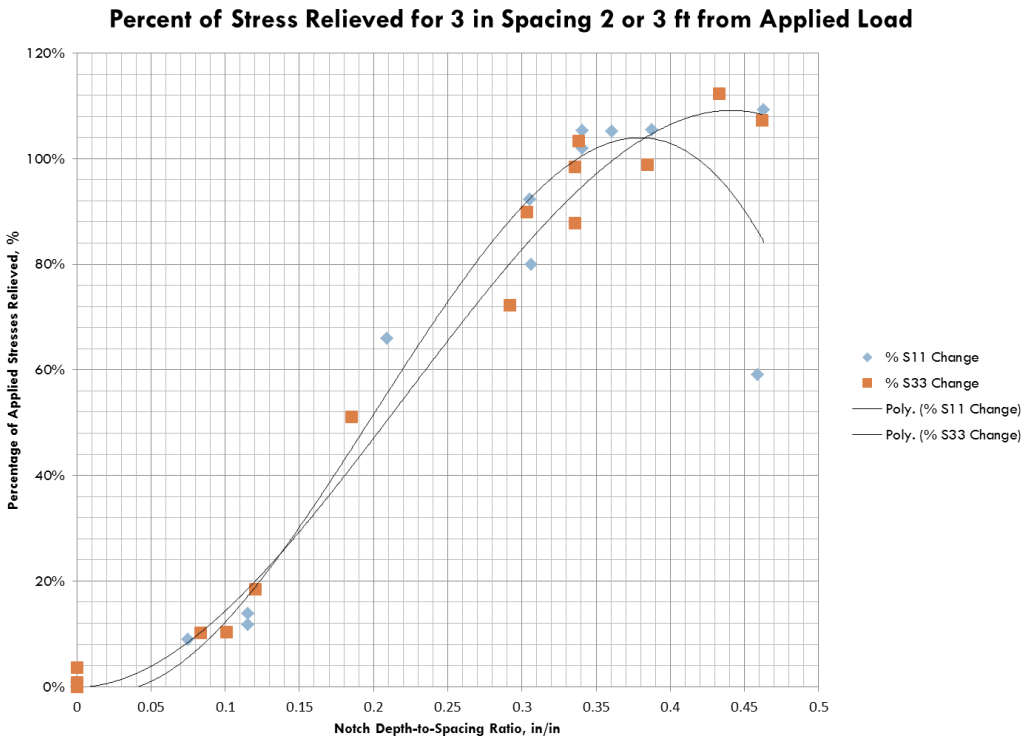

Figure 6.17 Percent of experimental applied stress relieved by increasing notch depth-to-spacing ratio

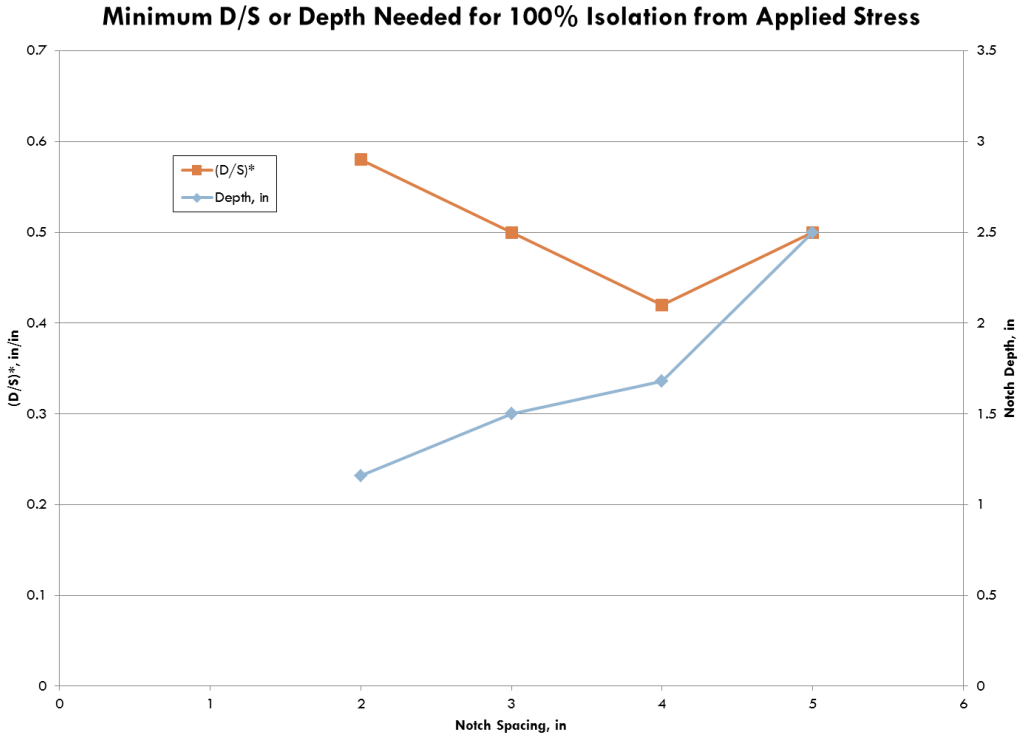

Figure 6.18 Minimum required notch depth-to-spacing ratio or notch depth to relieve 100% of applied stress

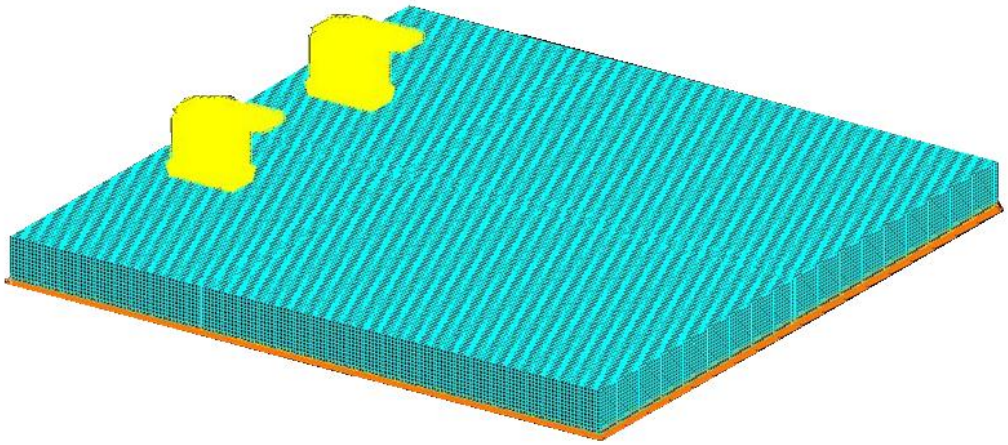

Figure 6.19 Isometric view of 15 foot x 15 foot x 12in modeled slab with spring supports and distributed loading

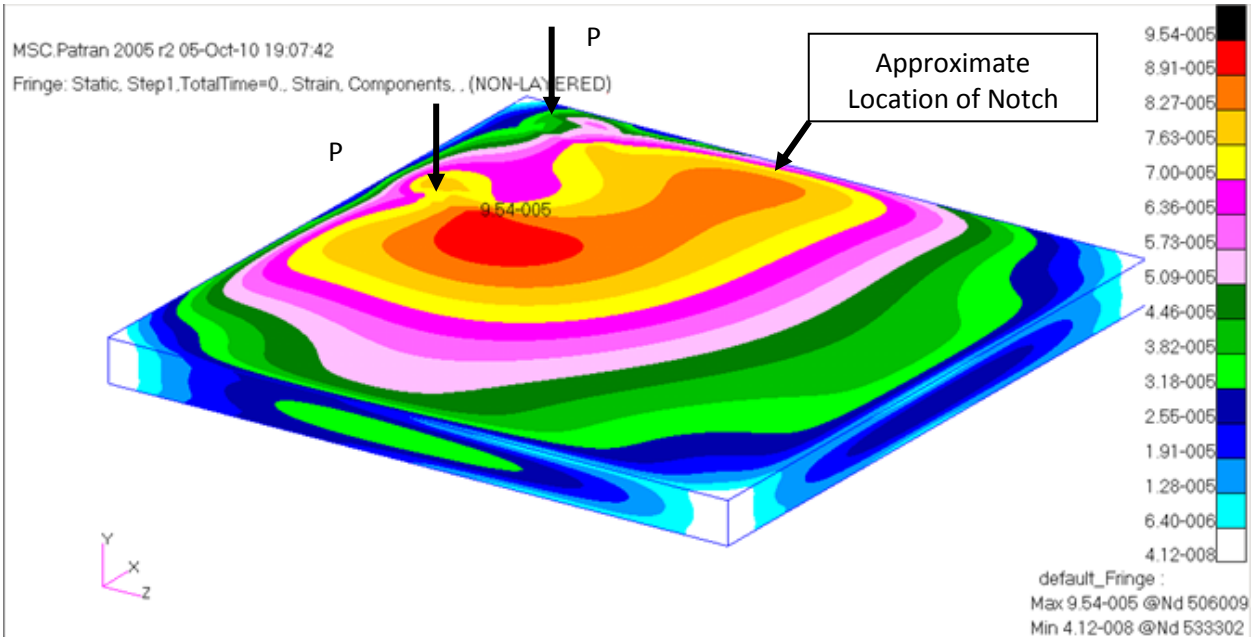

Figure 6.20 Distribution of Von Mises stresses in FEA Model of 15ft x 15ft x 12in Slab atop Winkler spring foundation with wheel loads positioned at center-edge-corner

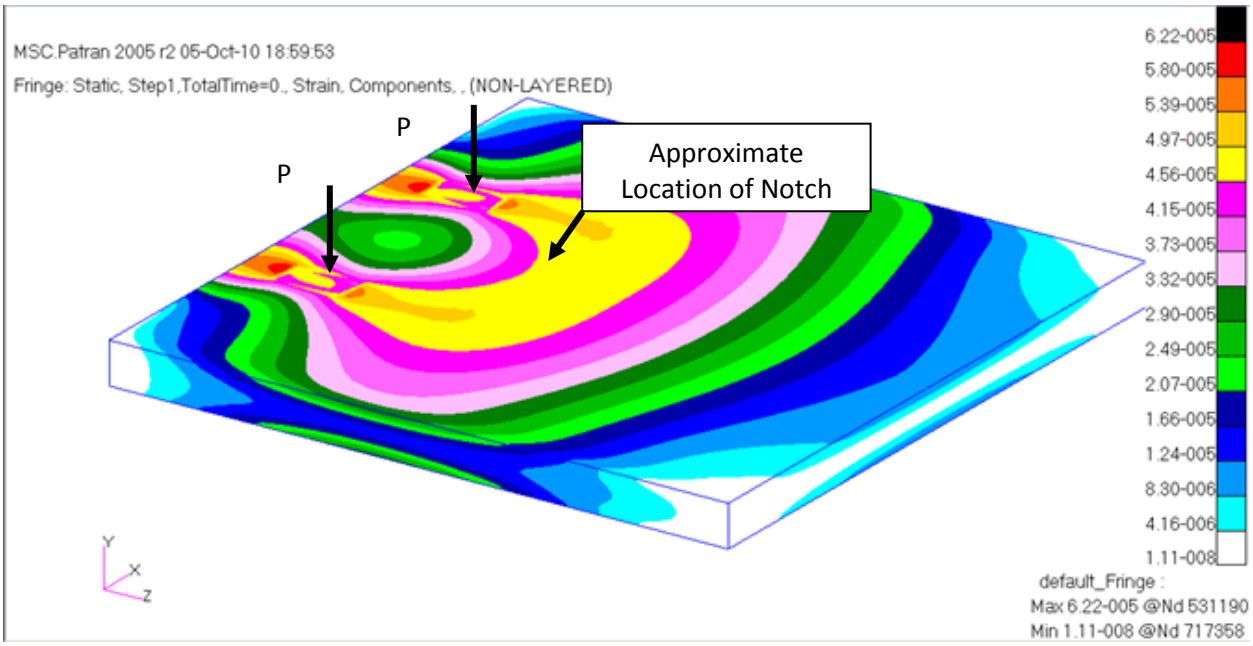

Figure 6.21 Distribution of Von Mises stresses in FEA Model of 15ft x 15ft x 12in Slab atop Winkler spring foundation with wheel loads positioned at center-edge

CHAPTER 7: DISCUSSION AND CONCLUSIONS

7.1 Introduction

The results obtained from experimental testing as well as those attained from FEA modeling offer insight into the validity of this testing procedure as a viable method for measuring the residual stress in plain concrete. Several observations and remarks are noted in the following sections for the experimental tests performed on the discarded slabs used for proof-of-concept testing, in-situ slabs at ATREL and the NAPTF slab.

7.2 Remarks for Discarded Slabs

The discarded slabs tested at ATREL were tested in an indoor, controlled environment. The results from these four experiments suggest that the testing procedure can be appropriately considered in larger-sized concrete slabs as well as beams. What these results more importantly demonstrate is that appreciable material stresses are present in concrete slabs without an applied load.

It is also important to realize that the geometry of the saw cuts can be modified, if needed. Their squared shape was maintained in order to calculate both principal stresses as well as stresses in the latitudinal and longitudinal directions. However, if the latter is not desired, then triangular or pentagonal cuts may be made. It is important to emphasize again that these cuts can be made granted that their application is a dry-cut. Previous testing using core-rings and cooling water demonstrate that the addition of water generates eventual drifting of the strain readings. This is likely due to the absorptive nature of the concrete material as it expands and relays that expansion through altered strain results. This problem occurs, naturally, because the cooling water seemingly introduces a moisture gradient into the tested material.

It is also important to realize that closely spaced notching can better alleviate material stresses than distantly spaced notching. This is potentially due to the ineffectiveness of distant saw cuts to alter the stress state of the immediate bulk material that the strain rosette directly measures. As such, a prescriptive methodology can be pursued for alternative notching geometries wherein an initial notch depth-to-spacing ratio of 0.40 is created and, after strain stabilization is achieved, can be followed by deepening the saw cuts by an additional 0.5 inches. If the change in stabilized strain between this second set of cuts differs from the first set of cuts, it is indicative that the full isolation from residual stresses has not been achieved. This necessitates additional cutting of the material. However, if the difference in stabilized strains is

within 5% of the previous set of stabilized strains, then the results demonstrate that the residual stresses have been appropriately identified.

7.3 Remarks for ATREL Slabs

The in-situ slabs tested at ATREL in an outdoor environment were tested with careful consideration to their environment which must be considered in any future application of this test. Their testing was performed during the early summer months were regular thunderstorms and high humidity rolled through the area. The addition of moisture and heat definitely affected the results of the pavement slabs in a manner to produce biased results. However, these results must be considered with respect to two items.

The first item to consider is that these slabs were tested in environments that typical concrete pavements are subjected to. As such, inducement of stresses due to thermal and moisture gradients are expected and validly affect the final strain measurements. However, great care must be taken, as it was during these tests, to ensure that either gradient is not actively affecting the test results during testing. In order to ensure this, the concrete pavement must be sufficiently dry so that active drying is not actively occurring in the span of the approximately 90 minute testing. Additionally, it is important that shading of the immediate testing site be considered. The shading of the immediate vicinity to be tested should be done at least an hour before testing so that it may cool from its temperature as a result of direct sunlight, but maintain an equilibrium temperature during testing.

While shading is not typical in most concrete pavements, the subjection of direct sunlight onto the strain gages will significantly alter their strain results. It is important, and potentially the driving goal, to measure the stresses induced by thermal effects. In order to do so, this must be done so that the ambient temperature during testing is stable so that an appreciable measurement can be made. If necessary, a secondary test can be performed such that the stresses can be determined at an altered ambient temperature environment.

7.4 Remarks for NAPTF Slab

The notch testing procedure for isolating the stresses continues to show promise as a viable technique for measuring the stress in a plain concrete pavement. However, lessons were learned in these five tests conducted at the NAPTF.

Test A2 reveals the potential limits in which this test can be performed on high-strength concretes. Excessive heating caused by high-strength materials suggests that due to the

equipment used, there may be a limitation of the test to measure concretes of a high stiffness or strength. One immediate remedy that can be performed in order to protect the saw blade from premature damage is to perform the notching in sequences such that the material being removed by notching is a fraction of the total material to be removed.

Test B1 also importantly demonstrates that the geometries of the notches cannot be ignored; all previous testing has been conducted along the interior of concrete slabs while test B1 has been the first to be performed along a free edge. In some instances, such as loss of subgrade support, the stresses at these edges will be of highest concern and it may be of interest to measure their total stress. However, the notch depth-to-spacing ratio of 0.40 shows to be an inadequate geometric configuration to fully isolate the stress observed by the strain rosette (as demonstrated in Figure 4). This brings to light that this testing procedure cannot be applied blindly to any plain concrete pavement without careful consideration for that slab's geometry and location of testing.

Tests C1 and D1 have the most interesting results since they were designed to be symmetric and identical testing situations. While the difference in the measured stress can be expected, the difference in response due to an applied is not. While there can be small discrepancies of the E-modulus and subgrade support resulting in dissimilar results, it is unclear whether these factors can range widely enough to produce the strain responses as depicted in these tests. However, these two tests, along with test A1, demonstrate that there is a correlation between the notch depth-to-spacing ratio and the isolation of the applied loads (to an extent) and the stresses can be achieved.

There remain at the NAPTF two strain rosettes, B1 and B2, which can be tested further. Strain rosette B1 proved to have been notched at an insufficient depth to fully isolate the stresses. To more fully comprehend its behavior, a follow-up test can be performed wherein the slab is similarly loaded along its corner edge and the strain response observed. Subsequently, the notch depths can be cut an additional 0.5 inches in depth resulting in a notch depth-to-spacing of approximately 0.53. The loading sequence can be applied thereafter and its observations noted. If the response of the strain rosette reverses direction (in this case, if a compressive, pinching effect is observed) it can be deduced that the stresses have been nearly fully isolated. Otherwise, if the change in strain from the previous testing is markedly similar before testing, it can be concluded

that the stresses had been already isolated beforehand. This however, is likely not the case for the already tested B1.

Test B2 is wholly available to be tested in any configuration as desired, although it would be interesting if another symmetrical case (say a fictitious strain rosette, B3, affixed 10 feet eastwards and 33 inches southward from the Northwest corner) were also performed. In this manner, another testing sequence similar to tests C1 and D1 can be performed to better understand the behavior of the slab and the results depicted in C1 and D1.

Suggestions from several persons who are closely following this project have voiced their favorability for limiting the minimum required depth of the notch to isolate stresses. Future testing should be planned which incorporate gages of smaller length so that a smaller square area can be isolated for. As such the notch depth-to-spacing ratio will be tested against these smaller dimensions and can potentially reduce the minimum required depth to successfully isolate the stresses from the strain rosette. However, caution should be undertaken since concrete is a material heterogeneous material. Using smaller length strain gages can result in erroneous strain data if it is affixed immediately above an unseen aggregate. It is recommended that an appropriate sized strain gage be used to better depict the behavior of the composite material.

7.5 Conclusions

While the bulk of testing for this thesis was performed on pavements, it is strongly believed that this testing procedure is generally applicable to concrete structures. This is because of the nature of the test and the observed FEM results. Despite the stress state or loading of a concrete structure, the percent of stress relieved at an internal location of the concrete surface should be remarkably similar to those found in these results. The determination of the total stress in the concrete structure can be compared with its computed stress and a residual stress can be found.

It is important to note the limitations of this proposed testing procedure once more. Its direct measurement is that of surface strains which can be computed into surface stresses. While induced stresses from applied loads may act in classical bending, shear or axial manners, the residual stresses may act in a non-linear fashion. This, again, is due to the nature of the development of the stresses where they are a result of differential drying and improper compaction in the plastic state of the freshly cast concrete.

Moreover, a given residual stress test result is an indication of the stress state at the time of testing, and the state of residual stress in known to change with time. This is because the measurement captures the stresses induced by non-changing thermal and moisture gradients at the time of testing. These stresses freely change over time as concrete undergoes daily thermal cycling and seasonal wetting and drying. Thus, it is prudent to consider repeated testing over time in order to better characterize the true effect of external gradients acting upon the plain concrete structure and to better understand its residual stress state.

REFERENCES

ASTM E837. Standard Test Method for Determining Residual Stresses by the Hole-Drilling Strain-Gage Method. 2008.

"Modeling aggregate interlock load transfer at concrete pavement joints." In *Dissertation Thesis*, by Anna C. Brink. University of Pretoria, 2003.

Caliendo, Ciro, and Alessandra Parisi. "Stress-Prediction Model for Airport Pavements with Jointed Concrete Slabs." *Journal of Transportation Engineering*, 2010: 664-677.

Cervantes, V., and J. Roesler. *Performance of Concrete Pavements with Optimized Slab Geometry.* Rantoul, IL: Illinois Center for Transporation Series 09-053, 2009.

Guo, E. H., F. Pecht, L. Ricalde, D. Barbagallo, and X. Li. "Data Analysis on Residual Stresses Measured in Concrete Beams." *9th International Conference on Concrete Pavements.* San Francisco, CA, 2008.

Guo, E., and F. Pecht. *Application of surface strain gages at the FAAs NAPTF.* Atlantic City, NJ: FAA Worlwide Airport Technology Transfer Conference , 2007.

Guo, Hua, Frank Pecht, and Lia Ricalde. "Analysis of concrete pavement strain data and behavior during joint formation." *International Journal of Pavement Engineering*, 2010: 173-187.

Hiller, Jacob A. M. , and Jeffery R. Roesler. "Simplified nonlinear temperature curling analysis for jointed concrete pavements." *Journal of Transportation Engineering*, 2010: 654-664.

Huang, Y. H. *Pavement Analysis and Design, 2nd Ed.* Upper Sadle River: Pearson Prentice Hall, 2004.

James, M. R. , and J. Lu. *Handbook of Measurement of Residual Stresses.* Lilburn: The Fairmont Press, 1996.

Marks, D. G., and D. A. Lange. *Development of Residual Stress Measurement for Concrete Pavements through Cantilevered Beam Testing.* MS Thesis, University of Illinois at Urbana-Champaign, 2009.

Mohamed, A. R., and W. Hansen. "Prediction of Stresses in Concrete Pavements Subjected to Non-Linear Gradients." *Cement and Concrete Composites 18*, 1996: 381-387.

Rao, S., and J. R. Roesler. "Nondestructive testing of concrete pavements for characterization of effective built-in curling." *Journal of Testing and Evaluation*, 2005: 1-8.

Richards, A. M. "Measurement of Stres in Concrete Pavements." *Transporation Research Record 713*, 1979: 9-15.

Wells, S. A., B. M. Phillips, and J. M. Vandenbossche. "Quantifying built-in construction gradients and early-age slab deformation caused by environmental loads in a jointed plain concrete pavement." *International Journal of Pavement Engineering*, 2006: 275-289.

APPENDIX: DRAFT ASTM PROCEDURE DOCUMENT

Introduction

This test method directly measures the total stresses at the surface of a plain concrete pavement and indirectly measures the residual stresses. A rectangular strain rosette is affixed atop the surface and the change in strain is observed when four symmetrical, quadrilateral cuts are sawn around it. The residual stress is subsequently calculated using a series of equations.

1. Scope

1.1 *Residual Stress Determination*

1.1.1 This test method measures residual stress at a point on a concrete surface. The method involves mounting strain gages and saw-cutting around them to relieve the stress. The stresses may remain approximately constant with depth ("uniform" stresses) but are more likely to vary with depth ("non-uniform" stresses). The depth of the notches cannot exceed the thickness of the concrete material. Uniform and non-uniform stress measurements are specified for these thick concrete materials.

1.2 *Stress Measurement Range*

1.2.1 This test method identifies in-plane stresses at the surface of a concrete material. It is a localized measurement that is dependent upon the temperature, moisture, location and time of day during testing. As such, the result is a measure of the total stresses on a pavement surface and cannot alone quantify the stresses due to material effects (residual stresses) or applied loads. However, if the environmental conditions are controlled appropriately, then a clear inference can be drawn for the residual stress.

1.3 *Damage and Repair*

1.3.1 This test method requires partial-depth notches to be cut in the concrete. The damage is local and should not be detrimental to the load carried by the concrete structure (assuming a sufficiently large thickness). Precautions must be taken to ensure that the structural capacity of the concrete is not compromised. The notches can be filled with concrete repair material after the testing procedure in order to restore its appearance to a satisfactory condition.

2. Referenced Documents

2.1 *ASTM Standards*

C469 Standard Test Method for Static Modulus of Elasticity and Poisson's Ratio of Concrete in Compression

C873 Standard Test Method for Compressive Strength of Concrete Cylinders Cast in Place in Cylindrical Molds

E837 Standard Test Method for Determining Residual Stresses by the Hold-Drilling Strain-Gage Method

3. Materials Required

3.1 *Equipment*

3.1.1 Surface strain gages of sufficient length for concrete (approximately 20 mm in length or at least sufficiently larger than the largest aggregate contained within the concrete). It is preferable to use (at minimum) 3-wire temperature compensating gages for exact measurements.

3.1.2 Suitable epoxies and polyurethanes are needed to secure the surface strain gages in place. It is preferable to use quick-curing epoxies so that testing times can be shortened.

3.1.3 Data-logging device suitable for up to three strain channel readings and capable of displaying the real-time strain value. It is preferable if the data-logger can record the data at a 1 Hz frequency and it is desired to have a resolution of $\pm 1 \times 10^{-6}$.

3.1.4 Circular saw capable of notching up to desired depth and fitted with suitable masonry blade (diamond-edge blade is preferable).

4. Summary of Test Method

4.1 *Concrete Pavement Surface*

4.1.1 Identify a point of interest on the surface of the concrete. The surface should be a smooth, flat area appropriate for testing based on pavement conditions and availability of pavement depth for saw notches to be made. Locations near edges, joints, large cracks or other irregularities should be avoided as the stresses in these areas may not be representative of the pavement as a whole. The concrete should be sufficiently dry in order to mitigate volumetric changes due to moisture gradients. The immediate area of testing should be adequately shaded from direct sunlight before the start of testing so that the strain readings are not affected by either volumetric changes in the concrete or by heating of the strain gage itself. The temperature of this area of concrete should be stable before the start of testing (neither heating nor cooling due to sunlight or shade).

4.2 *Strain Gage Rosette*

4.2.1 A strain gage rosette with three or more elements should be securely adhered to the prepared surface of the concrete pavement nearest to the center of the area to be isolated. They should be affixed per the strain gage manufacturer's recommendations. A suggested orientation for the strain gages is shown in Figure A.1.

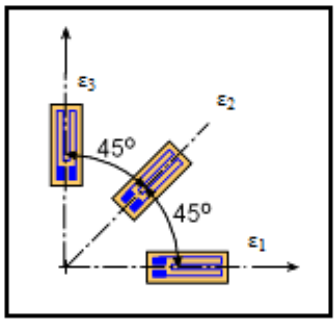

Figure A.1 Rectangular Strain Rosette

4.3 *Circular Masonry Saw*

4.3.1 An adjustable, circular saw fitted with a diamond-edge blade is used to notch around the strain rosette. The residual stresses in the material are effectively isolated when the depth of the notch is in accordance with the geometric spacing outlined in Table A.1. Heat is generated when cutting the notches, so a cooling period is required before noting final strain gage readings. Cooling water cannot be used because wetting the concrete will affect the strain reading significantly. Thus a circular saw that can dry-cut is necessary.

4.4 *Residual Stress Calculation*

4.4.1 The residual stresses originally existing in the concrete material are calculated from the change in strain when the saw notches are cut. These raw measurements are transformed into principal strains and stresses using the bi-axial form of Hooke's Law, the elastic modulus of the concrete and Poisson's ratio. The residual stresses in a concrete material can be either uniform or non-uniform in nature with respect to depth.

5. Significance and Use

5.1 *Summary*

5.1.1 Residual stresses are present in almost all materials. Residual stress in concrete can arise from temperature gradients, moisture gradients, or any other volume change, particularly when the concrete material is structurally restrained. In plain concrete pavements, the presence of residual stress can reduce the load capacity or cause premature failures such as faulting or blow-outs.

6. Concrete Surface Preparation

6.1 *Requirements*

6.1.1 The concrete surface should be prepared in accordance to the manufacturer's recommendations to properly affix surface strain gages. This process usually comprises the hand-sanding of efflorescence and other debris from the surface followed by an application of a thin epoxy layer. Grinding is not

recommended as this will cause an excess amount of damage along the surface of the concrete.

7. Strain Gages and Instrumentation

7.1 *Rosette Geometry*

7.1.1 Selected strain gages and strain rosettes should be of an appropriate size for measuring strain in concrete (usually on the order of magnitude of 20 mm to 30 mm in length). This size varies based on the maximum sized aggregate contained in the concrete. The gages should be affixed in each of three directions: (1) a reference direction, (2) 45^{o} from the reference direction and (3) perpendicular to the reference direction (refer to Figure 1). Because of the heat generated during a saw cut, the strain measurement will increase and must be monitored during testing in order to determine when the specimen has sufficiently cooled and the reading has stabilized. It is also important to note whether the measured surface temperature of the concrete exceeds the operable temperature of the strain gage during testing as this invalidates the test results. Depending on the geometry of the cuts and other factors that influence cooling rate, this stabilization period may be longer than 40 minutes.

7.1.2 The instrumentation for the recording of strains shall have a strain resolution of $\pm 1 \times 10^{-6}$ while the stability and repeatability of the measurement shall be at least $\pm 1 \times 10^{-6}$. It is strongly recommended that the lead wires be as short in length as practical and a three-wire temperature-compensating circuit be employed.

8. Procedure

8.1 *Notching Equipment and Use*

8.1.1 A machine capable of sawing notches in a concrete surface without causing extensive damage to its surroundings, usually a circular saw, is required. The depth of the saw must be adjustable so that the desired depth of cut can be readily achieved. Guides that can ensure straight and accurately sawn notches are strongly recommended if the underside of the circular saw does not pass over the strain gage rosette. However, if the underside of the circular saw's guard passes over the strain rosette, guides must be used to protect the strain rosette and ensure uninterrupted data collection and undamaged strain gages as shown in Figure A.2.

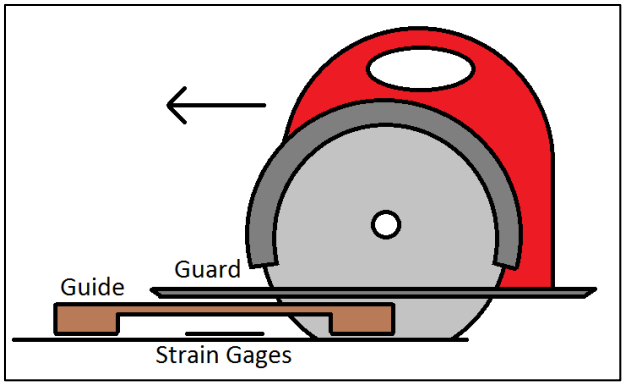

Figure A.2 Temporary guide protects the gages from the abrasive underside of the circular saw

8.1.2 The circular saw blade must be suitable for dry cuts because the use of cooling water is prohibited. A diamond edge blade is encouraged so that the notch can be sawn in a single pass. Multiple passes, if necessary, can be made to reach the desired depth, but note that the strain stabilization time will be lengthened as additional heat is introduced into the material.

8.1.3 An infrared thermometer, or other appropriate tool, should be employed to measure the temperature of the concrete surface during testing. These temperature values should be recorded in the Data Sheet along with the strain measurements.

8.2 *Load Application (Optional)*

8.2.1 A load may be applied and removed in the vicinity of the strain rosette to induce an amplified strain response. This response can be used to ensure whether the location of the strain rosette has been appropriately isolated from induced stresses. The magnitude of the required load varies and should be considered thoughtfully as to ensure the continual operation of the structure. For plain concrete pavements, a load of approximately 18,000 lbf (an equivalent single-axle load) should be considered for a pavement thickness of 8 inches or more. Depending on the environment of the testing procedure, one of two methods should be employed to ensure a reliable, safe procedure:

8.2.1.1 The load can be applied throughout testing. Load the pavement in a controlled manner such that the response by the strain rosette is linear elastic. This can be achieved with loading rates of approximately less than 1000 lbf per minute and at a distance from the strain rosette of several feet. Ensure that no other load is applied (such as a vehicle load or other heavy equipment) as this will alter the expected strain response if later modeled via FEM analysis. If the strain rosette response due to the applied load is immediate and stable, then proceed with the saw notching procedure as detailed in the following section. If the strain response due to

the applied load is unstable, consider removing the load and re-applying at a reduced rate or diminishing the magnitude of the load until a stable strain response is achieved. Once stabilized, proceed with the testing procedure as described in the following section. Before testing is concluded, remove the load and record the strain rosette response of the unloaded pavement. It is recommended that this load be once more applied and removed at the end of testing, as these strain values should demonstrate the isolation of the strain rosette.

8.2.1.2 The load can be applied and removed before testing and re-applied after testing. If the testing environment hinders the safe notching procedure to be performed while the pavement is loaded, then the loading can be applied and removed before the notching procedure occurs. Before the termination of data recording, a second loading and unloading sequence should be performed.

8.2.2 After saw cutting, the response of the strain rosette will be significantly reduced in magnitude from the response measured before saw cutting. The reduced response demonstrates that the strain rosette is properly isolated from the applied load. If the response after saw cutting is less than approximately 15% of the original response for the same applied load, then the majority of the stresses related to the applied load has been relieved. Accordingly, the difference in strain readings without the applied load represents the total stress present in the slab prior to the saw cut. If the response after saw cutting is more than 15% of the original response for the same applied load, consider deepening the depth of the saw cut by another 0.5 inches in order to isolate the applied stresses. Alternatively if the strain response due to an applied load is reversed (e.g., tensile strains are transformed into compressive strains), then the applied stresses have been appropriately isolated and no further testing is required.

8.3 *Notching Procedure*

8.3.1 Identify a 2x2 inch squared area onto which the surface strain gages can be applied. This area should be free of irregularities and prepared in accordance with the strain gage manufacturer's recommendation. This typically involves the sanding of efflorescence and other debris and the application of thin epoxy layers. Secure the strain rosette in a manner to ensure viable and continuous data readings within this 2x2 in square area. The strain gages should be placed as near the center-mark of the square area as possible. However, the outer boundary of the strain gage in any direction should not violate the 2x2 in square area.

8.3.2 Refer to Table A.1 to select a recommended Notch Separation distance. The distance selected should be drawn as a square that is symmetric with the 2x2

in square and that shares the same center-mark. The markings of the outer square should ensure a minimum ½ in separation of the strain gages from a notch at all times. If necessary, separate the lead wires to gain more flexibility in repositioning them out of the path of each saw pass. Extend the 4 edges of the outer square as necessary to produce lines of length 10 in resulting in geometry similar to a hash-mark, #, as shown in Figure A.3.

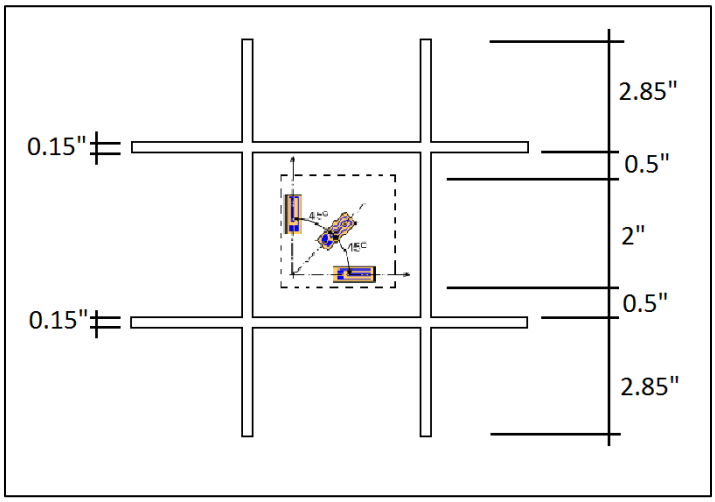

Figure A.3 Dimensions of notches around strain rosette after saw cutting

8.3.3 Ensure that the data-logger has been properly calibrated before testing. Begin strain measuring and recording. Allow for the excitation voltage to heat the strain gages for some time before beginning testing. These initial values are considered the "zero state" and serve as the point of reference for necessary calculations.

8.3.4 If guides are being employed, calibrate the depth of the saw blade with respect to the height of the guide in order to ensure that the appropriate notch depth is attained. Refer to Table A.1 for the minimum design depth which must coincide with the designed notch spacing. The two guides should be placed so that one fully covers the strain rosette and the other provides the saw guards a flush surface along its path. Most circular saws are constructed in a manner where the weight of the motor lays to one side of the saw blade. It is preferable to orient the saw pass in a manner so that the weight of the circular saw rests atop the guide that is away from the strain rosette.

8.3.5 When cutting, bring the circular saw to full speed and lower the center of the saw blade at one end of a 10 in line. When the circular saw guards are flush with the guides, proceed to move the saw forward along the line at an appropriate pace. Take precaution to not slide the guides against the strain rosette as this can potentially damage the gages and lead to erroneous results. When the center of the saw blade reaches the end of the 10 in line, safely lift

the circular saw up from the notch and thereafter switch the blade off. Per the saw blade manufacturer's recommendation, allow time for the saw blade to cool before proceeding with the second cut, usually 2 minutes. If the saw blade overheats or the circular saw is overworked, it is possible to decrease the depth of the cut to an intermediary one. This modification should be noted in the final report.

8.3.6 It is recommended that the second cut be made parallel to the first cut. It is also recommended that the direction of the cut be reversed as to prevent excess force from the circular saw from pressing on the strain rosette. Adjust the strain gage lead wires as necessary in order to protect them from damage and move the guides as necessary over the second 10 in line. Repeat the procedure for notching the 10 in line. After the saw blade cools, proceed with the third and fourth cuts in the same manner. Upon completing the fourth cut, measure the average depth of the notches and their parallel separation to include in the final report. Allow for the strain readings to stabilize before terminating the testing procedure. When the change in strain is less than $1x10^{-6}$ in 10 minutes for all three gages, the strain has recovered sufficiently and data collection can end.

Table A.1

Notch Separation, in	3.0	3.5	4.0
Recommended Minimum Notch Depth, in	1.2	1.4	1.6

8.3.7 It may be necessary to conduct a second set of 4 cuts along the same notches in order to ensure that the total stresses have been adequately isolated at the location of the strain rosette. This can be determined either by evaluating whether the effect of the strain rosette by the optional induced load has been diminished to within 15% of its original magnitudes, if an increase in depth of the notch by another 0.5 in produces a relaxed strain response within 5% of the previous strain response or if the desired notch depth was reached. If any of the aforementioned cases are met, testing may be concluded. Otherwise, consider an additional increase of depth of 0.5 in.

8.4 *Repair of Surface Damage*

8.4.1 Remove and collect the strain gages from the concrete surface and sand away thin epoxy layers as necessary. Excess dust and debris should be brushed or washed away and discarded as non-hazardous waste material. The notches can be filled with an appropriate cement based repair material as directed by the manufacturer's recommendation.

9. Computation of Stresses

9.1 *Poisson's Ratio and Elastic Modulus*

9.1.1 The Poisson's Ratio, ν, is needed in order to calculate the principal stresses from the principal strains; however, this value can be estimated as 0.15 for plain concrete. The modulus of elasticity for the concrete pavement is required to determine the stresses from the strain data. This stiffness, E, can be obtained with the following experimental methods:

9.1.1.1 Direct testing of the pavement using sample cores and subsequent laboratory testing. Refer to ASTM C469.

9.1.1.2 If the geometry of the structure is well understood, a load can be applied to the concrete and its strain measured at a known point. This response can be calculated to a stiffness value given the material's response is linear elastic.

9.1.1.3 Modulus estimation based on the strength or materials in the pavement. Refer to ASTM C873.

9.1.1.4 A Portable Seismic Property Analyzer (PSPA) or other non-destructive tests can be employed to determine the modulus of the material

9.2 *Stress Calculations*

9.2.1 Plot graphs of strains ε_1, ε_2 and ε_3 versus the average depth of the notches and confirm that the data follow generally smooth trends. Expected trends are typified in Figure A.4 where there is an immediate drop in strain readings due to the passing saw cut followed by an extended period in which the strains will rebound (or over-rebound) before stabilizing to a value. Investigate substantial irregularities and obvious outliers. If necessary, repeat the test (either at further depths or in an alternate location). Additionally if a load application was performed, ensure that the strain response at the end of testing is appropriately isolated (i.e. no response is observed). Note that the stabilized strain value will not necessarily coincide with the point at which the applied load is first isolated.

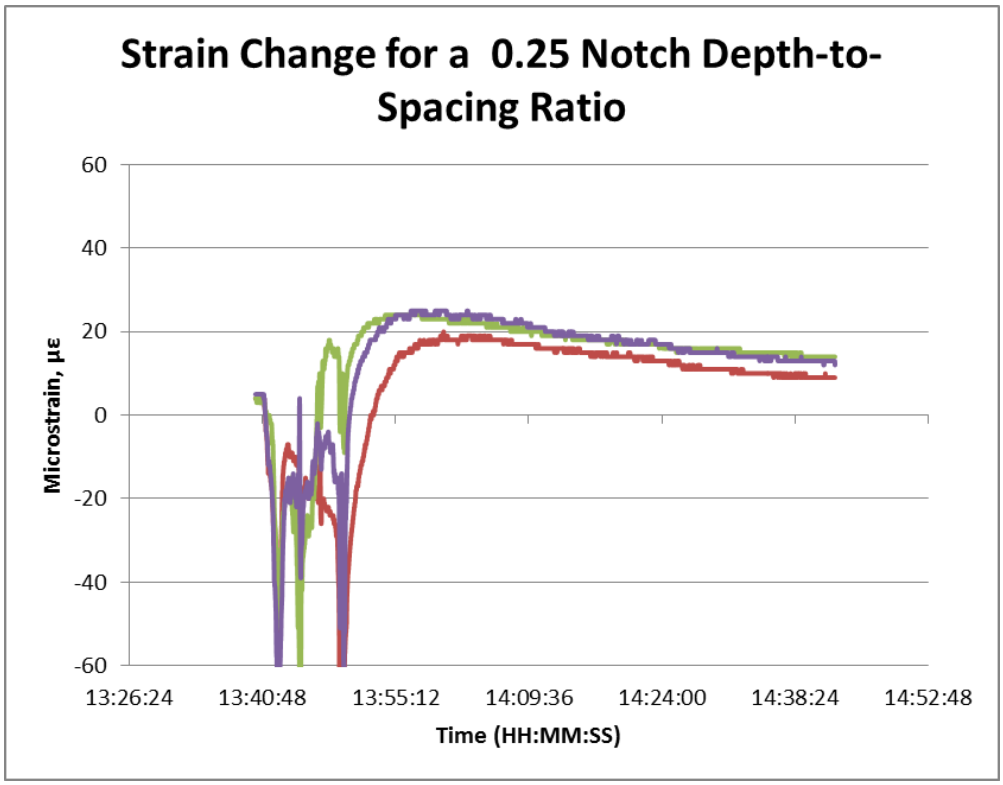

Figure A.4 Typical strain rosette response for quadrilateral cuts isolating

9.2.2 For the set of ε_1, ε_2 and ε_3 measurements of interest, calculate the corresponding principal strains *P* and *Q* along with orientation θ per Hooke's Law as given below:

$$\varepsilon_{P,\,Q} = \tfrac{1}{2}\,(\varepsilon_1 + \varepsilon_3) \pm (\tfrac{1}{2})^{0.5}\,[(\varepsilon_1 - \varepsilon_2)^2 + (\varepsilon_2 - \varepsilon_3)^2]^{0.5}$$

$$\theta = \tfrac{1}{2}\tan^{-1}\,[(\varepsilon_1 - 2\varepsilon_2 + \varepsilon_3) / (\varepsilon_1 - \varepsilon_3)]*180/\pi$$

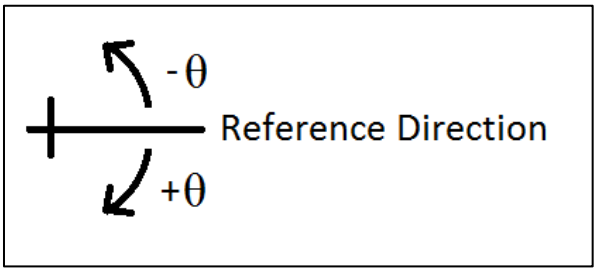

Figure A.5 Depiction of angle theta from reference axis to principal axis

9.2.3 Where ε_1 and ε_3 are separated by 90° and ε_2 lays either 45° or 225° from the reference strain measurements. θ is the angle *from* the principal axis *to* the reference axis implying that negative values of θ serve as the angle *from* the reference axis *to* the principal axis, counter-clockwise, as depicted in Figure A.5 above. The principal strains of ε_P and ε_Q can be used in the biaxial form of Hooke's law to find σ_P and σ_Q as follows:

$$\sigma_P = [E/(1-\nu^2)](\varepsilon_P + \nu\varepsilon_Q)$$
$$\sigma_Q = [E/(1-\nu^2)](\varepsilon_Q + \nu\varepsilon_P)$$

9.2.4 If the equations are combined, the principal stresses can be solved directly using:

$$\sigma_{P,Q} = \tfrac{1}{2} E [(\varepsilon_1 + \varepsilon_3)/(1-\nu) \pm [2^{0.5}/(1+\nu)][(\varepsilon_1 - \varepsilon_2)^2 + (\varepsilon_2 - \varepsilon_3)^2]^{0.5}]$$

9.2.5 The residual stress is considered to be the maximum principal stress as calculated if all other parameters (moisture, thermal and induced load) have been accounted for elsewhere. This value does not necessarily coincide with the induced stresses by any applied load, so it is necessary subtract any applied stresses in order to ascertain the residual stress value that is not attributable to load, moisture or thermal gradients.

10. Items to Report

10.1 *Test Description*

10.1.1 Description of the concrete pavement including its geometry,

10.1.2 Location of strain gage rosettes,

10.1.3 Model and type of rosettes used,

10.1.4 Rosette geometry, and

10.1.5 Equipment used to saw the notches.

10.2 *Strain Measurements and Stress Calculations*

10.2.1 Plot of maximum, principal strain versus depth for each rosette at 10 min intervals

10.2.2 Tabulation of strains ε_1, ε_2 and ε_3 for each rosette before and after notching,

10.2.3 Tabulation of calculated principal stresses for each rosette,

10.2.4 Tabulation of residual stresses after subtraction of applied stresses.

11. Precision and Bias

11.1 *Experimental Technique*

11.1.1 Strain values should be reported based on the noise levels of the data. The typical precision is usually about $\pm 2 \times 10^{-6}$.

11.1.2 Additionally, the strain reading will experience smooth trends of heating and cooling which will lead to parabolic and decaying behaviors. This is acceptable as long as the strain reading ultimately stabilizes in the span of approximately 60min. If the strain reading has not stabilized, it is possible that excessive heating (due to direct sunlight, e.g.), moisture or other micro-creep mechanisms have evolved and as such, the test results must be discarded.

11.1.3 It is important to realize that this testing method captures the stress state of the concrete in a specific instance of time. The sole measurement of a single test cannot wholly capture the changing stress states induced in the concrete due to seasonal variations (leading to curling) and eventual stress relaxation over time. Numerous tests should be run over a span of time in order to better characterize the concrete's residual stress state.

Draft ASTM Standard Test Method for Measuring Residual Stress in Plain Concrete Data Collection Sheet

Name of Test Conductor: _____ Date: ___ / ___ / ___
Sample Specimen Number: _____ Description: _____
Location: _____ Testing Conditions: _____

Strain Rosette Configuration

Gage Type: _____
Gage Length: _____
Gage Factor: _____ ± ____%
Gage Resistance: _____ ± ____Ω
Temp. Compensation: _____
Lead Wires: _____

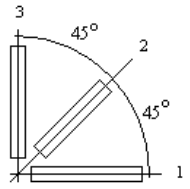

Figure 1 Rectangular Strain Rosette

Notching Configuration

Notch Spacing (in): _____ (S)
Design Depth (in): _____ (D)
1st Pass: _____ in.
2nd Pass: _____ in.
Designed Notch Depth-to-Spacing:
D / S = _____

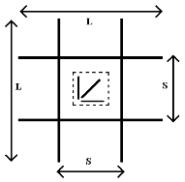

Figure 2 Sequence of Notches

Description of Machine Used:
_____
_____ .

Average of Notch Depths

Side 1:	Side 2:	Side 3:	Side 4:
_____	_____	_____	_____
_____	_____	_____	_____
_____	_____	_____	_____

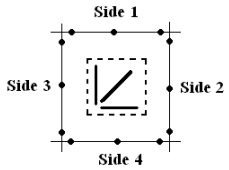

Figure 3 Depth Measurements

Average Depth (in): _____ (D')
Actual Notch Depth-to-Spacing:
D' / S = _____

Data Collection

Calibrate the data-logger and view (or record) data as the notches are made. Use an infrared thermometer to collect the average temperature of the concrete surface in the immediate area of testing. Note the strain readings and average temperatures at 600 ± 100 second increments. Testing is concluded when the change in strain for all three gages is no more than $1x10^{-6}$.

Time (sec)	Strain 1 (με)	Strain 2 (με)	Strain 3 (με)	Temp (°F)
0	*0*	*0*	*0*	
600				
1200				
1800				
2400				
3000				
3600				
4200				
4800				
5400				
Other:				

Depiction of Location of Strain Rosette

Description of Plain Concrete Section: _____
_____.
Drawing:

Computation of Total Stresses

Select ε_1, ε_2 and ε_3 as the final, stabilized strain readings at the conclusion of testing.

ε_1 = ____ ε_2 = ____ ε_3 = ____

Principal Stresses:

$A = \varepsilon_1 - \varepsilon_2$ = _____ $D = A^2 + B^2$ = _____
$B = \varepsilon_2 - \varepsilon_3$ = _____ $F = D^{0.5}$ = _____
$C = \varepsilon_1 + \varepsilon_3$ = _____ G = 0.707*F = _____
H = 0.5*C = _____

P = H + G = _____
Q = H – G = _____

Young's Modulus = E = _____ ksi
Poisson's Ratio = ν = _____ (0.15 to 0.25)

$J = E / (1 - \nu^2)$ = _____
K = P + ν*Q = _____ x 10^{-6}
L = Q + ν*P = _____ x 10^{-6}

Maximum Principal Stress = J * K = _____
Minimum Principal Stress = J * L = _____

The greater of the two values above is the largest total stress acting upon the plain concrete section and is the reported stress.

Reported In-Situ Stress: _____ psi.

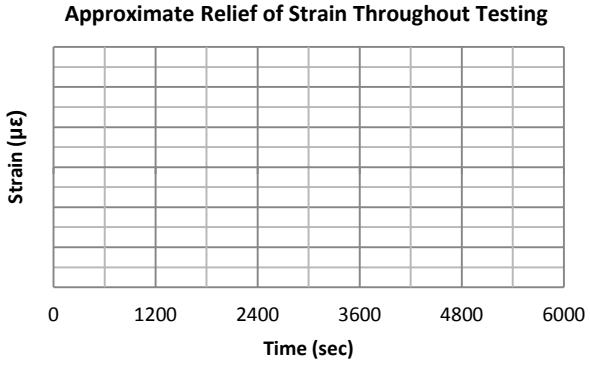

Figure 4 Graph of Stabilizing Strain Readings